Radboud University Nijmegen

Institute for Mathematics, Astrophysics and Particle Physics

Asymptotically Safe Amplitudes

No Strings Attached

Master Thesis Particle and Astrophysics

Author:
Tom Draper

Supervisor:
dr. Frank Saueressig

In collaboration with:
dr. Benjamin Knorr
dr. Chris Ripken

Date:
May 17, 2021

Abstract

In this thesis, I will discuss the most general gravity-mediated scattering of scalar particles compatible with a Lorentzian quantum effective action. I will use this framework to recover that scattering amplitudes originating from the Einstein-Hilbert action supplemented by minimally coupled scalar fields diverging quadratically with the centre-of-mass energy. The introduction of new interactions associated with terms quadratic in spacetime curvature cure this problem at the cost of unitarity. I will demonstrate that dressing the monomials with momentum-dependent form factors provides enough room to circumvent both problems, allowing for finite, unitary and causal scattering amplitudes beyond the Planck scale. These structural demands can be met without the introduction of non-localities or higher spin-degrees of freedom. These results constitute prototypical examples for scattering amplitudes expected within the gravitational asymptotic safety program. Furthermore, the form factor formalism allows for a parametrization of a class of higher-derivative theories of gravity. Our framework allows us to pinpoint the problems that present themselves in here. In this thesis, we will analyze effective field theory, Stelle gravity, infinite derivative gravity and Asymptotic Safety within this formalism as an illustration and as a stepping stone towards realizing Lorentzian asymptotically safe scattering amplitudes.

Acknowledgements

There are a number of people who have made the past year very special for me. First and foremost is Frank Saueressig, whom I would like to thank for his everlasting patience and unwavering support. I am not afraid to say that working from home has sometimes been difficult. Knowing that there was someone to whom I could ask anything and who would always make time for me was a comforting thought. Also, the detailed feedback to this thesis has been of immense help to finalize this project.

Of course, I would also like to thank Chris Ripken and Benjamin Knorr. The four of us have hosted the Tuesday Night Club every week for the past year, which ultimately resulted in two articles. For me it has been very special to be part of a new piece of physics and I would like to thank all three of you very much for letting me be part of it. I will fondly remember the serious discussions that were accompanied by a healthy dose of humour. The open atmosphere in this group has been great for a student like me. Thanks to you, I now know what it is like to be a scientist.

I want to say that it has been a great experience to work and learn with Sam Pirlo, who joined our collaboration halfway during my internship. Understanding the inner workings of Mathematica was much more fun doing together, and it was nice to have someone on my level to spar with. Our discussions helped me to pinpoint the topics I did not yet fully understand, and overcome the difficulties we encountered along the way.

I would like to thank Wim Beenakker for agreeing to be the second corrector of my thesis.

Finally, I would like to thank all the people that are close to me for their support over the past year. The social interactions I have had with you have been more important to me than the interactions studied in this thesis, especially during the restrictions due to COVID-19. No matter how hard I would have worked, I could not have done this without you.

Tom Draper - Nijmegen - May 17, 2021

Contents

Figures

CHAPTER 1

Introduction

The discussion about space and time is one that inspired many of the greatest minds of history. The ancient philosophers of Greece already wondered about the nature of these entities. Throughout the centuries, parallel to the development of mathematics, a framework was build to quantify these discussions into the laws of physics. The interplay between physics, mathematics and philosophy has boosted science to the point we are now. A remarkable feature that guided many scientist is a certain amount of beauty, elegance or simplicity that nature should preserve. Following these ontological principles, it is extraordinary how well the rules of calculus, algebra, group theory etc. lend themselves for the description of nature we have today.

A prime example of this is general relativity (GR), the theory of gravity we have today. Using tensor calculus, a complex set of highly non-linear partial differential equations is captured in a single line. Besides the mathematical marvel general relativity brought about, it also radically revolutionized the way we think about space and time. According to GR, they are one and the same and should be treated on equal footing. Previously, these were considered as separate entities, existing side-by-side, but the success of GR forced us to accept the notion of spacetime. No other theory could correctly described the precession of Mercury's perihelion, the deflection of light by the sun or gravitational redshift. On top of that is the prediction of gravitational waves and black holes, which have been observed in nature in just the last five years [1, 2].

Equally important, and roughly at the same time, was the development of quantum mechanics, and later quantum field theory. The classical particle interpretation of localized objects was replaced by formulating particles as excitations of an underlying Hilbert space, has proven to be extremely successful, although it was met with mixed reactions at that time.

Nevertheless, the irrefutable evidence of the quantum nature of matter was building up, which eventually culminated in the standard model (SM) of particle physics. The standard model incorporates three of the four fundamental forces of nature in a single quantum field theory by introducing a small set of elementary particles and force carriers. It uses the mathematical framework of quantum field theory to describe how they interact, and it allows us to calculate cross sections and decay rates to very high precision. Over the last decades, all particles that constitute the SM have been observed, with the Higgs boson being the last addition in 2012 [3, 4]. The standard model allowed us to calculate some of the most accurate predictions to date, such as the anomalous magnetic dipole moment of the electron where experiment and theory agree up to ten parts in a billion [5].

1.1 Problems with gravity

Despite the successes of the standard model, there are still some big questions left unanswered. For instance, very little is known about dark matter and dark energy, even though they proved the most significant contributions to the energy budget of the universe. Secondly, the observed neutrino oscillations contradict the assumed masslessness of the standard model neutrinos. Maybe the biggest issue is the absence of gravity. As physicists, we are looking for one elegant theoretical framework to describe nature, so naturally the standard model and general relativity should be unified into one theory. In order to treat gravity on equal footing with the other fundamental forces, it is of paramount importance to understand how gravity behaves as a quantum theory. However, the standard model does not describe gravity. It does not include its force carrier, the so-called *graviton*, as it does for the other fundamental forces (photons, gluons and $W^{\pm}$-, Z-bosons).

Gravitons appear naturally when general relativity is treated as a quantum field theory. However, problems start piling up quickly when gravitational interactions are evaluated at very short distances or at very high energies. In this UV-regime, observables defined through their scattering amplitudes are plagued by divergences. A general procedure in quantum field theory introduces a counter Lagrangian to the action whose goal is to absorb these infinities. To each term in the counter Lagrangian, a coupling constant is associated, whose value should be determined by experiments. The problem with gravity is that this approach requires an infinite number of counter terms. Thus, one needs an infinite number of observations to determine all the coupling constants. Formally, this is called the *perturbative nonrenormalizability* of general relativity. It has been proven that gravity interacting with scalar particles is perturbatively nonrenormalizable at the one-loop level [6, 7], and pure gravity at the two-loop level [8].

A second problem is due to the difficulty of measuring quantum gravity effects. It is expected that these effects become relevant at the Planck scale $\sqrt{\hbar c^5/G_N} \simeq 10^{19}$ GeV, which is many orders of magnitude higher than what we can currently measure at the LHC and it is even well-beyond the highest detected energies of cosmic rays. The branch of quantum gravity phenomenology is looking for quantum gravity signatures which are accessible experimentally. Although building a galaxy-sized particle collider might be cumbersome, there might be hope to measure quantum gravity in other processes. Some of the proposals build on the idea that Lorentz invariance or the principles of relativity might be broken near the Planck-scale, and that quantum gravity effects are important in the description of neutron stars. A more elaborate discussion on the current status can be found in [9–11]. Nevertheless, it is still notoriously hard to link theory to any reasonable detection and with current technology, these ideas are still out of reach.

1.2 A new hope

At this point one might wonder if the quest for quantum gravity is doomed to fail. Certainly, there are many issues, both theoretically and experimentally, that need to be overcome. Concerning general relativity, we know that problems arise in the UV, but this does not mean we cannot draw any conclusions in the low energy regime. Regarding general relativity as an effective field theory, predictive statements can be made below a certain cut-off scale [12–14]. It is beyond this scale that a new quantum gravity theory is required.

The scientific community has not been sitting still in the last decades, making massive progress towards understanding the intricate subtleties of quantum gravity. At this point, there is a wide range of quantum gravity proposals, each solving some of the issues raised in the previous section, although there is no clear "winner" yet. Among the more popular proposals are string theory and loop quantum gravity. Due to the non-perturbative nature of quantum gravity, these theories abandoned

the quantum field theory formalism. However, they have problems of their own. Loop quantum gravity has issues with restoring general relativity in the semi-classical limit [15–17]. Conversely, predictivity of string theory has always been up for debate, due to its enormous number of degrees of freedom. From a pragmatic point of view, no characteristic fingerprint of string theory (including, e.g., supersymmetry, extra dimensions and Regge poles) have seen experimental confirmation.

A second look at the QFT-approach to gravity shows that there is actually much to be gained. As shown by Stelle, it turns out that the addition of higher curvature terms to the Einstein-Hilbert action yields a renormalizable theory [18]. There is, however, a cost to be paid. Stelle gravity introduces a negative norm state, also called a ghost state, in the spin-two part of the graviton propagator (which will be shown in detail in chapter 5). This spin-two ghost is unphysical and it is known to violate the unitarity of the S-matrix [19]. Nevertheless, quantum field theories should not simply be disregarded. Currently, there is a plethora of higher-curvature and higher-derivative theories, potentially resolving the unitarity issues that typically arise in this sector [20, 21].

The analysis of a quantum field theory generally starts from an action. It tells us which interactions between particles are allowed, incorporates all the symmetry conditions of the theory, and allows to compute observables (at least in principle). A priori, we have no information about the interaction monomials that enter the action. A natural starting point is to order contributions to the action by power counting arguments. Generically, the argument is that interaction monomials coming with a higher mass dimension are suppressed in the low-energy regime. Following this logic, we could then start to include higher and higher orders of curvature tensors. However, this procedure proves to be problematic when truncated at a finite order. As was with Stelle gravity, unitarity-breaking ghosts modes appear in higher derivative theories. There are several ways to deal with ghosts [22]. In the context of asymptotic safety, they can be dealt with through an interacting fixed point. If the mass of the ghost state is pushed to infinity by the renormalization group equation, it is effectively decouple from the theory and unitarity is saved. Due to the complexity of the renormalization group equation, an analysis of a generic action is currently out-of-reach, but over the years, an incredible amount of evidence is building up that gravity is asymptotically safe in four dimensions [23–34], for a more complete discussion I refer to [35–37]. One of the open questions is if asymptotically safe gravity is unitary [38] and how the mechanism can be formulated for Lorentzian signature metrics. In this thesis we take first, important steps towards answering these questions.

The key idea of the present approach is to collect all orders of the Laplacians acting on a monomial X, conspire into an entire function. Schematically,

$$\int \mathrm{d}^4x\sqrt{-g}\Big(\alpha_0 X^2 + \alpha_1 X\Delta X + \alpha_2 X\Delta^2 X + \dots\Big) \longrightarrow \int \mathrm{d}^4x\sqrt{-g}X f_{\mathrm{XX}}(\Delta)X \tag{1.1}$$

where $\Delta = -g^{\mu\nu}D_\mu D_\nu$. Each monomial gets dressed with a *form factor*, which captures the entire momentum dependence of that specific term. This approach allows to study a broad class of quantum gravity theories in a unifying language. For example, in four dimensional theories, there are only two independent tensor structures that appear at $\mathcal{O}(R^2)$ in the pure gravity part of the action [39]; the squared Ricci scalar and the squared Weyl tensor (see section 3.2.1). The constant form factors of Stelle gravity, which generated the spin-two ghost, is now a momentum-dependent function. The idea is that appropriate form factors circumvent the ghost modes. The form factor model has been studied to resolve the black hole singularity [40], while they can simultaneously modify gravity on cosmic scales [41, 42]. The current question is which form factors result in a good theory of quantum gravity. This can be divided into two subquestions. We should understand what constraints need to be imposed on the form factors to abide to a list of physical requirements, e.g. unitarity and causality. Secondly, we need to know how to construct a theory that satisfies these criteria from first principles. In the work done in this thesis, the focus is on the first question.

1.3 Outline

The goal of this thesis is to use the form factors to study the requirements of unitarity and causality of scattering events. At the heart of this analysis will be the scattering of (in)distinguishable scalar particles, mediated by a graviton. The starting point will be the quantum effective action of gravity coupled to scalar fields, containing all interaction monomials that contribute to the tree-level scattering amplitudes in a flat Minkowski background. This also contains a self-interaction of the scalar particles, which plays an essential role in taming the growth of the amplitude. Dressing each term with a form factor, we obtain the most general quantum effective action that contributes to this scattering process.

This thesis starts with familiarising the reader with the mathematical background of the quantum effective action in chapter 2. In the final section of this chapter, I will also list the important constraints we wish to impose on the action, which restricts the monomials that enter. We then derive the most general action which can be attributed to scalar-scattering in chapter 3. From this, we derive the relevant n-point functions, from which we get the graviton propagator and the scalar-graviton vertex. This sets the stage for constructing the scattering amplitude, partial wave amplitudes, and cross section in chapter 4. The result allows us to derive constraints on the form factors to yield unitary, causal and scale-free amplitudes, without introducing massive higher-spin particles and non-localities. Also, it allows for an analysis of different higher-derivative theories of gravity in a unified language in chapter 5. As a proof of principle, a specific set of form factors are introduced in chapter 6 which are compatible with the list of constraints, showing that the form factors give enough freedom for a physical quantum gravity theory. We close with some concluding remarks and an outlook to future research in chapter 7.

The constants $\hbar$ and c will be set to one throughout the calculations, while Newton's constant will remain in the calculation. The calculations will done in a Lorentzian metric signature.[1] The cosmological constant is also set to zero. It is assumed that this does not influence the conclusions of the work done in this thesis.

During my internship, I have had the opportunity to join a research collaboration from Nijmegen, Waterloo and Mainz, consisting of dr. Frank Saueressig, dr. Benjamin Knorr, dr. Chris Ripken and me. The results of this thesis can partially be found in the two articles, [43, 44], we wrote in this time.

[1] Asymptotic safety calculations are usually done in Euclidean signatures.

CHAPTER 2

Time for action

In this chapter, the theoretical foundation for the remainder of this thesis will be laid down. The object that we will work towards is the quantum effective action. It is a generating functional which encodes all one-particle irreducible vertices of the theory. Having this in our toolkit, calculating scattering amplitudes becomes easy. Only tree-level diagrams are needed to obtain the amplitude. No renormalization techniques are required here, since all loop corrections are already included in the effective vertices. The downside to this is that full insight in the microscopic quantum fluctuations of the theory is required. In this sense, full information of the system is necessary. In this thesis, the quantum effective action will be parametrized in terms of unspecified form factors which capture all (non-perturbative) momentum dependence of the quantum fields. These functions account for the momentum behaviour of the vertices and propagators beyond leading order. Starting from a quantum effective action is therefore perfectly fine, although a derivation of these form factors from first principles is beyond the scope of this thesis.

The first part of this chapter shows how the quantum effective action is derived in the path integral formalism, starting from the ground up and going through the derivations step-by-step. The final part of the chapter introduces the physical requirements which need to be imposed on a theory.

2.1 Generating functionals

Typically, observables can be calculated from scattering amplitudes. There are different procedures to derive them from an action. Some QFT textbooks follow the way of canonical quantization. Classical fields are promoted to quantum operators which satisfy the canonical commutation relations, which is why QFT is sometimes bluntly referred to as "the art of putting hats on stuff". A different, but equivalent, approach is the path integral formalism. Following [45] an intuitive approach to the path integral can be achieved by studying the double-slit experiment. Suppose a sheet with two small slits is placed in between a particle source and a screen. This results in a interference pattern on the screen, due to the wave-particle duality of matter. It cannot be said through which hole a particle travelled to end up at the screen, and the detection amplitude is given by the sum of the amplitudes of the particle travelling through either hole. Would anything change if more holes were poked in the sheet? Similarly, would anything fundamentally change if more than one sheet was placed in between the source and the screen? The answer to both questions is no, the same principle still holds. The total amplitude is given by summing over the probability amplitudes of all possible

trajectories through the sheets and holes. The real magic happens considering an infinite number of sheets and holes. Effectively, the sheets are removed altogether, and the detection amplitude is given by summing over all possible paths between the source and screen. There are two questions which needs to be answered. We should know what the probability amplitude of any given path connecting the two points x_a at $t = 0$ and x_b at $t = \tau$ is and we should know how to "sum over paths".

The propagation amplitude in quantum mechanics is given by the evolution operator $\widehat{U}$, sandwiched between the initial state $|x_a\rangle$ and final state $|x_b\rangle$. It is a unitary operator which can be written as the exponential of a Hermitian operator. For a time-independent Hamiltonian $\widehat{H}$, this is given by

$$\widehat{U}(\tau) = \exp\left(-\frac{i}{\hbar}\widehat{H}\tau\right). \tag{2.1}$$

By the completeness relation, it is enough to know how the amplitude evolves in a tiny interval. Suppose the points x_i define a partition of the interval $[x_a, x_b]$, such that $x_0 = x_a$ and $x_N = x_b$ for some $N \in \mathbb{N}$ and $x_{i+1} > x_i$. Furthermore, the propagation between subsequent points is equitemporal, meaning that it takes $\delta\tau = \tau/N$ to propagate from x_i to x_{i+1}. The total amplitude is obtained by multiplying over all intermediate amplitudes

$$\langle x_b|\,\widehat{U}(\tau)\,|x_a\rangle = \prod_{i=1}^{N}\left(\int \mathrm{d}x_i\right)\langle x_i|\,\widehat{U}(\tau)\,|x_{i-1}\rangle\,. \tag{2.2}$$

Starting from a Hamiltonian $\widehat{H} = \widehat{p}^2/2m + \widehat{V}(x)$, the intermediate amplitudes can readily be calculated by making use of the completeness relation for a second time. For the explicit calculations, I refer to [45, 46]. A functional integral is obtained by plugging the result back and taking the continuum limit $N \to \infty$

$$\begin{aligned}\langle x_b|\,\widehat{U}(\tau)\,|x_a\rangle &= \int Dx(t)\,\exp\left(\frac{i}{\hbar}\int_0^\tau \mathrm{d}t\left[\frac{1}{2}m\dot{x}^2 - V(x)\right]\right)\\ &= \int \mathcal{D}x(t)\,\exp\left(\frac{i}{\hbar}\int \mathrm{d}t\,L[x,\dot{x}]\right).\end{aligned} \tag{2.3}$$

The functional integral integrates over all possible paths such that $x(0) = x_a$ and $x(\tau) = x_b$. Both of the initial questions are answered. The path integral is calculated through an integration procedure over a discrete interval, followed by taking the continuum limit. Simultaneously, this representation of the amplitude shows that the weight of each path is given by an exponential of a phase factor. Each path has the same modulus, and the phase factor is given by the action of the theory. The expectation value, where the initial and final state are the ground state is called the partition function, and it denoted by Z.

Befitting to any good quantum theory, the semi-classical limit $\hbar \to 0$ should retrieve the classical equations of motion. In this limit, the stationary phase approximation shows that only paths that extremize the action, solving the Euler-Lagrange equations, contribute to the action. This shows that the semi-classical limit gives the classical equations of motion.

At this point, it is time do start doing quantum field theory. This means all components in equation (2.3) should be identified with Lorentz invariant building blocks. First, the "path" is replaced by the quantum field ϕ, which is a function of spacetime, rather than just the variable t. Secondly, the action is defined as an integral of the Lagrangian density. The correct kinetic term contains two time-derivatives, contrary to Schrödinger's equation, to treat space and time on equal footing. Finally, we use the freedom to choose the initial and final configurations as the ground state to obtain the partition function of the quantum field theory. It has the interpretation of the

transition amplitude of the vacuum $|\Omega\rangle$, i.e. the vacuum energy, picking up all possible quantum fluctuations along the way

$$Z_0 = \langle\Omega|\,\widehat{U}(\tau)\,|\Omega\rangle = \int \mathcal{D}\phi\, \exp\left(i\int \mathrm{d}^4x \mathcal{L}[\phi]\right). \tag{2.4}$$

Here $|\Omega\rangle$ is the vacuum state of the fully interacting Hamiltonian of the system. At some instance of time, we would like to create a particle, watch it propagate for a while, and finally annihilate it into the vacuum. The way to achieve this, is by including a small perturbation to the vacuum by means of a source term J, linearly coupled to the field ϕ

$$Z\,[J] = \int \mathcal{D}\phi\, \exp\left(i\int \mathrm{d}^4x \Big[\mathcal{L}[\phi] + J(x)\phi(x)\Big]\right). \tag{2.5}$$

The ϕ-integral has no explicit solution in a closed form. In general, an expansion procedure of some kind is required, which is the starting of perturbation theory in QFT's. However, a solution can be found for a massive, free particle. In this case, the potential is set to $V(\phi) = \frac{1}{2}m^2\phi^2$, resulting in

$$Z[J] = Z_0 \exp\left(-\frac{i}{2}\int \mathrm{d}^4x \int \mathrm{d}^4y\, J(x)D(x-y)J(y)\right) = Z_0 \exp\big(iW[J]\big), \tag{2.6}$$

where W is defined as the exponent sitting in $Z[J]$

$$W[J] = -\frac{1}{2}\int \mathrm{d}^4x \int \mathrm{d}^4y\, J(x)D(x-y)J(y), \tag{2.7}$$

and D is the propagator of the scalar field ϕ, satisfying

$$-\left(\partial^2 + m^2\right) D(x-y) = \delta^{(4)}(x-y). \tag{2.8}$$

It is clear that $W[J] \simeq -i\log Z[J]$ contains the interesting information about a free particle, namely the propagator. Taking variations with respect to the source term gives us exactly that

$$\frac{\delta^2 iW[J]}{\delta J(x)\delta J(y)} = -iD(x-y). \tag{2.9}$$

It is not a coincidence that this happens. In fact, equation (2.9) holds for any action, not just for a free particle. Understanding W and Z in terms of correlation functions, or equivalently, in terms of Feynman diagrams turns out to be crucial. To show what is going on, Z and W will be expanded around $J = 0$, starting with Z first.

$$\begin{aligned} Z[J] &= \int \mathcal{D}\phi\, \exp\left(i\int \mathrm{d}^4x \mathcal{L}[\phi]\right) \sum_{n=0}^{\infty} \frac{i^n}{n!}\left(\int \mathrm{d}^4x J(x)\phi(x)\right)^n \\ &= Z_0\left(1 + i\int \mathrm{d}^4x\, J(x)\,\langle\phi(x)\rangle - \frac{1}{2}\int \mathrm{d}^4x \int \mathrm{d}^4y\, J(x)J(y)\,\langle\phi(x)\phi(y)\rangle + \dots\right). \end{aligned} \tag{2.10}$$

What is being shown here is that Z is a generating functional, whose coefficients give the n-point correlation functions. Of course, we know that the two-point correlation function is exactly the propagator, so it was indeed no coincidence that it appeared in eq. (2.7). In general, we have

$$\frac{1}{Z[J]}\frac{\delta^{(n)}Z[J]}{\delta J(x_1)\dots\delta J(x_n)}\bigg|_{J=0} = i^n\,\langle\phi(x_1)\dots\phi(x_n)\rangle\,. \tag{2.11}$$

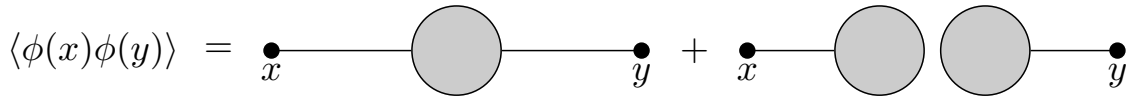

Figure 2.1: *Representation of the two-point correlation function in Feynman diagram language. It includes all diagrams, both connected (1st term) and disconnected (2nd term), propagating from x to y. The shaded grey area consists of all connected contributions.*

It is time to show the exact difference between W and Z. As an example, I will calculate the first and second order functional derivatives of $W[J]$ with respect to two non-zero source terms $J(x)$ and $J(y)$.

$$\frac{\delta W[J]}{\delta J(x)} = -i\frac{\delta \log Z[J]}{\delta J(x)} = -i\frac{1}{Z[J]}\frac{\delta Z[J]}{\delta J(x)} = \langle\phi(x)\rangle \tag{2.12}$$

This is the same result as we got for $Z[J]$. From the next order onwards, the result will be different however.

$$\begin{aligned}
\frac{\delta^2 W[J]}{\delta J(x)\delta J(y)} &= -i\frac{\delta^2 \log Z[J]}{\delta J(x)\delta J(y)} \\
&= -i\frac{\delta}{\delta J(x)}\frac{1}{Z[J]}\int \mathcal{D}\phi\, i\,\phi(y)\exp\left(i\int \mathrm{d}^4z\Big[\mathcal{L}[\phi]+J(z)\phi(z)\Big]\right) \\
&= -i\Bigg[-\frac{1}{Z[J]^2}\int \mathcal{D}\phi\, i\,\phi(x)\exp\left(i\int \mathrm{d}^4z\Big[\mathcal{L}[\phi]+J(z)\phi(z)\Big]\right) \\
&\qquad\qquad \times\int \mathcal{D}\phi\, i\,\phi(y)\exp\left(i\int \mathrm{d}^4z\Big[\mathcal{L}[\phi]+J(z)\phi(z)\Big]\right) \\
&\qquad + \frac{1}{Z[J]}\int \mathcal{D}\phi\, i\,\phi(x)\, i\,\phi(y)\exp\left(i\int \mathrm{d}^4z\Big[\mathcal{L}[\phi]+J(z)\phi(z)\Big]\right)\Bigg] \\
&= i\Big(\langle\phi(x)\phi(y)\rangle - \langle\phi(x)\rangle\,\langle\phi(y)\rangle\Big).
\end{aligned} \tag{2.13}$$

We can immediately interpret the difference between W and Z. While Z is the generating functional for *all* correlation functions, W generates only the *connected* ones. A diagrammatic representation of this result is shown in figure 2.1 and 2.2. As a matter of convention, the RHS of equation (2.13) is abbreviated to $i\,\langle\phi(x)\phi(y)\rangle_c$. In general, taking the n-th derivative of W with respect to J gives the n-th order connected correlation function

$$\frac{\delta i W[J]}{\delta J(x_1)\dots\delta J(x_n)} = i^n\,\langle\phi(x_1)\dots\phi(x_n)\rangle_c\,. \tag{2.14}$$

It is because of this reason that our interest lies in W; only connected and amputated diagrams are relevant in the calculation of scattering amplitudes.

The connected two-point function generated by W consists of all possible diagrams which cannot be separated without cutting an internal line. These diagrams can be divided into two classes. First, we consider the class where cutting an arbitrary internal line does not produce a disconnected graph. The collection of these diagrams are known as the one-particle irreducible diagrams. Next, we consider the classes where cutting one, two, ... internal lines produces one-particle irreducible diagrams. All these reducible diagrams can be produced by stringing together the irreducible parts in all possible ways, as illustrated in figure 2.2. In this sense, the connected two-point function gives the exact propagator. In the next section, we introduce the quantum effective action, which produces not only the exact propagator, but also all exact n-point vertices.

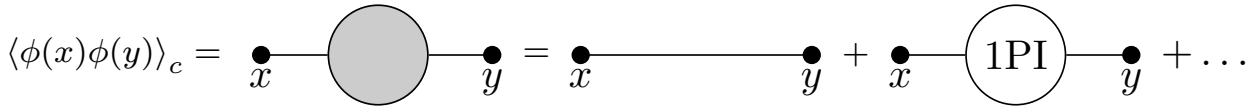

Figure 2.2: *Representation of the connected correlation functions in Feynman diagrams; it the total correlation function minus the disconnected part. The shaded grey area consists of all connected contributions.*

2.2 The quantum effective action

Right now, we are familiar with the generating functional Z, whose logarithm gives access to all the connected correlation functions. Although this result is already insightful, it is possible to go one step further. The connected diagrams still contain external lines, which should be removed to obtain the exact vertices of the theory. Taking the Legendre transform of W turns out do to the trick. This produces Γ, which is a generating functional for all exact one-particle irreducible vertices. This object is known as the *quantum effective action* and has many applications in particle physics, scattering theory and condensed matter physics. Subsequently, Γ is a functional of the expectation values of the fields and not of the source terms.

To incorporate the exact 1PI propagator and vertices in a path integral representation, the first thing to do is to promote W to a more general functional which includes loop corrections. A step-by-step explanation is given in [46]. Define $W_{\Gamma,\hbar}$ as the sum of all connected diagrams, where each external line is the exact 1PI propagator, and where each vertex is the exact 1PI vertex. The bare action is replaced by the more general effective action Γ. By definition, it is a richer object as it needs to contain all quantum corrections at this level. The dimensionless parameter $\hbar$ keeps track of the order of the connected diagrams. It is implemented in the following way

$$Z_{\Gamma,\hbar}[J] = \int \mathcal{D}\phi \, \exp\left[\frac{i}{\hbar}\left(\Gamma[\phi] + \int \mathrm{d}^4x \, J(x)\phi(x)\right)\right] = \exp\left(iW_{\Gamma,\hbar}[J]\right) \tag{2.15}$$

The original W is obtained if only tree-level contributions to W_Γ are considered. Every propagator is multiplied with a factor $\hbar$, whereas sources and vertices get an additional factor $\hbar^{-1}$. The combined factor is then equal to $P - E - V$, where P is the number of propagators, E is the number of sources and V the number of vertices. On the other hand, we can count the number of closed loops L by evaluating the number of unfixed internal momenta. The total number of internal momenta is equal to $P - E$, but some of these are fixed by constraints coming from the vertices. Also, one vertex is required to provide energy-momentum conservation, which brings to total number of unfixed momenta, i.e. loops, to $L = P - E - V + 1$. This allows for a loop expansion for $W_{\Gamma,\hbar}$

$$W_{\Gamma,\hbar}[J] = \sum_{L=0}^{\infty} \hbar^{L-1} W_{\Gamma,L}[J]. \tag{2.16}$$

For small $\hbar$, the dominant contribution comes from the connected tree-level diagram, giving us $W[J] = W_{\Gamma,L=0}[J]$.

The final piece of the puzzle is the new quantum equations of motion derived from (2.15). By the stationary phase approximation, the solution is given by the field configuration which satisfies

$$\frac{\delta\Gamma[\phi]}{\delta\phi(x)} = -J(x). \tag{2.17}$$

So far, we have studied the path integral in the vicinity of $J = 0$. Now the source term is set to a finite value, making the solution $\Phi(x)$ to the equations of motion J-dependent. In the stationary

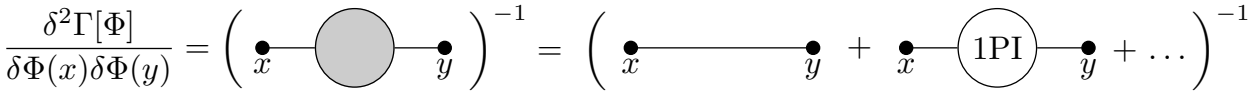

Figure 2.3: *The second variation of the quantum effective action is inversely proportional to the exact propagator, consisting of all possible combinations of one-particle irreducible corrections.*

phase approximation, the path integral (2.15) reduces to

$$Z_{\Gamma,\hbar}[J] = \exp\left[\frac{i}{\hbar}\left(\Gamma[\Phi] + \int \mathrm{d}^4x\, J(x)\Phi(x)\right) + \mathcal{O}(\hbar^0)\right]. \tag{2.18}$$

Now that the dust has settled, we can see the relation between W and Γ. Combining equations (2.15), (2.16) and (2.18) shows that the quantum effective action is given by the Legendre transform of W

$$\Gamma[\Phi] = W[J] - \int \mathrm{d}^4x\, J(x)\Phi(x), \tag{2.19}$$

where

$$\frac{\delta W[J]}{\delta J(x)} = \langle\Omega|\,\phi(x)\,|\Omega\rangle_J \equiv \Phi(x). \tag{2.20}$$

The last step follows from the observation that the vacuum expectation value of $\phi(x)$ in the presence of a non-zero source function is also the solution to the quantum equations of motion.

$$\begin{aligned}\langle\Omega|\phi(x)|\Omega\rangle &= \frac{\delta W[J]}{\delta J(x)} \\ &= \frac{\delta\Gamma[\Phi]}{\delta J(x)} + \frac{\delta}{\delta J(x)}\int \mathrm{d}^4y\, J(y)\Phi(y) \\ &= \frac{\delta\Gamma[\Phi]}{\delta J(x)} + \Phi(x) + \int \mathrm{d}^4y\, J(y)\frac{\delta\Phi(y)}{\delta J(x)}.\end{aligned}$$

The first term in this expression can be evaluated using the chain rule, giving

$$\begin{aligned}\langle\Omega|\phi(x)|\Omega\rangle &= \int \mathrm{d}^4y\, \frac{\delta\Gamma[\Phi]}{\delta\Phi(y)}\frac{\delta\Phi(y)}{\delta J(x)} + \Phi(x) + \int \mathrm{d}^4y\, J(y)\frac{\delta\Phi(y)}{\delta J(x)} \\ &= \int \mathrm{d}^4y\, \left[\frac{\delta\Gamma[\Phi]}{\delta\Phi(y)} + J(y)\right]\frac{\delta\Phi(y)}{\delta J(x)} + \Phi(x).\end{aligned} \tag{2.21}$$

By definition, Φ is the solution to (2.17), making the term in the large square brackets disappear. Hence, what remains is

$$\langle\Omega|\phi(x)|\Omega\rangle = \Phi(x). \tag{2.22}$$

So far, I claimed that Γ produces all one-particle irreducible correlation functions. It is time to prove that statement, which we will do along the lines of [47]. The statement is slightly more nuanced. The second order derivative generates the inverse of the two-point correlation function. This can be shown from the general properties satisfied by Legendre transforms. Recalling (2.17) we

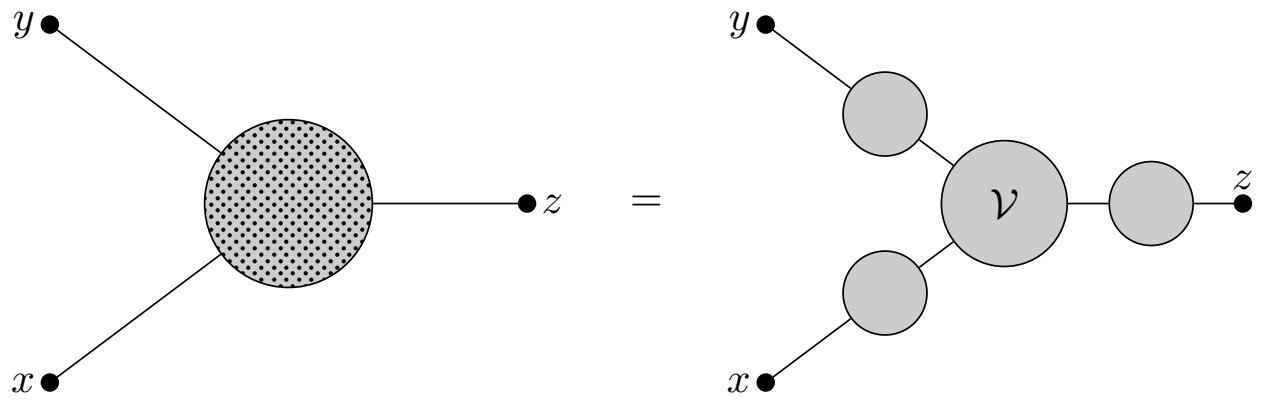

Figure 2.4: *The connected three point correlation function consists of three complete external lines attached to the one-particle irreducible three point vertex* $\delta^3\Gamma[\Phi]/(\delta\Phi)^3$.

have

$$\begin{aligned}\delta(x-y) &= -\frac{\delta}{\delta J(y)}\frac{\delta\Gamma[\Phi]}{\delta\Phi(x)} \\ &= -\int \mathrm{d}^4z \frac{\delta\Phi(z)}{\delta J(y)}\frac{\delta^2\Gamma[\Phi]}{\delta\Phi(z)\delta\Phi(x)} \\ &= -\int \mathrm{d}^4z \frac{\delta^2 W[J]}{\delta J(y)\delta J(z)}\frac{\delta^2\Gamma[\Phi]}{\delta\Phi(z)\delta\Phi(x)},\end{aligned} \tag{2.23}$$

where we applied the chain rule for the second line and equations (2.20), (2.22) give the final result in the third line. Given that W generates the connected two-point function, this shows that $\delta^2\Gamma[\Phi]/(\delta\Phi)^2$ is proportional to the inverse propagator,

$$\frac{\delta^2\Gamma[\Phi]}{\delta\Phi(x)\delta\Phi(y)} = -\left(\frac{\delta^2 W[J]}{\delta J(x)\delta J(y)}\right)^{-1} = D^{-1}(x-y). \tag{2.24}$$

What now about higher order variations. Using the standard rules for differentiating inverse matrices, the next order gives

$$\frac{\delta^3 W[J]}{\delta J(x)\delta J(y)\delta J(z)} = -\int \mathrm{d}^4u\mathrm{d}^4v\mathrm{d}^4w D(x-u)D(y-v)D(z-w)\frac{\delta^3\Gamma[\Phi]}{\delta\Phi(u)\delta\Phi(v)\Phi(w)}. \tag{2.25}$$

The result is the connected three-point correlation function. So let us see what is written in the integral. The three propagators denote external lines, which have to be joined together at a vertex. Because the result is the fully connected three-point function, this implies that $\delta^3\Gamma[\Phi]/(\delta\Phi)^3$ has to be the exact three-point vertex,

$$-\frac{\delta^3\Gamma[\Phi]}{\delta\Phi(x)\delta\Phi(y)\delta\Phi(z)} = \mathcal{V}(x,y,z). \tag{2.26}$$

The same argument and calculation can be extended to show that Γ generates all one-particle irreducible n-point vertices. In general

$$-\frac{\delta^{(n)}\Gamma[\Phi]}{\delta\Phi(x_1)\dots\delta\Phi(x_n)} = \mathcal{V}(x_1,\dots,x_n) \qquad \forall n \geq 3. \tag{2.27}$$

We conclude this section with the following remark. So far the derivation of the quantum effective action has been limited to scalar fields. The exact same principles hold for vector and tensor fields. To obtain the graviton propagator, variations of the effective action with respect to the metric perturbation $h_{\mu\nu}$ can be taken using the relation

$$\frac{\delta h_{\alpha\beta}}{\delta h_{\mu\nu}} = \mathbb{1}_{\alpha\beta}^{\ \ \mu\nu} = \frac{1}{2}\Big(\delta_\alpha^{\ \mu}\delta_\beta^{\ \nu} + \delta_\alpha^{\ \nu}\delta_\beta^{\ \mu}\Big), \tag{2.28}$$

such that $\mathbb{1}$ acts a the unit tensor for all symmetric rank-two tensors. Also, the graviton propagator is defined as the inverse of the two point function with respect to this unit tensor.

2.3 Constraining the action

Right now, we know what we can do given a quantum effective action Γ. The exact propagators and vertices are easily found through differentiation with respect to the relevant fields, and in order to obtain the amplitude for a scattering process, only tree-level diagrams are required. This makes it an extremely powerful tool in a physicist's toolkit. The cost to be paid is that we need a-priori knowledge of the interacting monomials that enter in the action, including momentum-dependent form factors which usually come from renormalization techniques.

First and foremost, the model should agree with observations and measurements. For gravity, this path is quelled by the weakness of gravitational interactions, which are expected to appear at the Planck scale. This makes it hard to tie experiments to constraints on form factors of local theories.[2] On the other hand, the quantum effective action should be theoretically consistent, providing a theory which abides to fundamental properties. Haphazardly extending GR with higher-derivative terms is known to cause problems, violating unitarity and causality. At this point, it should be clarified what these properties exactly are, and how they translate to constraints on the action and on scattering amplitudes.

Symmetry:
Symmetry conditions often form the basis for a physical theory. The mathematical language to parametrize symmetries is given by group theory. All symmetries found in nature can be associated to a symmetry group. The concept of symmetries is long known. For instance, the equations of motion underlying classical mechanics exhibit invariance under translation and rotation transformations.

Symmetries in QFT's are often captured in a special class of groups; the Lie groups. If the action is invariant under local transformations of a Lie group, then we call that a gauge symmetry. Initially, an action with a gauge symmetry is problematic and needs to be fixed. The reason is that in the path integral formalism, we are redundantly integrating over an infinite family of physically equivalent field configurations. Also, two-point functions can become singular. A well known example is QED, where gauge fixing of the $U(1)$ symmetry group is required to obtain a well-defined photon propagator. This gauge-fixing procedure was introduced by Faddeev and Popov [50–52]. They solve the issue by including an extra term in the action which captures all gauge-equivalent field configurations. In the case of non-Abelian gauge symmetries, a second term is required, which introduces ghost fields to the theory. These extra fields do not satisfy the spin-statistics theorem and have to be virtual. No ghost fields appear in QED. The $U(1)$ gauge symmetry of QED is Abelian, so no ghosts appear here, but for gravity this is not the case. Here, ghost fields are essential for a well-defined theory. Standard choices such as the harmonic gauge generate a "ghost action" quadratic in the ghost fields.

[2] There are non-local models which provide an infrared modification of gravity [48, 49]. In particular, this leads to interesting cosmological effects, such as a dynamical dark energy density that can account for the presently observed value of $\Omega_{\rm DE}$ without the introduction of a cosmological constant. Effects like these might be experimentally viable.

Secondly, symmetries severely limit the form of monomials that can enter in the action. Only monomials which are invariant under transformations of the underlying symmetry group can appear. That is the motivation of using tensors to construct the action, since this allows to construct Lorentz-invariant combinations rather efficiently. Invariance at the level of the action ensures that all observables also respect this symmetry. In the case of gravity, the field equations are written in terms of curvature tensors. These field equations are invariant under diffeomorphisms, which ensure that a change of coordinates do not affect the form of the equations of motion. In the case of gravity, only monomials which are derived from the Riemann tensor can appear. At the two-derivative level, only one monomial is non-zero due to symmetry, which constitutes the Ricci scalar for the Einstein-Hilbert action. At the next order, as we will see in section 3.2.1, only two extra monomials appear.

Unitarity:
The way to understand unitarity in quantum field theories is by means of the scattering matrix S. The components of the S-matrix are called scattering amplitudes and they relate how asymptotic free initial and final states are related. In order to understand the scattering amplitudes as probabilities, it is required that the S-matrix is unitary.

There is a direct relationship between unitarity of the S-matrix, and boundedness of the individual scattering amplitudes and consequently, cross sections. This result is known as the Froissart bound, named after the French physicist who first derived it in 1961 in [53, 54]. It uses the optical theorem to derive that the total scattering cross section cannot grow faster than $\log^2 \mathfrak{s}$, where $\mathfrak{s}$ is the square of the centre-of-mass energy. Considering Feynman rules derived from a bare action, the optical theorem relates tree-level diagrams and loop corrections to obtain unitarity. The question arises how the optical theorem extends to the quantum effective action formalism, and how it constrains the form factors. In this work, we will understand unitarity by means of a partial wave decomposition of the scattering amplitudes (see section 4.2). Bounding the partial wave amplitudes

$$|a_j(\mathfrak{s})| \leq 1 \qquad \forall j \geq 0, \tag{2.29}$$

the scattering amplitude is confined to the Argand plane. Consequently, the model introduced in chapter 6 satisfies the Froissart bound.

Causality:
Causality means that two spacelike separated events cannot affect each other, as it requires superluminal exchange of information. To meet this demand, it is required that the commutator of field operators vanish outside the light cone. Consequently, only local terms can be added to the action. Causality constrains scattering amplitudes in two ways. The Cerulus-Martin bound implies that amplitudes cannot fall faster than $\exp(-\mathfrak{s}\log\mathfrak{s})$ [55, 56]. In the forward scattering limit, when t is fixed, scattering amplitudes are polynomially bounded, having to grow slower than $\mathfrak{s}^2$ [57, 58].

Scale-invariance:
Some quantum field theories, even those who are perturbatively renormalizable, are not expected to hold for infinitely large energies. A prime example is ϕ^4-theory in four dimensions, with the bare Lagrangian given by

$$\mathcal{L}[\phi] = \frac{1}{2}\partial_\mu\phi\partial^\mu\phi - \frac{1}{2}m^2\phi^2 - \frac{1}{4!}\lambda\phi^4 \tag{2.30}$$

where λ is the coupling constant of the ϕ^4-interaction. The theory is perturbatively renormalizable, i.e. the one-loop divergences can be absorbed in the renormalized coupling constant. This leads to

a renormalization group equation

$$\frac{\mathrm{d}\lambda}{\mathrm{d}\log\Lambda^2} = \frac{3\lambda^2}{32\pi^2} + \mathcal{O}(\lambda^3) \tag{2.31}$$

with the UV cut-off scale Λ. The solution to this differential equation introduces a logarithmic term and a reference scale μ

$$\lambda(\Lambda^2) = \frac{\lambda(\mu^2)}{1 - \frac{3}{32\pi^2}\lambda(\mu^2)\log\left(\frac{\Lambda^2}{\mu^2}\right)}. \tag{2.32}$$

The problem that appears in this equation is that the denominator vanishes at a finite UV-scale. This is known as a Landau pole, and appears in theories that are not asymptotically free. The only way to get rid of the Landau pole, is to push the location of the pole to infinity. The only freedom is by taking μ to infinity. Subsequently, the renormalized coupling constant tends to zero. This is known as quantum triviality: an initially interacting theory becomes trivial when we demand that the coupling constant is finite for all energies.

In an asymptotically free theory, the problems of a Landau pole are circumvented because the coupling constants vanish in the UV. Asymptotic safety is a generalization. Coupling constants don't necessarily need to vanish, but they can approach finite values. In both cases, the "running" of the coupling constants stop, meaning that the interacting strength approaches a finite value. Subsequently, observables are automatically guaranteed to be finite and scale invariant, i.e. a momentum-dependent field redefinition does not affect observables in the high-energy limit [59].

It has to be noted that the constraints above can be met outside the framework of quantum field theory. Particularly in string theory, the Veneziano and Shapiro-Virasoro amplitude meet all unitarity and causality demands [60–62]. The underlying mechanism is an infinite tower of massive higher-spin resonances. The goal of the form factor approach is to show that unitarity and causality constraints can also be met in a Lorentzian quantum field theory. There is enough room in the form factor formalism to provide a UV-completion of gravity without introducing the resonances of string theory. As a proof of principle, a model will be introduced in chapter 6, where the form factors assume the form of a carefully chosen analytic function to prove this claim. To realize the asymptotic safety scenario for a non-minimally model of gravity coupled to matter, it is expected that matter self-interactions are crucial [38, 63]. During the analysis of the model, matter self-interactions will indeed prove to be essential to provide a bounded and scale-free scattering amplitude.

CHAPTER 3

Feynman rules from the quantum effective action

In the previous chapter, the theoretical framework for exploring quantum gravity as a QFT has been given. It has always been the goal to see if a quantum effective action can be written down which abides to many of the constraints given in section 2.3. Of the local theories that go beyond first order in the curvature terms, all of them struggle with at least some of the topics in section 2.3. We do not derive a quantum effective action, and in this sense, we do not formulate a QFT which has these nice properties. We rather focus on the apparent freedom of form factors to show that QFT's can produce a physical theory for quantum gravity in the high-energy regime.

As a simplest test case, the scattering process of two scalar particles will be studied, which interact through the emission and absorption of a graviton. Scalar particles are easy to use from a computational point-of-view, as they do not have tensor indices and do not introduce γ-matrices associated to representations of the Clifford algebra. This limits the possible tensor contractions significantly, and makes calculations less tedious. In this regard, photon scattering requires much more work, as the number of independent tensor structures ramp up quickly with the additional tensor indices. Nevertheless, the relevant Feynman rules for scalar scattering requires meticulous bookkeeping skills, which is why the results found in the section have also been verified with the *xAct* programming suite in Mathematica [64].

In this thesis, we shall discuss the scattering of distinguishable and indistinguishable scalar particles. Hence, two flavours of particles, ϕ and χ, are introduced, which can be distinguished by their mass. The first part of this chapter derives the most general quantum effective action compatible with relativistic QFT that can possibly contribute to gravity-mediated scattering of these particles. This will include the Einstein-Hilbert term and a kinetic term for the scalar field, as well as higher order terms such as R^2 and $R\phi\phi$. All of the invariant contractions of the curvature tensors and the scalar fields up to this order will be deduced and each monomial will be dressed with a form factor, such that the momentum dependence of the couplings is squeezed into functions.

In the upcoming section, we will first familiarize ourselves with the graviton. Without doing any hefty calculations, we can already derive some of the important properties, which can be used for the remainder of the chapter. It will be shown that the graviton is a rank-two tensor derived from the full metric. The second part of this chapter is dedicated to the Feynman rules derived from the quantum effective action. The main ingredients for the scattering amplitude are the graviton propagator and the graviton-matter vertex, which will be derived here. The scalar self-interaction will also be given at the end of the chapter.

3.1 Lessons from classical gravity

All forces described by the Standard Model are carried by some mediator. Electromagnetism has the photon, the strong nuclear force has the gluons and the weak nuclear force has the $W^{\pm}$- and Z-bosons. By this logic, it is only natural to expect a force mediator for gravity. This theorized particle is what we call the graviton.

Some simple observations reveal quite a lot about the nature of the graviton. First, we know that the graviton is a massless particle. We know that general relativity produces Newtonian gravity in the semi-classical limit which describes the long-range force of gravity with the inverse power law

$$V(r) = -G_N \frac{m_1 m_2}{r}. \tag{3.1}$$

The potential is similar to that of the classical Coulomb potential, which also has a massless mediator. A massive force carrier would have resulted in a suppression term, such as the exponential damping factor in Yukawa theory.[3]

Next, we can see that the graviton must be a spin-two particle. Any particle with half-integer spin, enters the action as a particle-anti particle pair, which is the reason why fermions are unfit to be force carriers. The graviton also cannot have odd spin. The reason can again be deduced from the gravitational potential. The mass of particles, which take the place of a charge in the potential, is positive. The minus sign tells us that gravity is an attractive force, at least in the classical realm. If the graviton would have spin s, then the sign of the gravitational potential would change as $(-)^{s+1}$. This still leaves the possibility for a spin-zero boson. But this is not feasible, as a scalar particle cannot produce the Einstein equations of motion in a semi-classical limit.

In general relativity, the linearized Einstein's field equations were obtained by perturbing the metric around a flat Minkowski spacetime.

$$g_{\mu\nu} = \eta_{\mu\nu} + h_{\mu\nu} \tag{3.2}$$

Expanding the Einstein field equation up to linear order in the metric perturbation gives (see appendix B)

$$\mathcal{O}_{\mu\nu\rho\sigma} h^{\rho\sigma} = -16\pi G_N T_{\mu\nu}, \tag{3.3}$$

where the differential operator $O_{\mu\nu\rho\sigma}$ is given by

$$\mathcal{O}_{\mu\nu\rho\sigma} = \eta_{\mu\rho}\eta_{\nu\sigma}\partial^2 - \left(\eta_{\nu\sigma}\partial_\mu\partial_\rho + \eta_{\mu\sigma}\partial_\nu\partial_\rho\right) + \eta_{\rho\sigma}\partial_\mu\partial_\nu + \eta_{\mu\nu}\partial_\rho\partial_\sigma - \eta_{\mu\nu}\eta_{\rho\sigma}\partial^2. \tag{3.4}$$

Then, diffeomorphism invariance allows for an suitable gauge choice. In linear gravity, the harmonic gauge condition

$$\mathcal{F}_\nu = \partial^\mu h_{\mu\nu} - \frac{1}{2}\partial_\nu h = 0, \tag{3.5}$$

where $h = \eta^{\mu\nu} h_{\mu\nu}$ is the trace of the metric perturbation, simplifies the equations of motion to an inhomogenous wave equation

$$\partial^2 h_{\mu\nu} = -16\pi G_N \Big(T_{\mu\nu} - \frac{1}{2}\eta_{\mu\nu} T\Big). \tag{3.6}$$

The wave solutions are the gravitational waves of general relativity. In four dimensions, the metric perturbation $h_{\mu\nu}$ has initially sixteen degrees of freedom. Ten of these are fixed by Poincaré symmetry,

[3] Massive gravitons are being studied in the literature, as they affect the low-energy behaviour of gravity [65]. The study of massive gravitons was instigated by the Fierz-Pauli action and later extended to a broader class of theories.

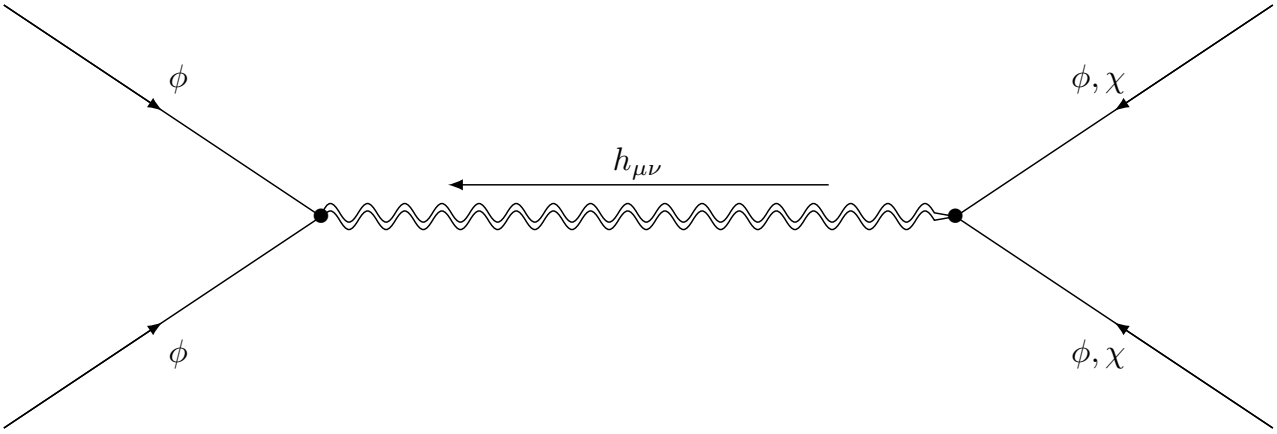

Figure 3.1: *A schematic representation of the diagrams we wish to calculate. The outgoing particles can be either identical or different from the ingoing particles.*

and another four by diffeomorphism invariance. They remaining two give rise to two independent polarization modes.

Much of this discussion extends to a quantized version of gravity. The metric perturbation $h_{\mu\nu}$ is promoted to a quantum field operator and loses its geometrical meaning. In typical QFT-language, this field operator can be represented in terms of creation and annihilation operators, and gravitons are interpreted as excitations of an underlying Fock space with respect to these operators. The two polarizations of the gravitational waves are now the $(++)$ and $(--)$ helicity states of the graviton. The gauge freedom has to be dealt with explicitly in the action with the help of the Faddeev-Popov procedure. This will be studied more closely in section 3.2.2.

3.2 Components of the action

The goal of this thesis is to analyze the scattering amplitudes associated to Feynman diagrams such as figure 3.1, i.e. external scalar particles which interact through a mediated graviton in a flat Minkowski background. The two essential ingredients that need to be derived are the graviton propagator and the graviton-matter vertex. To do this, the quantum effective action is split into two parts. One part contains purely gravitational monomials, which defines the propagator, while the other one contains matter and matter-gravity terms, defining the vertex.

3.2.1 Gravitational sector

The goal of the gravitational monomials is to construct the most general gravitational propagator in a flat Minkowski background. To do this, it is necessary to include all terms in the action which could possible contribute. From the quantum effective action, we know that we only need to consider terms that are at most quadratic in the metric perturbation $h_{\mu\nu}$. Each curvature tensor introduces an extra order of $h_{\mu\nu}$, so only monomials which are at most quadratic in the Riemann tensor or its contractions need to be considered. The curvature tensors exhibit a lot of symmetries in the indices, which reduce the number of unique contributing monomials drastically. A list of internal symmetries and the Bianchi identities can be found in appendix B. Additionally, we can use two more symmetries to reduce the number even further.

1. Covariant derivatives can be swapped freely. This will play a significant role in the R^2 and $R\phi\phi$ sector, where multiple covariant derivative terms can appear, whose indices need not to

be contracted with one another. If two or more covariant derivatives act on a single field, they can all be swapped. Initially, this can only be done if

$$\left[D_\mu, D_\nu\right] = 0 \tag{3.7}$$

This is not the case, because (3.7) is a well-known representation of the Riemann tensor. However, this contributes to higher order structures in the action; R^3 and $R^2\phi\phi$ respectively, which is not of interest to us.

2. The goal of the form factors is to capture the non-trivial momentum dependence of the graviton propagator and vertices. For general building blocks X_i, scalar, vector or tensor, the arguments of the form factors contain all possible combinations of covariant derivatives. This results in a term of the form

$$\int \mathrm{d}^4x\sqrt{-g}\mathrm{X}_1,\dots\mathrm{X}_n\left(\{D_iD_j\}_{i\leq j}\right)X_1,\dots X_n, \tag{3.8}$$

where

$$D_i\big(X_1\dots X_n\big) = X_1\dots D\big(X_i\big)\dots X_n, \tag{3.9}$$

i.e., the index i indicates the building block on which the covariant derivative acts. Switching to momentum space and imposing momentum conservation at each vertex, we are allowed to remove one D_i from the arguments. This gives in total $\frac{1}{2}n(n-1)$ arguments to each form factor. In this work, we will encounter two types of monomials. The first type is of the form X^2. Following the convention of [66], we have

$$\frac{1}{2}\int \mathrm{d}^4x\sqrt{-g}X f_{\mathrm{XX}}(\Delta)X, \tag{3.10}$$

where the canonical factor of $\frac{1}{2}$ is preserved. The second type is of the form XYY. We use the freedom of momentum conservation to remove mixed derivatives D_iD_j, where $i \neq j$, from the form factors. This gives a functions which solely depends on the Laplacian operators.

$$\int \mathrm{d}^4x\sqrt{-g}f_{\mathrm{XYY}}\left(\Delta_1,\Delta_2,\Delta_3\right)XYY. \tag{3.11}$$

In the low energy regime, all observables should comply with general relativity. This fixes the linear term in the action: the Einstein-Hilbert action

$$\Gamma_{\mathrm{EH}} = -\frac{1}{16\pi G_N}\int \mathrm{d}^4x\sqrt{-g}R. \tag{3.12}$$

This is also the only non-trivial contraction of the Riemann curvature tensor, so there really is no other choice in this sector. This is also the single unique monomial that will not be dressed with a form factor. When Laplacians act on the Ricci scalar, the total term is equivalent to a surface term and these do not affect the theory.

Next are the quadratic curvature terms. From the work of Fulling et al. [67], it is known which monomials appear at this order. Keeping track of all index contractions and symmetries, they characterize the maximally reduced set in terms of Young tableaux. At this level, it is still possible to do the calculation by hand and in the following paragraph, we will show that only two quadratic curvature monomials appear.

Let us first consider two curvature tensors, and no covariant derivatives. At this level, two curvature tensors can be contracted in four independent ways

$$\Big\{R^2, \quad R_{\mu\nu}R^{\mu\nu}, \quad R_{\mu\nu\rho\sigma}R^{\mu\nu\rho\sigma}, \quad R_{\mu\rho\nu\sigma}R^{\mu\nu\rho\sigma}\Big\}. \tag{3.13}$$

This list can be generated with the *AllContractions* function of *xAct*, which keeps track of the internal symmetries of the curvature tensors only. Imposing the first Bianchi identity, the third and fourth term are equivalent

$$R_{\mu\rho\nu\sigma}R^{\mu\nu\rho\sigma} = \frac{1}{2}R_{\mu\nu\rho\sigma}R^{\mu\nu\rho\sigma}. \tag{3.14}$$

This reduces the set to three structures, and for a generic spacetime dimension, this is all we can do. In four dimensions, a specific combination of squared curvatures tensors reduces to a topological surface term, the so-called Gauss-Bonnet term

$$\mathcal{GB} = R_{\mu\nu\rho\sigma}R^{\mu\nu\rho\sigma} - 4R_{\mu\nu}R^{\mu\nu} + R^2. \tag{3.15}$$

This term can be written as a total derivative in four dimensions, giving rise to a surface term when integrated over. Such terms do not affect the theory, and can therefore be removed. This constraint will be used to remove the squared Ricci tensor from the basis. As a matter of convention, we can replace the squared Riemann tensor by the squared Weyl tensor by the following relation

$$C_{\mu\nu\rho\sigma}C^{\mu\nu\rho\sigma} = R_{\mu\nu\rho\sigma}R^{\mu\nu\rho\sigma} - 2R_{\mu\nu}R^{\mu\nu} + \frac{1}{3}R^2. \tag{3.16}$$

This reduces the basis to

$$\Big\{R^2, \quad C_{\mu\nu\rho\sigma}C^{\mu\nu\rho\sigma}\Big\}. \tag{3.17}$$

The reason to choose the Weyl tensor over the Riemann tensor is as follows. In linearized gravity, we know that there are two physical degrees of freedom, which correspond to the polarization of a massless spin-two particle. Including the quadratic curvature terms (without form factors), six more degrees of freedom are introduced to the theory [18, 19, 68]. Five of them correspond to a massive spin-two graviton and the sixth corresponds to a massive scalar particle. Choosing the basis (3.17) the degrees of freedom decompose cleanly in the propagator representation. Using the spin projection operators, the massive spin-two degrees of freedom are generated by the squared Weyl tensor, and the massive spin-zero particle comes from the squared Ricci tensor. In section 3.3, we will see explicitly that this also happens when these basis terms are dressed with form factors.

The next step is to see if new terms appear when curvature tensors are contracted with covariant derivatives. This will not be the case. At the next order, two covariant derivatives appear, whose indices need to be contracted with indices of the curvature tensors. Applying the Bianchi identities and the constraints at the start of this section systematically, all contractions either vanish or can be mapped to the form factor contributions

$$\Big\{R\Delta^n R, \quad R_{\mu\nu}\Delta^n R^{\mu\nu}, \quad C_{\mu\nu\rho\sigma}\Delta^n C^{\mu\nu\rho\sigma}\Big\}. \tag{3.18}$$

In [66], it is shown that the $R^{\mu\nu}\Delta^n R_{\mu\nu}$, can be mapped onto the remaining two structures, but again only in four dimensions, as the procedure relies on (3.15). Hence, the gravitational sector is captured in the action

$$\Gamma_{\rm grav} = \frac{1}{16\pi G_N}\int \mathrm{d}^4x\sqrt{-g}\bigg(-R - \frac{1}{6}Rf_{\rm RR}(\Delta)R + \frac{1}{2}C_{\mu\nu\rho\sigma}f_{\rm CC}(\Delta)C^{\mu\nu\rho\sigma}\bigg). \tag{3.19}$$

The normalization factors of the form factors are chosen for convenience and such that positive form factors will not introduce additional poles in the graviton propagator.

3.2.2 Gauge fixing

The kernel of the operator $\mathcal{O}$ in equation 3.3 is given by all fields of the form

$$h_{\mu\nu} = \partial_\mu \xi_\nu + \partial_\nu \xi_\mu. \tag{3.20}$$

Transformations of this kind are infinitesimal coordinate transformations. The existence of the infinite dimensional kernel is due to diffeomorphism invariance of the gravitational action. This can be understood as follows. Define the local transformation

$$x'^\mu = x^\mu + \xi^\mu(x). \tag{3.21}$$

The tensor ξ plays the role of an infinitesimal coordinate transformation. The full metric transforms as [69]

$$\delta g_{\mu\nu} = -D_\mu \xi_\nu - D_\nu \xi_\mu \tag{3.22}$$

In a linear split with a Minkowskian background, we obtain the expression (3.20), up to a minus sign which can be removed by redefining $\xi_\mu \to -\xi_\mu$. The diffeomorphism invariance in general relativity allows for a transformation of $h_{\mu\nu}$ to a special gauge, which simplified the classical equations of motion to the wave equation (3.6). In quantum field theories, gauge symmetries require some attention. Field configurations that are related by a gauge transformation should be marginalized. The way to do this was proposed by Faddeev and Popov, after whom this trick is named. Equivalent field configurations are captured by a gauge fixing function such as (3.5). This thesis uses a generalized linear version, introducing gauge parameters α and β. The gauge-fixing function is then given by

$$\mathcal{F}_\nu = \partial^\mu h_{\mu\nu} - \frac{1+\beta}{4}\partial_\nu h. \tag{3.23}$$

The harmonic gauge, (3.5) corresponds to $\beta = 1$. The generalized gauge fixing functions enters the action in the following way

$$\Gamma_{\text{gf}} = \frac{1}{16\pi G_N}\frac{1}{2\alpha}\int \mathrm{d}^4x\, \mathcal{F}_\mu \mathcal{F}^\mu. \tag{3.24}$$

We now have the ability to analyse a much broader class of gauge fixings. Setting $\alpha = 1$, we get the Feynman gauge, and $\alpha \to 0$ gives us the Landau limit. In this work, we will not fix α and β. Hence, the parameters will appear explicitly in the graviton propagator. But as we will see, contracting the propagator with the vertices remove any gauge dependence from the result. This gives us gauge-independent observables.

As a final remark of this section, we note that in principle, the gauge-fixing term is not enough to regularize the path integral for non-Abelian gauge theories. A second trick is necessary, which introduces ghost-particles to the theory. These are virtual particles and couple only to the graviton. Hence, they cannot contribute to the tree-level amplitudes which we are interested in here, and can therefore be omitted in the present analysis.

3.2.3 Matter sector

From conventional QFT, the action of a free massive scalar particle ϕ, is given by

$$\int \mathrm{d}^4x\sqrt{-g}\left(\frac{1}{2}g^{\mu\nu}D_\mu\phi D_\nu\phi - \frac{1}{2}m^2\phi^2\right). \tag{3.25}$$

This reduces to the Klein-Gordon equation in classical quantum field theories on a Minkowski metric. To implement scalar particles in the form factor program, we dress the action (3.25) with a form factor $f_{\phi\phi}$

$$\Gamma_{\phi\phi} = \int \mathrm{d}^4x\sqrt{-g}\left(\frac{1}{2}\phi f_{\phi\phi}(\Delta)\phi\right). \tag{3.26}$$

The form factor $f_{\phi\phi}$ has to satisfy certain on-shell relations. On a flat spacetime, ϕ satisfies the linearized equations of motion $f_{\phi\phi}(\Box)\phi = 0$, with $\Box = -\partial^2$. It has a unique zero, corresponding to the mass of the particle: $f_{\phi\phi}(m^2) = 0$. Secondly, ϕ is normalized such that it has the canonical kinetic term on-shell: $f'_{\phi\phi}(m^2) = 1$. The diagrams of interest contain only external scalar particles. Imposing the on-shell conditions ensures that no additional $f_{\phi\phi}$ form factors appear in the scattering amplitudes.

For the graviton-matter vertex, we should think of all the ways one curvature tensor can be contracted with two scalar particles. Without any derivatives, the only possible contraction is

$$R\phi\phi. \tag{3.27}$$

Like the quadratic curvature sector, things get a little more tedious at the next level. As soon as covariant derivatives are included, there are additional combinations that appear. With two derivatives, an extra monomial is necessary to accommodate for all contractions. Again with the help of *xAct*, we have the non-minimal set

$$\Big\{D_\mu D_\nu R^{\mu\nu}\phi\phi\,,\quad RD_\mu\phi D^\mu\phi,\quad R^{\mu\nu}D_\mu\phi D_\nu\phi\,,\quad R^{\mu\nu}\phi D_\mu D_\nu\phi\Big\}. \tag{3.28}$$

The first structure is proportional to $(\Delta R)\phi\phi$ by the contracted Bianchi identity. The second monomial can be mapped to $R(\Delta\phi)\phi$. These two structures are generated by a form factor acting on $R\phi\phi$. The remaining two structures are equivalent by partial integration, although they cannot be mapped back to the $R\phi\phi$. Hence the dressed $R^{\mu\nu}D_\mu\phi D_\nu\phi$ is added to the gravity-matter action.

No new terms appear at four derivatives. In principle, there could be a contribution from terms if the Riemann tensor has all indices contracted with covariant derivatives. All other contributions can automatically be mapped to form factor contributions. Two things can happen, which depends on how the derivatives are distributed among the Riemann tensor and the two scalar fields. The derivatives may be distributed in such a way that they form a commutator once the internal symmetries of the Riemann tensor are used. This generates a term which either vanishes or is quadratic in the curvature. Both structures do not contribute to the $h\phi\phi$-vertex in a flat background. Thus, we are left with the most general gravity-matter action

$$\begin{aligned}\Gamma_{\text{matter}} = \int \mathrm{d}^4x\sqrt{-g}\Big(&\phi f_{\phi\phi}(\Delta)\phi \\ &+ f_{\mathrm{R}\phi\phi}(\Delta_1,\Delta_2,\Delta_3)R\phi\phi + f_{\mathrm{Ric}\phi\phi}(\Delta_1,\Delta_2,\Delta_3)R^{\mu\nu}D_\mu\phi D_\nu\phi\Big).\end{aligned} \tag{3.29}$$

The contribution of the χ-particle to the action is identical (simply replace the labels $\phi \to \chi$), which means that the same on-shell conditions apply to $f_{\chi\chi}$ when m_ϕ^2 is swapped for m_χ^2. Also, preserving $\mathbb{Z}_2$ symmetry of the scalar fields excludes a $h\phi\chi$ vertex.

In total, the quantum effective action that contributes to the Feynman diagram, figure 3.1, that we will use in this work is given by

$$\Gamma_{\text{grav}} + \Gamma_{\text{gf}} + \Gamma_{\text{matter}}. \tag{3.30}$$

The graviton-matter vertices are then derived from Γ_{matter} and the graviton propagator from Γ_{grav} and Γ_{gf}, which will be the scope of the upcoming sections.

3.3 The graviton propagator

The part of the action that generates the graviton propagator is given by

$$\Gamma_{\text{grav}} + \Gamma_{\text{gf}} = \frac{1}{16\pi G_N}\Bigg[\int \mathrm{d}^4x\sqrt{-g}\Big(-R - \frac{1}{6}Rf_{\text{RR}}(\Delta)R + \frac{1}{2}C_{\mu\nu\rho\sigma}f_{\text{CC}}(\Delta)C^{\mu\nu\rho\sigma}\Big) + \frac{1}{2\alpha}\int \mathrm{d}^4x\,\mathcal{F}_\mu\mathcal{F}^\mu\Bigg]. \tag{3.31}$$

With the mathematical framework we set up in chapter 2, calculating the propagator is now a straightforward calculation. The calculation is however prone to errors due to the large number of tensors that appear in the intermediate steps. This is why the results have been verified with the *xAct* programming suite in Mathematica [64, 70]. A complete derivation of the graviton propagator can be found in appendices C and D. In appendix C, the action is expanded up to quadratic order in the metric perturbation, followed by taking variational derivatives with respect to h. The symmetry in the indices of h transfers to this object, and in the end also to the propagator, meaning that

$$\frac{\delta^2\big(\Gamma_{\text{grav}} + \Gamma_{\text{gf}}\big)}{\delta h^{\mu\nu}\delta h^{\rho\sigma}} \tag{3.32}$$

is symmetric in the indices $\{\mu\nu\}$ and $\{\rho\sigma\}$.

We can now think of all linearly independent ways to construct a rank-four tensor out of the background metric and momentum tensors, maintaining the symmetry. This is the basis which was chosen in [43]. Although the result is completely equivalent, we can also think of other bases. In appendix D, we introduce the spin-projection operators which allows us to decompose any symmetric two-tensor onto irreducible representations of $SO(3)$. We can therefore analyse the spin components that constitute the graviton propagator. The final result is given in equation (D.16), which I will reiterate here

$$\begin{aligned} D^{\mu\nu\rho\sigma}(q^2) = 16\pi G_N\Bigg(&2G_{\text{CC}}(q^2)\mathcal{P}_2^{\mu\nu\rho\sigma} + \frac{2\alpha}{q^2}\mathcal{P}_1^{\mu\nu\rho\sigma} - G_{\text{RR}}(q^2)\mathcal{P}_{0,\text{s}}^{\mu\nu\rho\sigma} \\ &+ \left[\frac{16\alpha}{(\beta-3)^2}\frac{1}{q^2} - 3\Big(\frac{\beta+1}{\beta-3}\Big)^2 G_{\text{RR}}(q^2)\right]\mathcal{P}_{0,\text{w}}^{\mu\nu\rho\sigma} \\ &+ \sqrt{3}\frac{\beta+1}{\beta-3}G_{\text{RR}}(q^2)\big(\mathcal{P}_{0,\text{sw}}^{\mu\nu\rho\sigma} + \mathcal{P}_{0,\text{ws}}^{\mu\nu\rho\sigma}\big)\Bigg), \end{aligned} \tag{3.33}$$

where

$$G_{\text{XX}}(q^2) = \frac{1}{q^2\big(1 + q^2 f_{\text{XX}}(q^2)\big)}. \tag{3.34}$$

Some of the coefficients have a singularity at $\beta = 3$. This choice of β is related to an incomplete gauge fixing. The gauge fixing operator works as a projection operator for this particular choice [71].

The only components of the propagator that are independent of the gauge parameters are the spin-two and the spin-zero singlets. All other contributions are unphysical, and can be removed by a convenient choice of gauge parameters. This also happens at the level of the Einstein-Hilbert action [35], so indeed the form factors do not introduce new physical sectors of the graviton. We also see that the inclusion of form factors alter the pole behaviour of the propagator in these sectors

$$G_{\text{XX}}(q^2) = \frac{1}{q^2} - \frac{1}{q^2 + f_{\text{XX}}^{-1}(q^2)}. \tag{3.35}$$

For constant form factors, this indicates a massive ghost particle or a tachyon sitting in the spin-zero or spin-two part of the graviton, depending on the sign. We will see this in more detail when we analyse Stelle gravity in chapter 5. Having momentum dependence in the form factors gives us full control over these particles. We will exploit this freedom to produce form factors which do not introduce any new massive degrees of freedom.

3.4 The graviton-matter vertex

The matter action 3.29,

$$\Gamma_{\text{matter}} = \int \mathrm{d}^4x\sqrt{-g}\Big(\phi f_{\phi\phi}(\Delta)\phi + f_{\mathrm{R}\phi\phi}(\Delta_1,\Delta_2,\Delta_3)R\phi\phi + f_{\mathrm{Ric}\phi\phi}(\Delta_1,\Delta_2,\Delta_3)R^{\mu\nu}D_\mu\phi D_\nu\phi\Big), \tag{3.36}$$

has already been used in a previous article to calculate the $h\phi\phi$-vertex [66]. The derivation of the vertex is slightly more involved. To derive the contribution of the $f_{\phi\phi}$ form factors to the $h\phi\phi$-vertex, it is necessary to expand the Laplacian operator Δ and the metric determinant $\sqrt{-g}$ up to first order in h. Then, taking variations with respect to the respective fields give the graviton-matter vertex. In appendix C, the complete derivation is given, following the conventions of [66]. The graviton-matter vertex is finally given by

$$\begin{aligned}\mathcal{V}^{\mu\nu}_{h\phi\phi}(q,p_{\phi_1},p_{\phi_2}) = {}& \frac{1}{4}\eta^{\mu\nu}f_{\phi\phi}(p^2_{\phi_1}) \\ & - \frac{1}{2}\frac{f_{\phi\phi}(p^2_{\phi_1}) - f_{\phi\phi}(p^2_{\phi_2})}{p^2_{\phi_1}-p^2_{\phi_2}}\Big(p^\mu_{\phi_1}p^\nu_{\phi_1} - \frac{1}{2}\eta^{\mu\nu}q\cdot p_{\phi_1} + \frac{1}{2}\Big(q^\mu p^\nu_{\phi_1} + q^\nu p^\mu_{\phi_1}\Big)\Big) \\ & + f_{\mathrm{R}\phi\phi}(q^2,p^2_{\phi_1},p^2_{\phi_2})\Big(q^2\eta^{\mu\nu} - q^\mu q^\nu\Big) \\ & - \frac{1}{2}f_{\mathrm{Ric}\phi\phi}(q^2,p^2_{\phi_1},p^2_{\phi_2})\Big(\frac{1}{2}\Big(q^2+p^2_{\phi_1}-p^2_{\phi_2}\Big)\Big(q^\mu p^\nu_{\phi_1}+q^\nu p^\mu_{\phi_1}\Big) + \\ & \qquad \frac{1}{4}\Big(q^2+p^2_{\phi_1}-p^2_{\phi_2}\Big)\eta^{\mu\nu} + q^2 p^\mu_{\phi_1}p^\nu_{\phi_1}\Big) \\ & + (p_{\phi_1}\leftrightarrow p_{\phi_2}).\end{aligned} \tag{3.37}$$

The graviton-matter vertex satisfies the following tranversality condition

$$q_\mu\mathcal{V}^{\mu\nu}_{h\phi\phi}(q,p_{\phi_1},p_{\phi_2}) = 0, \tag{3.38}$$

which only holds when the expression is evaluated on-shell and such that momentum conservation is imposed, i.e. $q = p_{\phi_1} + p_{\phi_2}$.

The $h\chi\chi$-vertex is completely similar, after replacing all the labels $\phi \to \chi$. In this notation, q is the momentum of the internal graviton, and p_{ϕ_1} and p_{ϕ_2} are the momenta of the external scalar particles. The on-shell conditions for $f_{\phi\phi}$ guarantee that the vertex is finite for all external momenta.

3.5 The scalar self-interactions

It has been known for a while that pure gravity is one-loop renormalizable, but gravity coupled to matter is not. The presence of scalar matter generates UV-divergences which necessitate a counter term in the action of the form [6, 38, 72]

$$\Gamma_{\text{self}} \simeq \int \mathrm{d}^4x\sqrt{-g}\,(D^\mu\phi D_\mu\phi)^2\,. \tag{3.39}$$

A self interaction of this form is currently not present in our theory, but it will play the crucial role to obtain a finite amplitude at all scales. This contribution is slightly different for $\phi\phi \to \phi\phi$ and $\phi\phi \to \chi\chi$. We include a ϕ^4 and $\phi^2\chi^2$ term in the action, and dress it with a form factor. Momentum conservation lets us remove four arguments, so we choose to remove the Laplace operators. The self interactions generate only the two-scalar-to-two-scalar vertex, which means we only consider the expansion up to zeroth order

$$\Gamma_{\phi\phi\chi\chi} = \frac{1}{4}\int \mathrm{d}^4x f_{\phi\phi\chi\chi}\left(-\partial_1\cdot\partial_2, -\partial_1\cdot\partial_3, -\partial_1\cdot\partial_4, -\partial_2\cdot\partial_3, -\partial_2\cdot\partial_4, -\partial_3\cdot\partial_4\right)\phi^2\chi^2, \tag{3.40}$$

$$\Gamma_{\phi\phi\phi\phi} = \frac{1}{4!}\int \mathrm{d}^4x f_{\phi\phi\phi\phi}\left(-\partial_1\cdot\partial_2, -\partial_1\cdot\partial_3, -\partial_1\cdot\partial_4, -\partial_2\cdot\partial_3, -\partial_2\cdot\partial_4, -\partial_3\cdot\partial_4\right)\phi^4. \tag{3.41}$$

Switching to momentum space, and taking variational derivatives, gives us the Feynman rules associated to the four-point interactions

$$\mathcal{V}_4^{\phi\phi\chi\chi} = f_{\phi\phi\chi\chi}\left(p_1\cdot p_2,\ p_1\cdot p_3,\ p_1\cdot p_4,\ p_2\cdot p_3,\ p_2\cdot p_4,\ p_3\cdot p_4\right), \tag{3.42}$$

$$\mathcal{V}_4^{\phi\phi\phi\phi} = f_{\phi\phi\phi\phi}\left(p_1\cdot p_2,\ p_1\cdot p_3,\ p_1\cdot p_4,\ p_2\cdot p_3,\ p_2\cdot p_4,\ p_3\cdot p_4\right). \tag{3.43}$$

Due to the symmetry of identical particles, we impose that $f_{\phi\phi\chi\chi}$ is symmetric upon interchanging $\{1,2\}$ and $\{3,4\}$ while $f_{\phi\phi\phi\phi}$ is symmetric in all its arguments.

In the upcoming chapter, the Feynman rules derived here will be used to construct scattering amplitudes, associated to Feynman diagrams such as figure 3.1. The essential ingredients are the graviton propagator, equation (3.33), and the graviton-matter vertex, equation (3.37). In the final chapter, the self-interactions, equations (3.42) and (3.43), will come into play.

CHAPTER 4

The most general amplitude

Now all the components for the scattering amplitudes have been calculated. In this chapter, the Feynman rules are used to calculate the scattering amplitudes of two processes. One of these considers scattering of identical particles $\phi\phi \to \phi\phi$. The other one with different incoming and outgoing particles $\phi\phi \to \chi\chi$. The latter scattering requires only one single amplitude to be calculated due to this symmetry. In terms of the Mandelstam variables (see appendix A), this is the $\mathfrak{s}$-channel diagram, where $\mathfrak{s}$ is the square of the centre-of-mass energy. The former scattering process of identical particles also permits a $\mathfrak{t}$- and $\mathfrak{u}$-channel diagram. These diagrams can now simply be obtained by crossing symmetry and relabelling the scalar mass. The contribution of the four-point interaction will also be calculated, although it will not be of primary interest until later. In the remainder of this chapter, the scattering amplitudes will be decomposed into partial wave amplitudes, and the cross section of both interactions will be calculated.

4.1 The scattering amplitude

Labelling the incoming particles with momenta p_1, p_2, and outgoing particles with p_3, p_4, we are interested in S-matrix elements of the form

$$\langle p_3, p_4 | \, \widehat{S} \, | p_1, p_2 \rangle \, . \tag{4.1}$$

In this notation $|p_i, p_j\rangle$ resembles a two particle momentum-state of scalar particles. Splitting $\widehat{S} = \widehat{\mathbb{1}} + i\widehat{T}$ distinguishes between the non-interacting part, $\widehat{\mathbb{1}}$ where no scattering happens, and an interacting part $\widehat{T}$. It is the interacting part that is of interest in quantum field theory. This is where the strength of the Feynman diagrams come into play. In momentum space, we know that [47]

$$\langle p_3, p_4 | \, i\widehat{T} \, | p_1, p_2 \rangle = (2\pi)^4 i\delta^{(4)} \left(\sum p_i \right) \mathcal{A} \left(p_1, p_2 \to p_3, p_4 \right) \tag{4.2}$$

The amplitude $\mathcal{A}$ includes the information of all scattering channels allowed by the theory. If the Feynman rules are known, that is, how to translate from diagrams to formulae and vice versa, then calculating tree-level scattering amplitudes is straightforward.

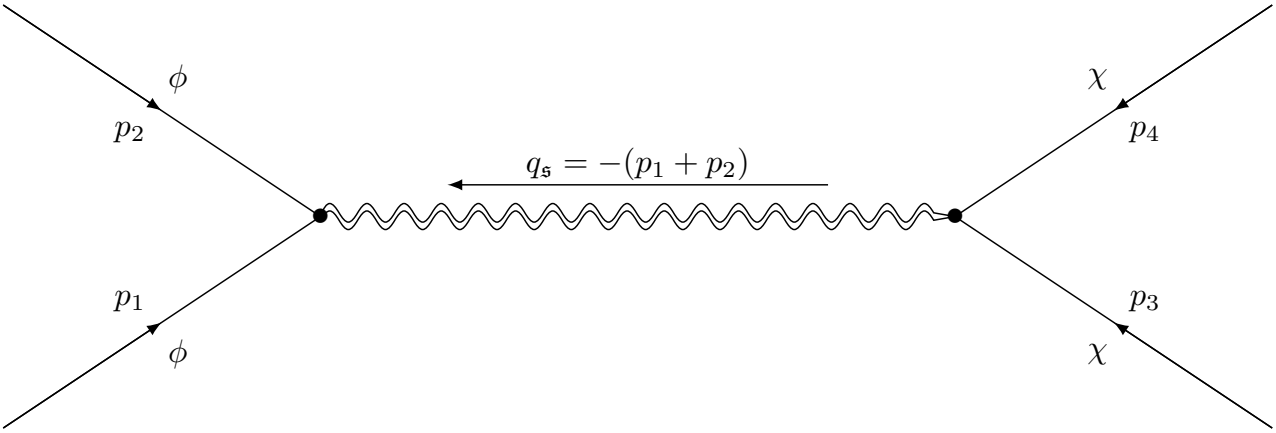

Figure 4.1: *The Feynman diagram underlying $\phi\phi \to \chi\chi$ scattering.*

$\underline{\phi\phi \to \chi\chi}$:
The first and hardest part is the calculation the scattering amplitude of $\phi\phi \to \chi\chi$. This segment produces all the physics necessary for $\phi\phi \to \phi\phi$ as well as all other related scattering amplitudes. $\widehat{S}$ encodes all the information how the initial state can propagate to the final state. Here, the only diagram contributing to the amplitude is the one shown in figure 4.1. The straight lines denote scalar particles ϕ or χ. The double wiggly line denotes the graviton. By convention, all momenta are incoming. The amplitude of this diagram $\langle p_3, p_4 | \, i\widehat{T} \, | p_1, p_2 \rangle$ is in momentum space given by

$$\begin{aligned} \langle p_3, p_4 | \, i\widehat{T} \, | p_1, p_2 \rangle &= \int \frac{\mathrm{d}^4 q}{(2\pi)^4} (2\pi)^4 \delta^{(4)}(p_1 + p_2 + q)(2\pi)^4 \delta^{(4)}(-q + p_3 + p_4) i\mathcal{A}\big(p_1, p_2, p_3, p_4; q\big) \\ &= (2\pi)^4 \delta^{(4)}\left(\sum p_i\right) i\mathcal{A}^{\phi\phi\chi\chi}\big(p_1, p_2, p_3, p_4; -(p_1 + p_2)\big) \end{aligned} \tag{4.3}$$

Momentum conservation is imposed at each vertex, and the internal graviton momentum q is integrated over. The remainder $\mathcal{A}^{\phi\phi\chi\chi}$ includes the vertices and propagator of the diagram. For a tree-level diagrams such as figure 4.1, this consists of contracting two scalar-matter vertices with the internal graviton propagator in the following way.

$$i\mathcal{A}_{\mathfrak{s}}^{\phi\phi\chi\chi}(p_1, p_2, p_3, p_4; q) = \mathcal{V}^{\mu\nu}_{h\phi\phi}(q, p_1, p_2) D_{\mu\nu\rho\sigma}(q) \mathcal{V}^{\rho\sigma}_{h\chi\chi}(-q, p_3, p_4). \tag{4.4}$$

Momentum conservation fixes the internal graviton momentum. This gives the scattering amplitude as a function of three variables. A convenient choice are the Mandelstam variables $\mathfrak{s}, \mathfrak{t}$ and $\mathfrak{u}$. Scattering is done in the centre-of-mass frame, and the scattering amplitude is written as a function of the combinations $p_1 + p_j$, with $j = 2, 3, 4$. The Mandelstam variables are defined in this way. For a thorough definition of the kinematics used here, I refer to appendix A. The appeal of the Mandelstam variables is that each tree-level diagram is characterized by the internal momentum. For instance, the amplitude associated to figure 4.1 has $q = -(p_1 + p_2)$, which is why it is called the $\mathfrak{s}$-channel diagram.

Using the Mandelstam variables and the spin-projection decomposition of the propagator, equation (4.4) simplifies once again. Contracting spin projectors with the two graviton-matter vertices, and evaluating the external scalar particles on-shell shows that only $\mathcal{P}_2$ and $\mathcal{P}_{0,\mathrm{s}}$ survive. Using the

propagator and vertex derived in sections 3.3 and 3.4 respectively, the result is

$$\begin{aligned}\mathcal{V}^{\mu\nu}_{h\phi\phi}\left(\mathcal{P}_2\right)_{\mu\nu\rho\sigma}\mathcal{V}^{\rho\sigma}_{h\chi\chi} &= -\frac{1}{24}\Big(1+\mathfrak{s}f_{\mathrm{Ric}\phi\phi}(\mathfrak{s},m_\phi^2,m_\phi^2)\Big)\Big(1+\mathfrak{s}f_{\mathrm{Ric}\chi\chi}(\mathfrak{s},m_\chi^2,m_\chi^2)\Big)\\ &\quad\times\Big(\mathfrak{t}^2-4\mathfrak{t}\mathfrak{u}+\mathfrak{u}^2+2\left(m_\phi^2-m_\chi^2\right)^2\Big) \qquad (4.5)\\ \mathcal{V}^{\mu\nu}_{h\phi\phi}\left(\mathcal{P}_{0,\mathrm{s}}\right)_{\mu\nu\rho\sigma}\mathcal{V}^{\rho\sigma}_{h\chi\chi} &= -\frac{1}{12}\Big(\left(\mathfrak{s}+2m_\phi^2\right)\left(1+\mathfrak{s}f_{\mathrm{Ric}\phi\phi}(\mathfrak{s},m_\phi^2,m_\phi^2)\right)-12\mathfrak{s}f_{\mathrm{R}\phi\phi}(\mathfrak{s},m_\phi^2,m_\phi^2)\Big)\\ &\quad\times\Big(\left(\mathfrak{s}+2m_\chi^2\right)\left(1+\mathfrak{s}f_{\mathrm{Ric}\chi\chi}(\mathfrak{s},m_\chi^2,m_\chi^2)\right)-12\mathfrak{s}f_{\mathrm{R}\chi\chi}(\mathfrak{s},m_\chi^2,m_\chi^2)\Big). \qquad (4.6)\end{aligned}$$

Contractions involving the other projection tensors vanish, but only after the on-shell conditions are imposed. It was not important to fix the gauge parameters α and β at the start of the calculation. Contracting the gauge-dependent propagator with the vertices and the on-shell conditions guarantee that the propagator is projected on its gauge-invariant parts. This means that the scattering amplitude is manifestly gauge invariant, as it ought to be. A deeper understanding is given in [73]. In linearized gravity, the equations of motion relate the metric perturbation $h_{\mu\nu}$ to the energy-momentum tensor $T_{\mu\nu}$. Splitting the metric perturbation $h_{\mu\nu}$ as a superposition of fields with spin zero, one and two, it can be shown that the spin-one part does not depend on $T_{\mu\nu}$. It satisfies a homogeneous differential equation, and is completely fixed by its initial conditions. The underlying reason is the transversal graviton-matter vertex, cf. equation (3.38). $\mathcal{P}_2$ and $\mathcal{P}_{0,\mathrm{s}}$ are the only two structures which contain metric tensors besides momentum tensors. Accounting for the coefficients of the graviton propagator in equation (3.33) gives us the full-fledged amplitude

$$\mathcal{A}_{\mathfrak{s}}^{\phi\phi\chi\chi}(\mathfrak{s},\mathfrak{t},\mathfrak{u})\equiv 16\pi G_N\mathcal{V}^{\mu\nu}_{h\phi\phi}\Big(2G_{\mathrm{CC}}(s)\left(\mathcal{P}_2\right)_{\mu\nu\rho\sigma}-G_{\mathrm{RR}}(s)\left(\mathcal{P}_{0,\mathrm{s}}\right)_{\mu\nu\rho\sigma}\Big)\mathcal{V}^{\rho\sigma}_{h\chi\chi}. \qquad (4.7)$$

Using equations (4.5) and (4.6), this can be written in its expanded form

$$\begin{aligned}\mathcal{A}_{\mathfrak{s}}^{\phi\phi\chi\chi}(\mathfrak{s},\mathfrak{t},\mathfrak{u}) = \frac{4\pi G_N}{3}\Bigg[&-\Big(1+\mathfrak{s}f_{\mathrm{Ricc}\phi\phi}(\mathfrak{s},m_\phi^2,m_\phi^2)\Big)\Big(1+\mathfrak{s}f_{\mathrm{Ricc}\chi\chi}(\mathfrak{s},m_\chi^2,m_\chi^2)\Big)\\ &\times\Big(\mathfrak{t}^2-4\mathfrak{t}\mathfrak{u}+\mathfrak{u}^2+2\left(m_\phi^2-m_\chi^2\right)^2\Big)G_{\mathrm{CC}}(\mathfrak{s})\\ &+\Big(\left(\mathfrak{s}+2m_\phi^2\right)\left(1+\mathfrak{s}f_{\mathrm{Ric}\phi\phi}(\mathfrak{s},m_\phi^2,m_\phi^2)\right)-12\mathfrak{s}f_{\mathrm{R}\phi\phi}(\mathfrak{s},m_\phi^2,m_\phi^2)\Big)\\ &\times\Big(\left(\mathfrak{s}+2m_\chi^2\right)\left(1+\mathfrak{s}f_{\mathrm{Ric}\chi\chi}(\mathfrak{s},m_\chi^2,m_\chi^2)\right)-12\mathfrak{s}f_{\mathrm{R}\chi\chi}(\mathfrak{s},m_\chi^2,m_\chi^2)\Big)G_{\mathrm{RR}}(\mathfrak{s})\Bigg]. \qquad (4.8)\end{aligned}$$

This result finalizes the calculation we set out to do at the start and is one of the most important results of this thesis. Related amplitudes can be deduced from this result from symmetry arguments. For instance, the $\phi\chi\to\phi\chi$ scattering also contains one tree-level diagram. The internal momentum in this case is given by the Mandelstam variable $\mathfrak{t}$, while the remainder of the calculation of the diagram is completely analogous to $\mathcal{A}_{\mathfrak{s}}^{\phi\phi\chi\chi}$. Crossing symmetry tells us that $\mathcal{A}_{\mathfrak{t}}^{\phi\chi\phi\chi}$ can be obtained by replacing $\mathfrak{s}\leftrightarrow\mathfrak{t}$.

Let us discuss the properties of (4.8) in detail. The scattering amplitude is invariant under momentum-dependent field redefinitions. Introducing the wave function renormalization tensor[4] $\sqrt{Z(q^2)}$ to transform

$$h_{\mu\nu}\mapsto\left(\sqrt{Z(q^2)}\right)_{\mu\nu}^{\ \ \rho\sigma}h_{\rho\sigma}, \qquad (4.9)$$

[4] In gravity, the wave function renormalization can be a tensor mapping a $(0,2)$-tensor to a $(0,2)$-tensor, including appropriate symmetries.

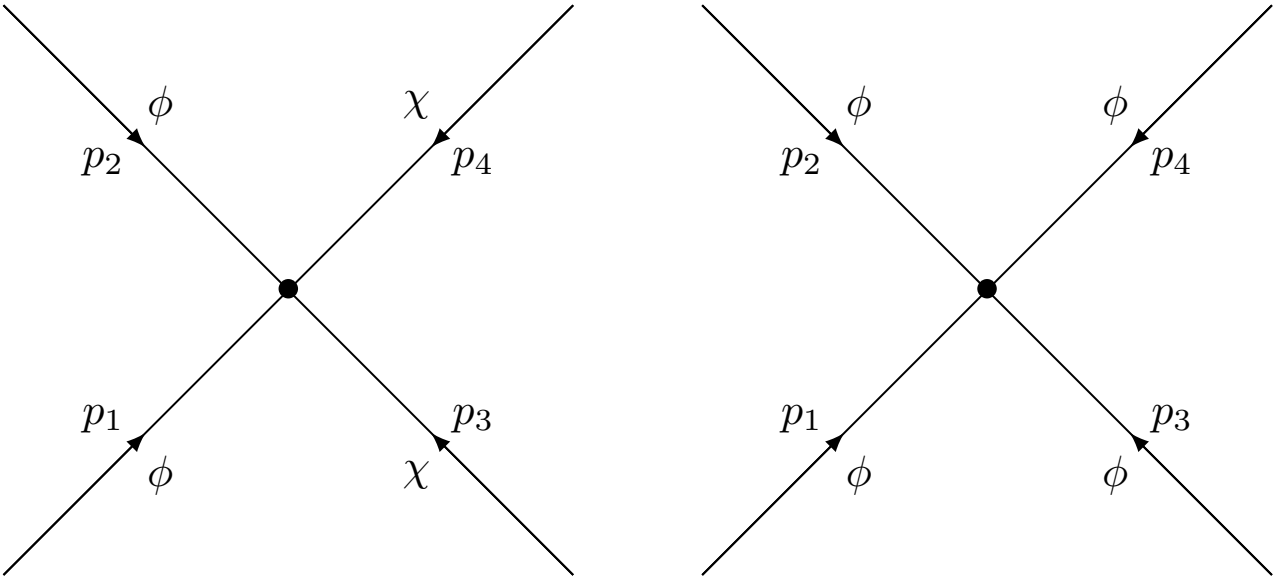

(a) *Self interaction of the $\phi\phi \to \chi\chi$ scattering. It is symmetric under $p_1 \leftrightarrow p_2$ and $p_3 \leftrightarrow p_4$.*

(b) *Self interaction of the $\phi\phi \to \phi\phi$ scattering. It is symmetric in all momenta.*

Figure 4.2: *Self interaction of the $\phi\phi \to \chi\chi$ scattering (left) and $\phi\phi \to \phi\phi$ scattering (right).*

does not affect the amplitude. The graviton propagator picks up a factor of $Z(\mathfrak{s})^{-1}$, which is cancelled by the $\sqrt{Z(\mathfrak{s})}$ terms appearing in the vertices. Secondly, the form factors $f_{\phi\phi}$ and $f_{\chi\chi}$ are absent in the amplitude. The reason is the presence of only external scalar particles which are evaluated on-shell. The on-shell conditions imposed on these form factors remove them from the amplitude. If a diagram contains internal scalar particles, these form factors would appear.

Equation (4.8) does not include the scalar self-interaction, whose Feynman diagram is given by figure 4.2a. This contribution to the amplitude is given by (3.42) evaluated on-shell

$$\mathcal{A}_4^{\phi\phi\chi\chi} = f_{\phi\phi\chi\chi}\left(\tfrac{\mathfrak{s}-2m_\phi^2}{2}, \tfrac{\mathfrak{t}-m_\phi^2-m_\chi^2}{2}, \tfrac{\mathfrak{u}-m_\phi^2-m_\chi^2}{2}, \tfrac{\mathfrak{u}-m_\phi^2-m_\chi^2}{2}, \tfrac{\mathfrak{t}-m_\phi^2-m_\chi^2}{2}, \tfrac{\mathfrak{s}-2m_\chi^2}{2}\right). \tag{4.10}$$

In total, the amplitude for the $\phi\phi \to \chi\chi$ is given by $\mathcal{A}_\mathfrak{s}^{\phi\phi\chi\chi} + \mathcal{A}_4^{\phi\phi\chi\chi}$, which finalizes the discussion of the $\phi\phi \to \chi\chi$ scattering amplitude calculation.

$\underline{\phi\phi \to \phi\phi}$:
Next, the focus shifts to the scattering of identical particles. Due to the symmetry, there are now three diagrams contributing to the total amplitude. These are given in figure 4.3. Having already calculated the amplitude (4.8) makes the calculation of the amplitudes easy. For the $\mathfrak{s}$-channel diagram $\mathcal{A}_s^{\phi\phi\phi\phi}$, the labels χ are replaced with ϕ in (4.8), yielding

$$\begin{aligned}\mathcal{A}_\mathfrak{s}^{\phi\phi\phi\phi}(\mathfrak{s},\mathfrak{t},\mathfrak{u}) = \frac{4\pi G_N}{3}\Bigg[&-\Big(1+\mathfrak{s}f_{\mathrm{Ric}\phi\phi}(\mathfrak{s},m_\phi^2,m_\phi^2)\Big)^2\Big(\mathfrak{t}^2-4\mathfrak{t}\mathfrak{u}+\mathfrak{u}^2\Big)G_{\mathrm{CC}}(\mathfrak{s}) \\ &+\Big(\big(\mathfrak{s}+2m_\phi^2\big)\big(1+\mathfrak{s}f_{\mathrm{Ric}\phi\phi}(\mathfrak{s},m_\phi^2,m_\phi^2)-12\mathfrak{s}f_{\mathrm{R}\phi\phi}(\mathfrak{s},m_\phi^2,m_\phi^2)\big)\Big)^2 G_{\mathrm{RR}}(\mathfrak{s})\Bigg].\end{aligned} \tag{4.11}$$

The amplitudes of the $\mathfrak{t}$- and $\mathfrak{u}$-channel are obtained by applying crossing symmetry to (4.11); replacing $\mathfrak{s}$ with $\mathfrak{t}$ and $\mathfrak{u}$ respectively.

$$\mathcal{A}_\mathfrak{t}^{\phi\phi\phi\phi}(\mathfrak{s},\mathfrak{t},\mathfrak{u}) = \mathcal{A}_\mathfrak{s}^{\phi\phi\phi\phi}(\mathfrak{t},\mathfrak{s},\mathfrak{u}), \qquad \mathcal{A}_\mathfrak{u}^{\phi\phi\phi\phi}(\mathfrak{s},\mathfrak{t},\mathfrak{u}) = \mathcal{A}_\mathfrak{s}^{\phi\phi\phi\phi}(\mathfrak{u},\mathfrak{t},\mathfrak{s}). \tag{4.12}$$

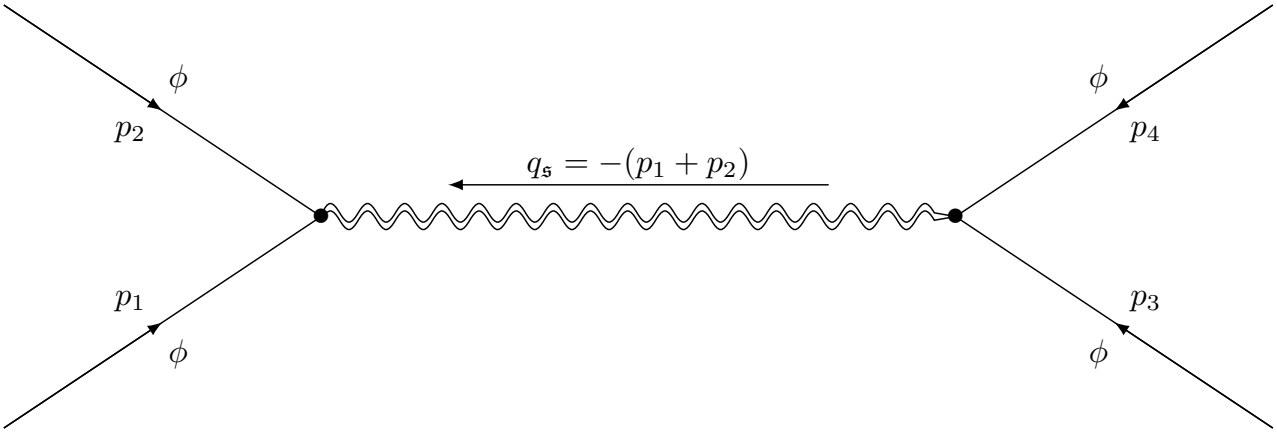

(a) $\mathfrak{s}$-*channel diagram.*

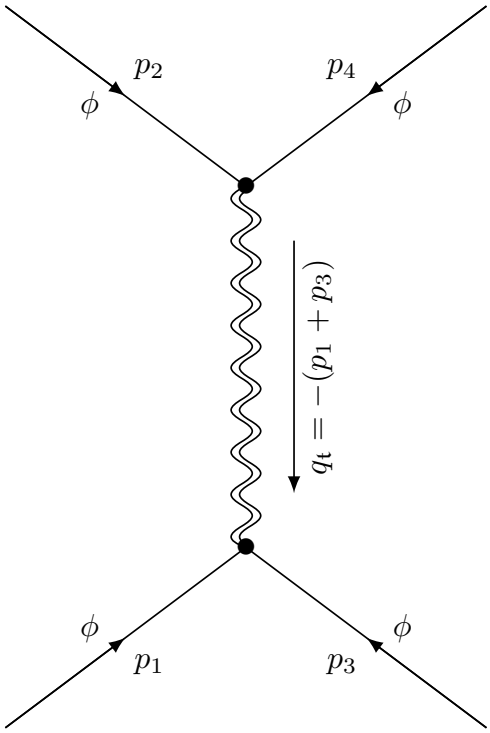

(b) $\mathfrak{t}$-*channel diagram.*

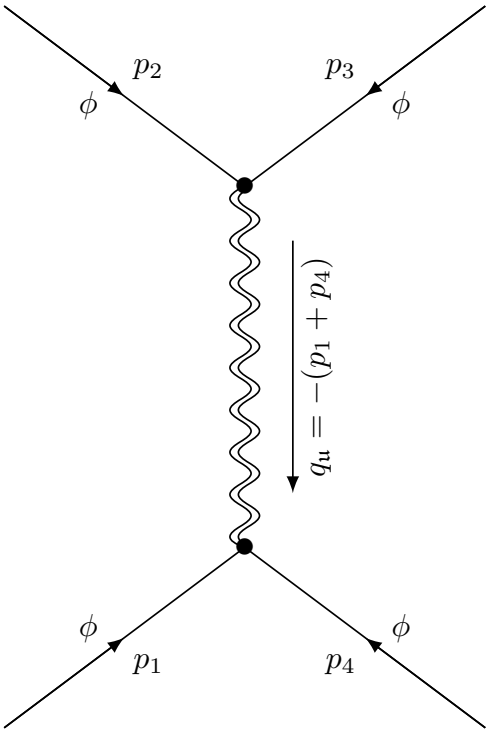

(c) $\mathfrak{u}$-*channel diagram.*

Figure 4.3: *The Feynman diagrams associated with the $\phi\phi \to \phi\phi$ scattering process. For indistinguishable particles, there are three channels, characterized by the momentum carried by the graviton. In terms of the Mandelstam variables, these are the $\mathfrak{s}$-, $\mathfrak{t}$- and $\mathfrak{u}$-channel diagrams respectively.*

The self-interaction is given by evaluating (3.43) on the mass shell and replacing the momenta by the Mandelstam variables

$$\mathcal{A}_4^{\phi\phi\phi\phi} = f_{\phi\phi\phi\phi}\left(\tfrac{\mathfrak{s}-2m_\phi^2}{2}, \tfrac{\mathfrak{t}-2m_\phi^2}{2}, \tfrac{\mathfrak{u}-2m_\phi^2}{2}, \tfrac{\mathfrak{u}-2m_\phi^2}{2}, \tfrac{\mathfrak{t}-2m_\phi^2}{2}, \tfrac{\mathfrak{s}-2m_\phi^2}{2}\right). \tag{4.13}$$

The total amplitude for $\phi\phi \to \phi\phi$ scattering is given by $\mathcal{A}_\mathfrak{s}^{\phi\phi\phi\phi} + \mathcal{A}_\mathfrak{t}^{\phi\phi\phi\phi} + \mathcal{A}_\mathfrak{u}^{\phi\phi\phi\phi} + \mathcal{A}_4^{\phi\phi\phi\phi}$.

4.2 Partial wave decomposition

An often used technique in the analysis of scattering amplitudes is to use a partial wave decomposition to study individual angular momentum components of the amplitude. In two-to-two scattering, the amplitude has rotational symmetry, such that it does not depend on the azimuthal scattering angle ϕ. Therefore, the scattering amplitude can be characterized by two variables, the centre-of-mass energy $\mathfrak{s}$ and the scattering angle θ. In classical quantum mechanics, this symmetry is used to decompose the amplitude into partial waves characterized by their angular momentum. This method also lends itself to any other system exhibiting rotational symmetry. For example, in [74], this method was employed to study the UV-completion of gravity via scattering of two scalar particles in the spin-helicity formalism, and in [75] it gave insight in the angular momentum rules for massive gravity. The exchange of a generic spin-J particle in the scattering amplitude is captured in the index of the Legendre polynomials, $P_n(z)$. For example, the coefficient belonging to $P_2(z)$ gives the contribution of the scattering process mediated by a spin-two particle.

Let us start by recapitulating the relevant properties of the Legendre polynomials and our definition of the partial wave expansion. For the majority, we will follow the conventions in [74]. A compact definition of the Legendre polynomials is given by Rodrigues' formula,

$$P_n(x) \equiv \frac{1}{2^n n!} \frac{\mathrm{d}^n}{\mathrm{d}^n x} \left(x^2 - 1\right)^n . \tag{4.14}$$

The Legendre polynomials form an orthogonal set on the Hilbert space of square integrable functions on the interval $[-1, 1]$, commonly denotes as $L^2\big([-1, 1]\big)$. The inner product on this space is defined as

$$\langle f, g \rangle = \int_{-1}^{1} \mathrm{d}x \, f(x) \, g(x). \tag{4.15}$$

The Legendre polynomials satisfy the orthogonality condition.

$$\langle P_n, P_m \rangle = \frac{2}{2n+1} \delta_{nm}. \tag{4.16}$$

Introducing an appropriate scaling factor transforms the Legendre polynomials to an orthonormal set. As an immediate consequence, we are now in the position to expand any function in $L^2\big([-1, 1]\big)$ in this basis.

$$f = \sum_{j=0}^{\infty} a_j P_j, \qquad\qquad a_j = \frac{2j+1}{2} \langle f, P_j \rangle . \tag{4.17}$$

In scattering amplitudes, we are seeking to encode their dependence on the scattering angle θ in terms of the Legendre polynomials. We define the expansion with an extra overall factor of 32π. The coefficients a_j are the so-called *partial wave amplitudes*

$$\mathcal{A}(\mathfrak{s}, \cos\theta) = 32\pi \sum_{j=0}^{\infty} \frac{2j+1}{2} a_j(\mathfrak{s}) P_j(\cos\theta), \tag{4.18}$$

where

$$a_j(\mathfrak{s}) \equiv \frac{1}{32\pi} \int_{-1}^{1} \mathrm{d}\left(\cos\theta\right) \mathcal{A}(\mathfrak{s}, \cos\theta) P_j(\cos\theta). \tag{4.19}$$

$\underline{\phi\phi \to \chi\chi}$:
With the toolbox of partial wave amplitudes at our disposal, equation (4.8) can now neatly be decomposed, such that two partial wave amplitudes are appearing

$$a_0^{\phi\phi\chi\chi}(\mathfrak{s}) = \frac{G_N}{12} G_{\mathrm{RR}}(\mathfrak{s}) \left[\left(\mathfrak{s} + 2m_\phi^2\right) \left(1 + \mathfrak{s} f_{\mathrm{Ric}\phi\phi}(\mathfrak{s}, m_\phi^2, m_\phi^2)\right) - 12\mathfrak{s} f_{\mathrm{R}\phi\phi}(\mathfrak{s}, m_\phi^2, m_\phi^2) \right] \times \left[\left(\mathfrak{s} + 2m_\chi^2\right) \left(1 + \mathfrak{s} f_{\mathrm{Ric}\chi\chi}(\mathfrak{s}, m_\chi^2, m_\chi^2)\right) - 12\mathfrak{s} f_{\mathrm{R}\chi\chi}(\mathfrak{s}, m_\chi^2, m_\chi^2) \right], \tag{4.20}$$

$$a_2^{\phi\phi\chi\chi}(\mathfrak{s}) = -\frac{G_N}{60} G_{\mathrm{CC}}(\mathfrak{s}) \left(\mathfrak{s} - 4m_\phi^2\right) \left(1 + \mathfrak{s} f_{\mathrm{Ric}\phi\phi}(\mathfrak{s}, m_\phi^2, m_\phi^2)\right) \times \left(\mathfrak{s} - 4m_\chi^2\right) \left(1 + \mathfrak{s} f_{\mathrm{Ric}\chi\chi}(\mathfrak{s}, m_\chi^2, m_\chi^2)\right). \tag{4.21}$$

The partial wave amplitudes with $j = 1$ and $j \geq 3$ vanish. These expressions simplify significantly if we assume a minimally coupled theory and take the ultrarelativistic limit, i.e. the graviton-matter form factors are set to zero and the mass of the scalar particles is negligible compared to $\mathfrak{s}$,

$$a_0^{\phi\phi\chi\chi}(\mathfrak{s}) = \frac{G_N}{12} \mathfrak{s}^2 G_{\mathrm{RR}}(\mathfrak{s}), \quad a_2^{\phi\phi\chi\chi}(\mathfrak{s}) = -\frac{G_N}{60} \mathfrak{s}^2 G_{\mathrm{CC}}(\mathfrak{s}). \tag{4.22}$$

For now, the focus is purely on the graviton mediated amplitude and the analysis of the self-interaction is left for later. It should be noted however, that the self-interaction contributes to the even partial wave amplitudes, a_{2n}, which are associated to ladder diagrams exchanging n gravitons.

$\underline{\phi\phi \to \phi\phi}$:
The procedure we used to obtain the scattering amplitudes $\mathcal{A}_{\mathfrak{s}}^{\phi\phi\phi\phi}$, $\mathcal{A}_{\mathfrak{t}}^{\phi\phi\phi\phi}$ and $\mathcal{A}_{\mathfrak{u}}^{\phi\phi\phi\phi}$ from $\mathcal{A}_{\mathfrak{s}}^{\phi\phi\phi\phi}$ does not translate to the partial wave amplitudes. The problem arises in the $\mathfrak{t}$- and $\mathfrak{u}$-channel amplitudes. The partial wave amplitudes become ill-defined in this region, due to the $\mathfrak{t}^{-1}$ and $\mathfrak{u}^{-1}$ factors appearing in these diagrams. In the limit $\cos\theta \to 1$, the amplitude diverges, which is a general problem for all scattering amplitudes mediated by a massless particle.

4.3 Cross section

Scattering cross sections are the objects that relate theory to experiment. On the one hand, this is something that we can measure with great accuracy in particle colliders such as the LHC, while on the other hand, they are directly related to scattering amplitudes. Working in the centre-of-mass frame has the advantage that the differential cross section reduces to a simple expression. The result holds for all scattering amplitudes and is given by

$$\left(\frac{\mathrm{d}\sigma}{\mathrm{d}\Omega}\right)_{\mathrm{CM}} = \frac{1}{64\pi^2\mathfrak{s}} \sqrt{\frac{\mathfrak{s} - 4m_\chi^2}{\mathfrak{s} - 4m_\phi^2}} \left|\mathcal{A}(\mathfrak{s}, \mathfrak{t}, \mathfrak{u})\right|^2. \tag{4.23}$$

The massless limit is defined as taking both $m_\phi, m_\chi \to 0$, which removes the square root term from the equation. To obtain the total cross section, the differential cross section (4.23) is integrated over the solid angle $\mathrm{d}\Omega$. At this point we make the following observations. In case of a two-to-two scattering process, where $\mathcal{A}$ is independent of ϕ, an overall factor of 2π is obtained due to the ϕ-integral. Moreover, there are no mixed factors of partial wave amplitudes due to the orthogonality of the Legendre polynomials. For readability, the indices ϕ, χ of the partial wave amplitudes are omitted, and we obtain

$$\sigma_{\mathrm{CM}}^{\phi\chi} = \frac{16\pi}{\mathfrak{s}} \sqrt{\frac{\mathfrak{s} - 4m_\chi^2}{\mathfrak{s} - 4m_\phi^2}} \left(a_0^2(\mathfrak{s}) + 5a_2^2(\mathfrak{s})\right). \tag{4.24}$$

In these calculations, the coefficients of one and five appears in front of the partial wave amplitudes. These are generated by the normalization factor of the Legendre polynomials, and they indicate how many (off-shell) graviton helicity states appear; one in the spin-zero sector, and five in the spin-two sector. In the massless limit, the partial wave amplitudes (4.22) reduce to the cross section

$$\sigma_{\text{CM}}^{\phi\chi} = \frac{\pi G_N^2 \mathfrak{s}^3}{18}\Big(G_{\text{RR}}^2(\mathfrak{s}) + \frac{1}{5}G_{\text{CC}}^2(\mathfrak{s})\Big). \tag{4.25}$$

Here, we accounted for a factor $\frac{1}{2}$ due to identical external particles. Also, G_{XX} is given in equations (3.34), which reduces to $\mathfrak{s}^{-1}$ when we return to general relativity, where the form factors f_{XX} are set to zero. Hence, for general relativity, the cross section is

$$\sigma_{\text{CM}}^{\phi\chi} = \frac{\pi}{15}G_N^2\mathfrak{s}. \tag{4.26}$$

The inclusion of non-zero form factors will in general change the scaling behaviour of the cross section. In the upcoming chapter, we will see various manifestations of higher-derivative gravity models, and analyse how they change the scattering amplitudes, partial wave amplitudes and subsequently the scattering cross sections.

The differential cross section for $\phi\phi \to \phi\phi$ is obtained by squaring the complete amplitude $\mathcal{A}^{\phi\phi\phi\phi}$. Due to the divergence of the $\mathfrak{t}$- and $\mathfrak{u}$-channel amplitudes, integrating over the solid angle produces a divergent integral. This is not a problem that the form factors brought about. This divergence is also produced in general relativity and is due to the masslessness of the graviton. A potential cure came from Weinberg's soft graviton theorem [76]. Apart from the IR-divergence generated by the virtual graviton, a second source of IR-divergences appear from diagrams where soft external gravitons are radiated away. Weinberg showed that order for order in perturbation theory, the IR-divergences generated from both classes exactly cancel, meaning that it is expected that the emission of soft graviton removes the singularity.

CHAPTER 5

In context to other theories

Based on the form factor program, the comparison of different higher-derivative theories of gravity can be done in the form factor program with relative ease. They parametrize these theories, and allow for an analysis in an unifying language. The goal of this chapter is to analyze some of these theories, and to identify their properties with respect to the causality and unitarity conditions set up in section 2.3. Following the analysis of [43], the important properties of the different theories can be extracted from the gravity mediated scattering of distinguishable particles, $\phi\phi \to \chi\chi$. As seen in the previous chapter, this reduces the scattering amplitude to equation (4.8) which gives a well-defined partial wave decomposition. Secondly, we will study massless particles, setting $m_\phi, m_\chi = 0$. Finally, the theories all have gravity minimally coupled to matter, entailing that all form factors f_{Rxx} and f_{Ricxx} are set to zero.

5.1 General relativity revisited

The theory of general relativity is retrieved by setting all form factors to zero. In this way, all quadratic curvature contributions to the action are removed, and only the Einstein-Hilbert term remains (without the cosmological constant). We can immediately substitute this replacement rule into the scattering amplitude to obtain the well-known result of general relativity [77],

$$\mathcal{A}^{\phi\phi\chi\chi}(\mathfrak{s}) = 8\pi G_N \frac{\mathfrak{tu}}{\mathfrak{s}} = 2\pi G_N \mathfrak{s} \sin^2\theta. \tag{5.1}$$

The resulting partial wave amplitudes are

$$a_0^{\phi\phi\chi\chi}(\mathfrak{s}) = \frac{G_N}{12}\mathfrak{s}, \quad a_2^{\phi\phi\chi\chi}(\mathfrak{s}) = -\frac{G_N}{60}\mathfrak{s}. \tag{5.2}$$

We can immediately see that there is no hope of having a unitary S-matrix in the high energy limit. Both the scattering and the partial wave amplitudes scale linearly with $\mathfrak{s}$, which in turn implies that the dimensionless cross section $\mathfrak{s}\sigma_{\mathrm{CM}}$, where σ is given by equation (4.26), scales quadratically with the centre-of-mass energy squared. This is in line with the negative mass dimension of Newton's constant, $[G_N] = -2$. By construction, tree-level diagrams are linear in G_N and therefore must be proportional to $\mathfrak{s}$ in order to obtain a dimensionless amplitude.

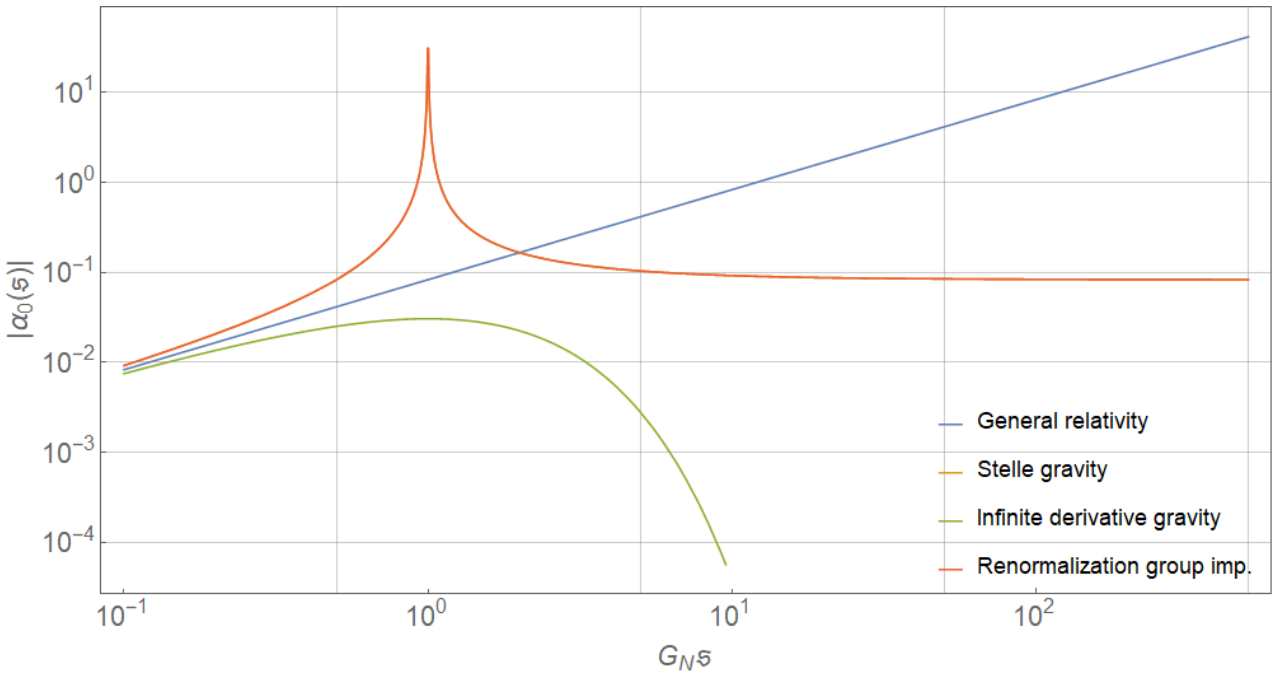

Figure 5.1: *The spin-zero partial wave amplitudes of general relativity, Stelle gravity, infinite derivative gravity and renormalization group improvements. Here, $\omega = c_R = 1$ for all models. The partial wave amplitude of Stelle gravity and renormalization group improvements completely overlap.*

5.2 Effective field theory

Effective field theories introduce a cut-off scale Λ^2 up to which a theory is valid. Beyond this scale, the theory should not be trusted, and a different theory which is appropriate at this scale should be employed. However, the idea behind effective field theories is that below the cut-off scale, the theory is predictable. In this way, general relativity makes sense when considered as a quantum theory. The cut-off scale of the effective field theory is the Planck scale, beyond which a complete quantum gravity theory is required.

An effective field theory cannot describe all quantum fluctuations in the action by definition, and thus we cannot employ the quantum effective action constructed in chapter 2. Scattering amplitudes can be calculated in a perturbative expansion as long as we consider the low-energy regime only. Tree-level amplitudes calculated from a bare action S give leading order contributions, and loop corrections are now required to obtain a more accurate result. A first order correction can be found by calculating all one-loop Feynman diagrams. For massless mediators such as the graviton or the photon, these loop corrections typically comprise non-analytic terms proportional to $\log \mathfrak{s}$ and $\mathfrak{s}^{-1/2}$ [78–81].

Alternatively, these non-analytic terms can be calculated directly from the bare action. A one-loop effective action contains these terms as form factors. Tree-level diagrams calculated from this object have the one-loop corrections already accounted for. The one-loop effective action is given by

$$\Gamma^{1-\text{loop}} = S - \frac{1}{2}\text{tr}\log\frac{S^{(2)} + \mathcal{R}_{\text{UV}}}{S^{(2)}}, \tag{5.3}$$

where $S^{(2)}$ is the second variation of S with respect to the fluctuation field, and $\mathcal{R}_{\text{UV}}$ is a regulator which ensures that the trace does not diverge at high energies. One of the first one-loop calculations for pure gravity was done by 't Hooft and Veltman, who calculated the one-loop divergences resulting

from the Einstein-Hilbert action [6]. A wide range of calculations have been done since then for Einstein-Hilbert gravity coupled to matter, such as scalar, Dirac and Maxwell fields [35, 82]. The logarithmic divergence for gravity coupled to N_s scalars is given by

$$\Gamma_{\text{one-loop}} = -\frac{1}{16\pi^2}\int \mathrm{d}^4x\sqrt{-g}\left[\frac{41+N_s}{120}R\log\left(\frac{\Delta}{\Lambda^2}\right)R + \frac{2+N_s}{240}R_{\mu\nu}\log\left(\frac{\Delta}{\Lambda^2}\right)R^{\mu\nu}\right]. \tag{5.4}$$

The gravity matter form factors can also be calculated in this framework [82, 83], although including matter fluctuations tend to complicate the calculations.

This works primarily focusses on the UV aspect of scattering amplitudes. Hence, the partial wave amplitude calculated from (5.4) is omitted from figure 5.1. Nevertheless, non-local effects in the infrared regime have been studied in the literature [41, 42, 84, 85] and can potentially account for dark energy in the universe [48, 49, 86]. Equation (5.4) serves as an illustration of the versatility of the form factor formalism.

5.3 Stelle gravity

In Stelle gravity, the form factors of the quadratic curvature monomials are set to a non-zero constant

$$f_{\text{RR}}(q^2) = -\frac{1}{c_{\text{R}}}, \quad f_{\text{CC}}(q^2) = -\frac{1}{c_{\text{C}}}. \tag{5.5}$$

The free parameters c_{R} and c_{C} set the scale at which the quadratic curvature corrections set in. At energies below this scale, the second order curvature terms are insignificant and Stelle gravity reduces to general relativity. At large energies, these extra terms tame the growth of the amplitude. We can see this from the partial wave amplitudes evaluated for the form factors (5.5)

$$a_0^{\phi\phi\chi\chi}(\mathfrak{s}) = \frac{G_N}{12}\mathfrak{s}^2\Big(\frac{1}{\mathfrak{s}} - \frac{1}{\mathfrak{s}-c_{\text{R}}}\Big), \quad a_2^{\phi\phi\chi\chi}(\mathfrak{s}) = -\frac{G_N}{60}\mathfrak{s}^2\Big(\frac{1}{\mathfrak{s}} - \frac{1}{\mathfrak{s}-c_{\text{C}}}\Big). \tag{5.6}$$

Indeed, as $\mathfrak{s}$ tends to infinity, the form factors (5.5) ensure a finite amplitude. A closer inspection reveals the problems that appear in Stelle gravity. The decomposition of the partial wave amplitudes show that, besides the massless pole at $\mathfrak{s}=0$, there are additional massive poles, sitting at $\mathfrak{s}=c_{\text{R}}$ and $\mathfrak{s}=c_{\text{C}}$ for the different spin modes. These additional contributions appear in the partial wave amplitudes with opposite sign. This is an indication that one of these extra poles is associated to a negative-energy state. A formal calculation of the residue of the massive poles shows that the spin-two pole is the culprit

$$\text{Res}|_{\mathfrak{s}=c_{\text{R}}}\big(a_0^{\phi\phi\chi\chi}(\mathfrak{s})\big) = \lim_{\mathfrak{s}\to c_{\text{R}}}\frac{c_{\text{R}}-\mathfrak{s}}{c_{\text{R}}}a_0(\mathfrak{s}) = \frac{G_N}{12}c_{\text{R}} > 0, \tag{5.7}$$

$$\text{Res}|_{s=c_{\text{C}}}\big(a_2^{\phi\phi\chi\chi}(\mathfrak{s})\big) = \lim_{\mathfrak{s}\to c_{\text{C}}}\frac{c_{\text{C}}-\mathfrak{s}}{c_{\text{C}}}a_2(\mathfrak{s}) = -\frac{G_N}{60}c_{\text{C}} < 0. \tag{5.8}$$

States with negative residue lack a physical interpretation, and should therefore be removed from the theory. Doing this however, violates unitarity of the S-matrix [87], showing that introducing quadratic curvature monomials à la Stelle generates a non-unitary theory.

It was already shown by Ostrogradski in the 1850s that classical systems containing time derivatives of order higher than two generate Hamiltonians whose kinetic energy is not bounded from below. The same principle applies here. The quadratic curvature monomials introduce higher order field derivatives, which in turn violate the unitarity of the theory. As summarized in [22], there are three ways to deal with this problem. We can accept that gravity is not causal at a microscopic level. The

$$k\partial_k\Gamma_k[\phi] = \frac{1}{2}\mathrm{Tr}$$ 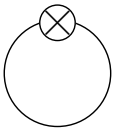

Figure 5.2: *A visualization of the Wetterich equation in Feynman diagram notation.*

massive modes that appear in the propagator are then interpreted as particles moving backwards in time. A second way is to break Lorentz invariance. Maintaining two time-derivatives and allowing for higher spatial derivatives, unitarity can be saved. This idea forms the basis of Hořava-Lifschitz gravity. The third way is what we initially set out to do with the form factor program. The derivative terms are compressed into a function, capturing the non-trivial momentum dependence. Stelle gravity shows that momentum-dependent form factors are paramount if one insists on unitarity and causality. An example is the infinite derivative models that we will encounter in the next section.

5.4 Infinite derivative gravity

Infinite derivative gravity [69, 80, 88, 89] generalizes Stelle gravity by including momentum-dependent form factors at the bare action. The choice for the form factors in this approach is an exponential function. In this way, the form factor has no zero, and therefore, the graviton propagator only contains the massless modes. It mimics the behaviour of the scattering amplitudes calculated from string theory, where exponential form factors appear as a class of higher-derivative theories [90]. Following [80, 91], the specific choice for form factors are

$$f_{\mathrm{RR}}(\Delta) = \frac{e^{c_{\mathrm{R}}\Delta}-1}{\Delta}, \qquad f_{\mathrm{CC}}(\Delta) = \frac{e^{c_{\mathrm{C}}\Delta}-1}{\Delta}, \qquad f_{\phi\phi}(\Delta) = e^{c_{\mathrm{S}}\left(\Delta-m_\phi^2\right)}\left(\Delta-m_\phi^2\right). \tag{5.9}$$

This is also the first encounter with a non-trivial scalar form factor $f_{\phi\phi}$. By construction, this form factor satisfies the on-shell conditions specified in section 3.2.3. The exponential form factors suppress the high energy behaviour of the scattering amplitudes, which generates an asymptotic free theory.

Work in this field suggests there should also be form factors in the gravity-matter sector, although the precise structure of these terms has not yet been worked out. Substituting (5.9) into the partial wave amplitudes of $\phi\phi \to \chi\chi$, we obtain

$$a_0^{\phi\phi\chi\chi}(\mathfrak{s}) = \frac{G_N}{12}\mathfrak{s}\, e^{-c_{\mathrm{R}}\mathfrak{s}}, \qquad a_2^{\phi\phi\chi\chi}(\mathfrak{s}) = -\frac{G_N}{60}\mathfrak{s}\, e^{-c_{\mathrm{C}}\mathfrak{s}}. \tag{5.10}$$

This clearly shows the exponential damping of the amplitudes in the UV-regime. This is also illustrated in figure 5.1. This also means that there are no ghost modes in infinite derivative gravity, or any new massive degrees of freedom at all for that matter.

By crossing symmetry, we obtain the scattering amplitude for $\phi\chi \to \phi\chi$ by interchanging $\mathfrak{s} \leftrightarrow \mathfrak{t}$. In this case, the partial wave amplitudes are exponentially increasing with $\mathfrak{s}$, which violates the Froissart bound. It is therefore unclear if infinite derivative gravity truly generates a finite, unitary theory.

5.5 Renormalization group improvements

Non-perturbative methods for gravity became available by the work of Reuter in the early nineties [86, 92–94]. The central object in this framework is the *effective average action*; a scale-dependent counterpart to the "ordinary" effective action. This is done by introducing a regulator $\mathcal{R}_k$. In this

case, k acts as an IR cut-off scale, which associates a mass k^2 to the low-energy modes. The effective average action is derived along the same lines as the ordinary quantum effective action. First, we define the functional $W_k[J]$

$$\exp\left(W_k[J]\right) \equiv \int \mathcal{D}\phi \exp\left(-\Gamma[\phi] - \Delta S_k[\phi] + \int \mathrm{d}^4x\, \phi(x)J(x)\right). \tag{5.11}$$

Here, the regulator term $\Delta S_k[\phi]$ is given in momentum space by

$$\Delta S_k[\phi] = \frac{1}{2}\int \frac{\mathrm{d}^4p}{(2\pi)^4}\phi_p \mathcal{R}_k(p^2)\phi_p. \tag{5.12}$$

We note that the effective average action is derived for spacetimes with an Euclidean signature, so the traditional factors of i do not appear in the path integral. We see that the regulator term has no impact on the vertices of the theory. Its only effect is to modify the momentum behaviour of the propagator. In this case, it is similar to the f_{XX} form factors encountered for the graviton propagator, although now the IR-behaviour is changed. For a regular suppression of the infrared modes of $\phi(x)$, the following list of requirements applies to the regulator [35, 95]

- $\mathcal{R}_k$ must be continuous and monotonically decreasing in both p^2 and k^2.
- For $p^2 > k^2$, $\mathcal{R}_k$ should tend to zero.
- For $p^2 \ll k^2$, $\mathcal{R}_k$ is approximately k^2.
- For $k \to 0$, $\mathcal{R}_k$ should tend to zero.

The effective average action is defined by taking the Legendre transform of $W_k[J]$

$$\Gamma_k\left[\phi\right] = -W_k[\phi] + \int \mathrm{d}^4x\, J(x)\phi(x) - \Delta S_k[\phi]. \tag{5.13}$$

A smooth regulator allows the derivation of a flow equation. This is known as the Wetterich equation, which provides the primary non-perturbative tool to investigate asymptotic safety of quantum gravity

$$k\partial_k\Gamma_k[\phi] = \frac{1}{2}\mathrm{Tr}\left[\left(\Gamma_k^{(2)} + \mathcal{R}_k\right)^{-1} k\partial_k\mathcal{R}_k\right]. \tag{5.14}$$

In this notation, $\Gamma_k^{(2)}$ is the Hessian containing two functional derivative with respect to ϕ. The trace is defined with respect to an arbitrary basis of eigenstates of the argument, which can be discrete or continuous. Figure 5.2 gives a visual representation of the Wetterich equation. The continuous line represents the exact propagator, regulated by $\mathcal{R}_k$

$$\left(\Gamma_k^{(2)} + \mathcal{R}_k\right)^{-1}, \tag{5.15}$$

and the cross on top symbolizes the insertion of $k\partial_k\mathcal{R}_k$. The effective average action interpolates between two special limit points. From equation (5.13) and the properties of the regulator, we see that $\lim_{k\to 0}\Gamma_k$ removes the regulator and the quantum effective action is retrieved. On the other hand, it can be shown that $\lim_{k\to\infty}\Gamma_k$ approaches the bare action [36].

The Wetterich equation is non-perturbative, in the sense that it does not rely on any expansion in coupling constants of any kind. Typically, one would like to start from a bare action S, and solve the Wetterich equation to obtain the renormalized coupling constants. In general, this is incredibly hard to do, and typically one has to settle for a truncated expansion of the action. Having a finite number

of monomials in the action, each associated with a coupling constant, results in a finite number of β-functions obtained from the Wetterich equation. This typically generates a set of non-linear, coupled differential equations which can be solved by means of numerical methods.

The basis of monomials used to construct the action can be thought of as spanning a *theory space*. The coupling constant correspond to coordinates in this high-dimensional space, and the β-functions trace out trajectories. In some cases, the trajectories will be pulled towards a fixed point. At the fixed point, the coupling constants are finite, the β-functions vanish and hence, the theory is saved from UV-divergences. A fixed point has been found when studying the action projected on a two-dimensional subspace spanned by $\sqrt{g}$ and $\sqrt{g}R$ [96]. The coupling constants are therefore the scale-dependent Newton's constant G_k and cosmological constant Λ_k. In four-dimensional gravity, the dimensionless coupling constants are obtained by multiplication with an appropriate factor of k to obtain a dimensionless object

$$g_k = G_N k^2, \qquad \Lambda_k = k^{-2}\Lambda_k \tag{5.16}$$

The negative mass dimension of Newton's constant dictates the quadratic scaling of g_k, showing that expanding in g_k well beyond the Planck scale is problematic. The Wetterich equation gives a new scaling behaviour in this regime. Following [96], the dimensionless coupling constants are substituted in the Wetterich equation to obtain the two β-functions. For a vanishing cosmological constant, we have

$$k\partial_k g_k = 2\frac{1-\omega' g_k}{1-(\omega'-\omega)g_k}g_k. \tag{5.17}$$

Having chosen the exponential regulator, the constants ω and ω' are

$$\omega = \frac{4}{\pi} - \frac{\pi}{36}, \qquad \omega' = \frac{14}{3\pi} - \frac{\pi}{36}. \tag{5.18}$$

Although $g_k = 0$ is a solution to (5.17), it implies that g_k is zero at all scales. Looking at the world around us, it is clear that this cannot be the case. A second non-trivial fixed point is given at

$$g^*_{\text{UV}} = \frac{1}{\omega'}. \tag{5.19}$$

Given that g_k is contained in the interval $[0, g^*_{\text{UV}}]$ for all k, then g_k has to be attracted towards zero in the infrared limit, and towards g^*_{UV} in the ultraviolet limit. Equation (5.17) cannot be solved explicitly, but for $\omega'/\omega \approx 1$ we find an accurate approximation. This choice is not unreasonable as from (5.18) we have $\omega'/\omega \approx 1.18$. Restoring k^2, Newton's constant is

$$G(k^2) = \frac{G_N}{1+\omega G_N k^2}. \tag{5.20}$$

For small k^2, the running is indeed close to the bare Newton's constant. For $k^2 \gg G_N^{-1}$, the coupling constant falls off as k^{-2}.

We perform a renormalization group improvement to the scattering amplitude by exploiting the information given by equation (5.20) to incorporate quantum corrections to the graviton propagator. In the amplitude, the only scale-dependent variable is the graviton momentum. Naturally, we identify $k^2 = q^2_{\text{E}}$. The subscript reminds us that we are still in an Euclidean background. Using a standard Wick rotation, we can switch from the Euclidean background to the Minkowski background. Taking the sign convention of the flat background into account, we have $k^2 \to -q^2$. The renormalizion group improvement of the scattering amplitude (5.1) gives,

$$\mathcal{A}^{\phi\phi\chi\chi}(\mathfrak{s}) = 8\pi G(-\mathfrak{s})\frac{\mathfrak{tu}}{\mathfrak{s}} = 8\pi\frac{G_N}{1-\omega G_N \mathfrak{s}}\frac{\mathfrak{tu}}{\mathfrak{s}}. \tag{5.21}$$

The partial wave amplitudes are

$$a_0^{\phi\phi\chi\chi}(\mathfrak{s}) = \frac{G_N}{12}\mathfrak{s}^2\Big(\frac{1}{\mathfrak{s}} - \frac{1}{\mathfrak{s} - G_N^{-1}\omega^{-1}}\Big), \quad a_2^{\phi\phi\chi\chi}(\mathfrak{s}) = -\frac{G_N}{60}\mathfrak{s}^2\Big(\frac{1}{\mathfrak{s}} - \frac{1}{\mathfrak{s} - G_N^{-1}\omega^{-1}}\Big). \tag{5.22}$$

The partial wave amplitudes show the same qualitative behaviour as Stelle gravity. The gravitational form factors are both equal to the constant $f_{\mathrm{XX}} = -G_N\omega$, which corresponds to the Stelle parameters $c_{\mathrm{X}} = G_N^{-1}\omega^{-1}$. The interacting fixed point guarantees finite observables in the UV. The renormalization group improvement implements this feature at the cost of a ghost particle in the spin-two sector of the graviton, similar to Stelle gravity. Setting $c_{\mathrm{R}} = c_{\mathrm{C}} = G_N^{-1}\omega^{-1}$, the partial wave amplitudes completely overlap is shown in figure 5.1.

The renormalization improvement assigns the same mass to the spin-zero and spin-two mode, which is already a simplification of Stelle gravity where the two could have different mass. Extending this analysis to more general scattering processes becomes more problematic. Renormalizing one single coupling constant is not enough to specify all the different form factors that might appear. Secondly, form factors generally carry more than one argument. For example, the matter form factors f_{Rxx} and f_{Ricxx} had three, each depending on independent scales. An underdetermined system appears when the single scale parameter k has to describe a multiple-parameter family of scale-dependent variables. Renormalization group improvements give an idea about how physics could look like, but one should not expect that it is able to reveal the full picture.

CHAPTER 6

Realizing asymptotic safe amplitudes

In this chapter, the model introduced in [44] is analysed. A carefully chosen analytic structure of the form factors realizes asymptotic safety at the level of scattering amplitudes. The model is a proof of principle, showing that the form factors have enough freedom to support a unitary and causal theory. There will be extra emphasis on the pole structure of the model, which has the resemblance of a Lee-Wick model in QED. This model is non-perturbative in the sense that a finite truncation of the model introduces massive poles signalling unitarity and causality problems. These massive poles are artefacts of the truncation scheme. An analysis of the full form factors shows that all poles are on the imaginary axis. Hence, it is essential that the full structure is maintained. It will also become clear that the form factors modifying the graviton propagator are not sufficient to guarantee finite observables. This is only possible with the addition of a matter self-interactions.

6.1 Lee-Wick models and microcausality - an interlude

In the 1960s, Lee and Wick proposed a special class of quantum field theories to provide a UV-completion to QED [97,98]. The goal was to circumvent the Landau pole which appears in the photon propagator for some finite energy, while retaining renormalizability and unitarity of the theory. Their idea was to modify the scalar part of the photon propagator according to

$$\frac{1}{q^2} \quad \longrightarrow \quad \frac{1}{q^2} - \frac{1}{q^2 - M^2} = -\frac{M^2}{q^2\big(q^2 - M^2\big)}, \tag{6.1}$$

where M is a finite mass scale. This modification is not completely new; this is also done in Pauli-Villars regularization. The difference is that M is not regarded as a cut-off scale, which can be send to infinity to return the classical theory. Instead, Lee and Wick regard M as a physical scale. This can be achieved by including a massive auxiliary field in the action. For example, the Abelian Lee-Wick model for QED, with an interaction fermion ψ, is [99]

$$\mathcal{L} = -\frac{1}{4}F_{\mu\nu}F^{\mu\nu} + \frac{1}{4}G_{\mu\nu}G^{\mu\nu} + \frac{1}{2}M^2 B_\mu B^\mu - \overline{\psi}\Big[\gamma^\mu\big(-i\partial_\mu - e(A_\mu + B_\mu)\big) + m\Big]\psi + J_\mu\big(A^\mu + B^\mu\big). \tag{6.2}$$

Here we have introduced the massive Lee-Wick photon field B_μ to the theory ($G_{\mu\nu} = \partial_\mu B_\nu - \partial_\nu B_\mu$) with mass M. Notice that it appears in the Lagrangian with the wrong sign, meaning that it is a ghost

state. Both the "normal" and the Lee-Wick photon couple to the electromagnetic current, and the interaction can be described in a combined propagator. In [99], this propagator has been calculated, and modified by integrating out the Dirac fields. This way, the propagator gets a contribution of the vacuum polarization, $\Pi(q^2)$,

$$iD_{\mu\nu}(q^2) = \frac{-i\eta_{\mu\nu}}{\left(q^2 + i\epsilon\right)\left[1 + \Pi(q^2) - q^2/M^2\right]}. \tag{6.3}$$

The vacuum polarization is given in a Källen-Lehmann spectral representation

$$\Pi(q^2) = q^2 \frac{\alpha}{3\pi} \int_{4m^2}^{\infty} \mathrm{d}s \frac{1}{s\left(s - q^2 + i\epsilon\right)} \sqrt{1 - \frac{4m^2}{s}} \left(1 + \frac{2m^2}{s}\right). \tag{6.4}$$

Calculating the vacuum polarization function $\Pi(q^2)$ of the photon propagator, shifts the pole of the heavy Lee-Wick particle into the complex plane. In [100], a numerical solution reveals the resonance structure, showing that the propagator is well approximated by

$$iD_{\mu\nu}(q^2) = \frac{-i\eta_{\mu\nu}}{q^2\left(q^2 - \mu^2 - iM\Gamma\right)}. \tag{6.5}$$

The imaginary part of the denominator yields a finite decay width, showing that the massive Lee-Wick particle is unstable. However, this decay width also comes with the wrong sign. Together, this implies that overall, the imaginary part of the propagator is the same as a propagator with the correct kinetic and resonance signs

$$\mathrm{Im}\, q^2 D_{\mu\nu}(q^2) = -\eta_{\mu\nu} \frac{M\Gamma}{(q^2 - \mu^2)^2 + M^2\Gamma^2}. \tag{6.6}$$

The negative sign of the massive Lee-Wick propagator in (6.1) is associated to a negative energy state, violating unitarity. In the classical limit, this negative state indicates instability of the theory, which can be removed by imposing boundary conditions such that certain modes are restrained. However, this procedure is known to violate causality, suppressed below the scales set by the Lee-Wick particles [101, 102]. In particular, [102] shows that the overlap of incoming and outgoing wave packets, mediated by the massive Lee-Wick particle, has non-zero overlap only when the mediator propagates backwards in time, i.e. the outgoing particles appear before the ingoing particles have collided. The time scale at which causality is violated is set by the imaginary part of the Lee-Wick resonance. A second problem that arises is the violation of Lorentz invariance at a certain point in the calculations [103–105]. A solution came by the hands of Cutkovsky, Landshoff, Olive and Polkinghorne [106], who redefined the contour of the momentum integral in such a way that unitarity and Lorentz invariance is eventually restored.

6.2 Analysis of the hyperbolic tangent form factors

Scattering of massless, distinguishable particles produced a single tree-level diagram (figure 4.1) and scattering amplitude (4.8). Omitting the gravity-matter form factors f_{Rxx} and f_{Ricxx}, we shift the analysis to the pure gravity form factors and the pole structure therein. Adopting the form factors of [44]

$$f_{\mathrm{XX}}(\Delta) = c_{\mathrm{X}} G_N \tanh\left(c_{\mathrm{X}} G_N \Delta\right), \tag{6.7}$$

we immediately get the scattering amplitude and partial wave amplitudes by plugging the form factors (in momentum space representation) in equations (4.8) and (4.22). The constants $c_{\mathrm{X}} > 0$

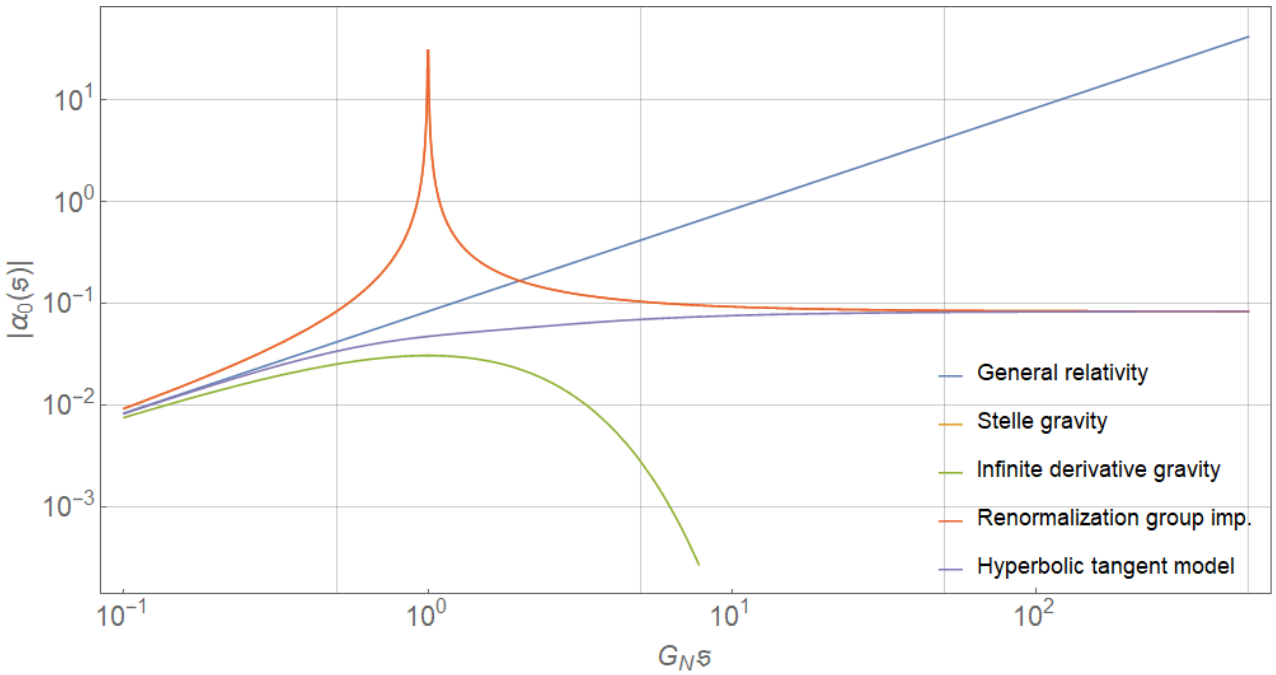

Figure 6.1: *The spin-zero partial wave amplitudes of figure 5.1, now with the hyperbolic tangent model included. Again $\omega = c_R = 1$ for all models.*

are strictly positive and dimensionless. In the centre-of-mass frame, the scattering amplitude (4.8) reduces under these assumptions to

$$\begin{aligned}\mathcal{A}_{\mathfrak{s}}^{\phi\phi\chi\chi}(\mathfrak{s},\cos\theta) &= \frac{4\pi G_N}{3}\Big(\mathfrak{s}^2 G_{\mathrm{RR}}(\mathfrak{s}) - \big(\mathfrak{s}^2+6\mathfrak{s}\mathfrak{t}+6\mathfrak{t}^2\big)\,G_{\mathrm{CC}}(\mathfrak{s})\Big)\\ &= \frac{4\pi G_N}{3}\mathfrak{s}^2\Big(G_{\mathrm{RR}}(\mathfrak{s})P_0(\mathfrak{s}) - G_{\mathrm{CC}}(\mathfrak{s})P_2(\mathfrak{s},\cos\theta)\Big),\end{aligned} \tag{6.8}$$

with

$$G_{\mathrm{XX}}(z) = \frac{1}{z\big(1+c_{\mathrm{X}}G_N z\tanh c_{\mathrm{X}}G_N z\big)}. \tag{6.9}$$

The corresponding partial wave amplitudes (4.22) will be reiterated here

$$a_0^{\phi\phi\chi\chi} = \frac{G_N}{12}\mathfrak{s}^2 G_{\mathrm{RR}}(\mathfrak{s}), \qquad a_2^{\phi\phi\chi\chi} = -\frac{G_N}{60}\mathfrak{s}^2 G_{\mathrm{CC}}(\mathfrak{s}). \tag{6.10}$$

Unitarity:
First we notice that $\mathfrak{s}\tanh\mathfrak{s}$ is a positive function. Therefore, these form factors do not introduce massive ghost degrees of freedom in the theory. At the same time, the partial wave amplitudes are bounded in the high energy regime. As $\mathfrak{s}$ tends to infinity, the tanh-function approaches unity. In this way the momentum behaviour of the propagator is smoothly altered from $\mathfrak{s}^{-1}$ to $\mathfrak{s}^{-2}$ which is exactly what was necessary to stop the linear growth of the partial wave amplitudes in general relativity (see figure 6.1). The smooth transition is what Stelle gravity was lacking. It also had the correct high energy behaviour of the propagator, but at the cost of a pole at finite energy. Imposing the unitarity constraint of of the partial wave amplitude, (2.29), gives a lower bound of the c_{X}.

$$c_{\mathrm{R}} \geq \frac{1}{12}, \qquad c_{\mathrm{C}} \geq \frac{1}{60}. \tag{6.11}$$

Causality

One of the conditions for a causality-abiding scattering amplitude was given by the upper bound mentioned in section 2.3. Any causal scattering amplitude should be polynomially bounded, growing slower than $\mathfrak{s}^2$. For $\phi\phi \to \chi\chi$, this is not a problem, but there is a related scattering process where this bound is violated.

Moving towards $\phi\chi \to \phi\chi$ scattering, we obtain the corresponding scattering amplitude equation (6.8) by crossing symmetry

$$\mathcal{A}_{\mathfrak{t}}^{\phi\chi\phi\chi} = \frac{4\pi G_N}{3}\Big(\mathfrak{t}^2 G_{\mathrm{RR}}(\mathfrak{t}) - \left(6\mathfrak{s}^2 + 6\mathfrak{s}\mathfrak{t} + \mathfrak{t}^2\right) G_{\mathrm{CC}}(\mathfrak{t})\Big). \tag{6.12}$$

This scattering process only has a $\mathfrak{t}$-channel. In the forward scattering limit, where $\mathfrak{t}$ is fixed, this amplitude scales with $\mathfrak{s}^2$, breaking the causality bound. The gravity form factors are insufficient to recuperate causality. This is where the scalar self-interaction plays a crucial role. The form factor $f_{\phi\phi\chi\chi}$ can be chosen in such a way that causality is restored. In the massless limit, the on-shell self-interaction to the $\mathfrak{t}$-channel amplitude is

$$\mathcal{A}_4^{\phi\chi\phi\chi} = f_{\phi\phi\chi\chi}\left(\tfrac{\mathfrak{t}}{2}, \tfrac{\mathfrak{s}}{2}, \tfrac{\mathfrak{u}}{2}, \tfrac{\mathfrak{u}}{2}, \tfrac{\mathfrak{s}}{2}, \tfrac{\mathfrak{t}}{2}\right) + \mathrm{sym}, \tag{6.13}$$

where "sym" means that all permutations of the arguments of $f_{\phi\phi\chi\chi}$, where $p_1 \leftrightarrow p_2$ and $p_3 \leftrightarrow p_4$, should be added. This way, crossing symmetry arises from the symmetrization of the form factors, which itself arises from the variational principle of the action. Different choices of $f_{\phi\phi\chi\chi}$ can generate the same amplitude, which is why only the full vertex is of our concern. Besides being crossing symmetric, the form factor should also vanish in the low energy limit $\mathfrak{s} \to 0$. In this regime, general relativity should be retrieved and corrections due to self-interactions should be suppressed at low energies. On the other hand, the self interaction cancels the quadratic divergence of the scattering amplitude, which gives

$$\lim_{\substack{\mathfrak{t}\text{ fixed}\\ \mathfrak{s}\to\infty}} \mathcal{A}_4^{\phi\chi\phi\chi} = -\lim_{\substack{\mathfrak{t}\text{ fixed}\\ \mathfrak{s}\to\infty}} \mathcal{A}_{\mathfrak{t}}^{\phi\chi\phi\chi} = 8\pi G_N \mathfrak{s}^2 G_{\mathrm{CC}}(\mathfrak{t}) + \mathcal{O}(\mathfrak{s}). \tag{6.14}$$

To achieve these goals, an interpolation function f_{int} is introduced to switch the self-interaction off and on in the correct regimes. For low $\mathfrak{s}$, this function reduces to zero, and in the limit $s \to \infty$, it tends towards one. The self-interaction is then defined as

$$\mathcal{A}_4^{\phi\chi\phi\chi} = g(\mathfrak{t}|\mathfrak{s},\mathfrak{u}) = 4\pi G_N G_{\mathrm{CC}}(\mathfrak{t})(\mathfrak{s}^2 + \mathfrak{u}^2) f_{\mathrm{int}}(\mathfrak{s}^2 + \mathfrak{t}^2 + \mathfrak{u}^2), \tag{6.15}$$

where we take f_{int} the same as in [44]

$$f_{\mathrm{int}}(z) = \frac{c_t G_N^2 z \tanh c_t G_N^2 z}{1 + c_t G_N^2 z \tanh c_t G_N^2 z}. \tag{6.16}$$

By construction, this function is invariant under crossing symmetry and at low energies, i.e. $G_N s \lesssim (G_N c_t)^{-1}$, the self-interaction is "switched off". The control parameter c_t sets the scale at which the self-interaction provides a relevant contribution to the complete amplitude. The full scattering amplitude is now linear in $\mathfrak{s}$ at high energies,

$$\lim_{\substack{\mathfrak{t}\text{ fixed}\\ \mathfrak{s}\to\infty}} \mathcal{A}^{\phi\chi\phi\chi} = \lim_{\substack{\mathfrak{t}\text{ fixed}\\ \mathfrak{s}\to\infty}} \mathcal{A}_{\mathfrak{t}}^{\phi\chi\phi\chi} + \mathcal{A}_4^{\phi\chi\phi\chi} = -8\pi G_N \mathfrak{s}\mathfrak{t} G_{\mathrm{CC}}(\mathfrak{t}) + \mathcal{O}(\mathfrak{s}^0). \tag{6.17}$$

Naturally, the self-interaction also contributes to the total scattering amplitude of the $\mathfrak{s}$-channel. One easily verifies that it does not affect the salient features at high energies,

$$\lim_{\substack{\mathfrak{t}\text{ fixed}\\ \mathfrak{s}\to\infty}} \mathcal{A}^{\phi\phi\chi\chi} = \lim_{\substack{\mathfrak{t}\text{ fixed}\\ \mathfrak{s}\to\infty}} \mathcal{A}_{\mathfrak{s}}^{\phi\phi\chi\chi} + \mathcal{A}_4^{\phi\phi\chi\chi} = \frac{4\pi G_N}{3}\mathfrak{s}^2\Big(G_{\mathrm{RR}}(\mathfrak{s}) + 2G_{\mathrm{CC}}(\mathfrak{s})\Big) + \mathcal{O}(\mathfrak{s}^0). \tag{6.18}$$

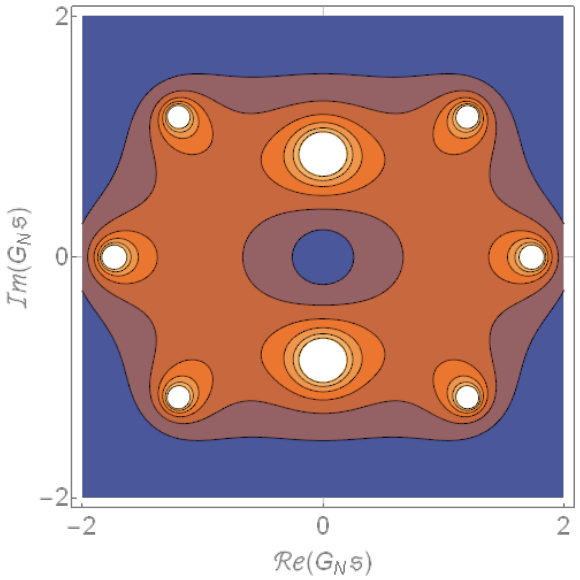

(a) *Pole structure of* tanh*-model at tenth order.*

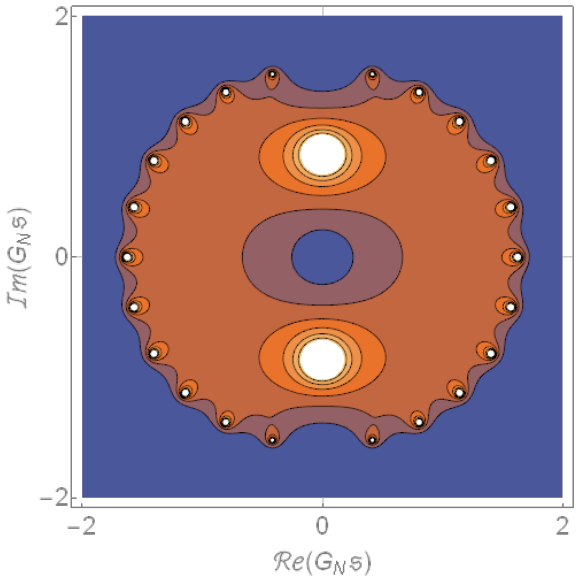

(b) *Pole structure of* tanh*-model at twenty-fifth order.*

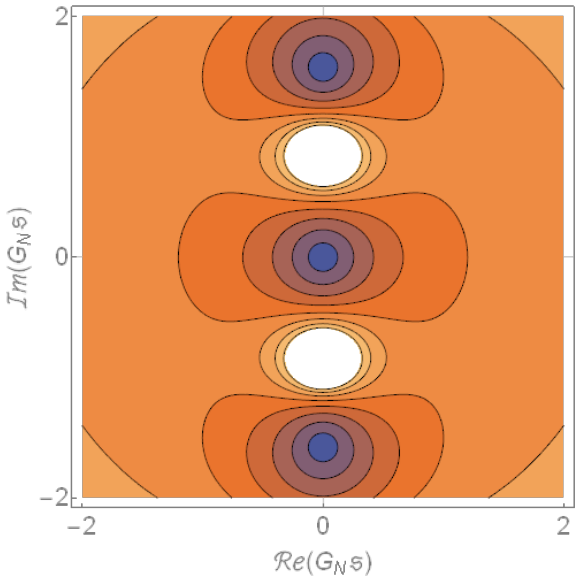

(c) *Pole structure of the untruncated form factor.*

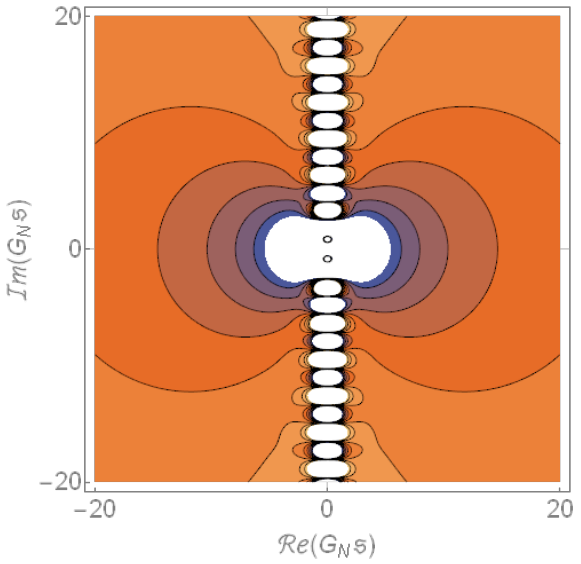

(d) *Pole structure of the untruncated form factor at a larger interval.*

Figure 6.2: *Contour diagrams of* $1 + z\tanh(z)$*. The figures signify the pole structure of the form factors, truncated at a finite order [6.2a, 6.2b] and in their exact form [6.2c, 6.2d]. The location of the poles are at the centre of the white circles.*

The functions $G_{\mathrm{XX}}(\mathfrak{s})$ decay asymptotically of order $\mathfrak{s}^{-2}$ so the amplitude is asymptotically constant in $\mathfrak{s}$. Thus, the qualitative behaviour of the $\mathfrak{s}$-channel amplitude is unchanged. Including a matter self-interaction only shifts the asymptotic limit to a different, finite value.

Pole structure:

Due to the symmetry of the form factor contribution in the propagator, there are no poles for any real $\mathfrak{s}$ (apart from the one corresponding to a massless graviton at $\mathfrak{s} = 0$). Analyzing the pole structure in

the complex momentum plane, all poles of the tanh-model are on the imaginary axis; their real part is always zero. The first pole is in the origin and is due to the massless graviton of general relativity. The position of the other poles are found by solving

$$ix\tanh(ix)+1=0 \qquad \longleftrightarrow \qquad x\tan(x)-1=0, \quad x\in\mathbb{R}. \tag{6.19}$$

There is no solution of this equations in closed form, and numerical methods are required to approximate the exact position of the poles. However, at large x, the poles approach the zeros of $\tan(x)$ increasingly better, showing that the poles have a Regge behaviour where they are equally spaced due to the periodicity of the tangent function. Reintroducing the constants c_{X} and G_N, the poles, $\Gamma^{(n)}$, are positioned at

$$\Gamma^{(n)}_{\mathrm{X}} \simeq \frac{\pi n}{G_N c_{\mathrm{X}}} i, \qquad \forall n\in\mathbb{Z}. \tag{6.20}$$

The exact solutions to equation (6.19) are illustrated in figure 6.2. In these contour diagrams, the poles are positioned at the centre of the white bubbles. In figures 6.2c and 6.2d we clearly see how the poles are positioned at the complex axis, becoming equidistant far away from the origin.

The fallacy of form factor truncations:
So far, we have seen that the poles of the full form factors are all on the imaginary axis. This is the underlying mechanism which gives us causal, unitary, Lorentz invariant scattering amplitudes. However, this form factor approach is relatively new, and so far quite a lot of the literature focuses on studying quantum gravity theories employing a truncated derivative expansion. This corresponds to approximating the form factors by a Taylor expansion of finite order. In this section, it will be shown that this procedure is prone to difficulties. First, we can perform a Taylor expansion of $z\tanh(z)$ around $z=0$

$$z\tanh z = \sum_{n=1}^{\infty} \frac{2^{2n}\left(2^{2n}-1\right)}{(2n)!} B_{2n} z^{2n}, \tag{6.21}$$

where B_n are the Bernoulli numbers. The expansion has a finite radius of convergence of $\pi/2$, where the tanh hits its first pole. Hence, we cannot expect a finite expansion to generate all the poles on the imaginary axis, especially those outside of the radius of convergence. The pole structure of the truncated model is shown in figures 6.2a and 6.2b, where (6.21) is expanded up to order ten and twenty-five respectively. Some of the poles are indeed on the imaginary axis and are present in the full form factors 6.2c, but the remaining poles arise at the boundary of the radius of convergence. Truncating the form factors therefore yield massive poles in the complex plane. This structure is identical to the one encountered in Lee-Wick models. From this context, it is known that poles with a non-zero real part lead to violation of microcausality.

In the context of asymptotic safety, the evolution of a scale-dependent effective action is described by a non-perturbative functional renormalization group equation. The difficulty is that the analysis of a general action with this technique is currently our of reach. At the moment, truncations of the action are studied to analyze the asymptotic safety scenario of gravity. Although there are strong indications of asymptotic safety of gravity [23–34], there is still a lot unknown about the unitarity of these theories. From the model here, it is clear that carefulness is required when unitarity is studied in a truncated theory. A similar conclusion is reached in [107]. The ghosts that enter in these theories, such as the spin-two ghost in Stelle gravity, might be artefacts of the truncation procedure, and might be absent in the full theory.

Microcausality of the hyperbolic tangent model:
The question then arises of the tanh-model violates causality at microscopic scales like the Lee-Wick models do. Following the analysis in [102] , it turns out that this is not the case. The multiplicative factor of $1 + f_{\mathrm{XX}}(q^2)$ appearing in the propagator is regular for all real q^2. Consequently, the causal behaviour of the scattering amplitude is equivalent to that of a massless particle. On the other hand, it is clear that a truncation of the form factor to some degree introduces massive Lee-Wick poles. This signals once again that it is crucial that the full form factor has to be kept.

CHAPTER 7

Conclusions and Outlook

In this thesis we developed the form factor program in the quantum effective action. Our main interest was in determining its ability to generate amplitudes compatible with Lorentzian asymptotic safety. Explicitly, the focus was on scattering of (massive) scalar matter, generating the scattering amplitude (4.8). This result was generated from the most general action that could describe the process. This includes up to R^2 monomials to properly account for the graviton propagator, and up to $R\phi\phi$ monomials for the vertices. Collecting the derivative acting on these monomials in the form factors, the most general action, vertices, propagators and amplitudes could be derived. This amounted for the first part of the thesis, from which the following conclusions can be drawn.

1. The amplitude (4.8), and all derived amplitudes, are manifestly gauge independent. The gauge-fixing term contributed to the spin-one and spin-zero sector of the off-shell graviton to ensure a well-defined propagator. Contracting the propagator with the graviton-matter vertices and imposing on-shell conditions, eliminates any gauge-dependence of the result.

2. A decomposition of the scattering amplitude into partial wave amplitudes has proven to be very insightful. In (4.20), it is shown that the Ricci form factor enters the spin-zero amplitude, and the Weyl form factor to the spin-two part. These form factors alter the momentum dependence of the graviton propagator derived from general relativity to

$$\frac{1}{q^2} \to \frac{1}{q^2\big(1+q^2 f_{\mathrm{XX}}(q^2)\big)}. \tag{7.1}$$

   It shows that a suitable choice for the form factor could cancel the typical q^2 divergence of the GR scattering amplitude (5.1).

3. The scattering amplitude is invariant under momentum-dependent field redefinitions of the graviton.

In the second part, the general amplitude was used to analyze some of the established higher-derivative theories. In this part, the scalars were assumed to be massless, and all $R\phi\phi$ form factors were dropped. In this setup, it was possible to analyze unitarity, boundedness and causality for these theories. Figure 5.1 summarizes the behaviour of the the theories studied in this thesis.

- In the absence of the quadratic curvature form factors, the scattering amplitude reduced to the one of GR. This showed the typical linear divergence of the amplitude in the centre-of-mass energy $\mathfrak{s}$.
- The main emphasis of this thesis was to study the high-energy behaviour of scattering amplitudes. Nevertheless, the form factor formalism can naturally be used to include logarithmic structures which arise from effective field theory. These terms account for the leading low-energy corrections to general relativity and are to be used below the corresponding cut-off scale.
- In Stelle gravity, the two curvature form factors are assumed to be constant. This choice introduced a massive pole with a negative residue in the spin-two sector of the off-shell graviton propagator. This ghost state, is known to violate unitarity. They are typical for theories that include time derivatives of the metric perturbation beyond second-order. At energies beyond the mass of the ghost mode, the scattering amplitudes are finite and scale-free.
- In the asymptotic safety program, the Wetterich equation is used to study if the renormalization of coupling constants approaches a fixed point in the UV. The scale-dependence of Newton's constant was determined by applying this method to the Einstein-Hilbert action. The result were two fixed points, a free fixed point, and a non-trivial one in the UV [96]. The running coupling (5.20) interpolates smoothly between these two regimes. The qualitative behaviour of the scattering amplitude due to the scale-dependent coupling constant is analogous to that of Stelle gravity. It has become clear that the renormalization group scheme is not sufficient to account for all momentum-dependence captured by the form factors.
- The exponential form factors of infinite derivative gravity dampen the partial wave amplitudes of the $\mathfrak{s}$-channel amplitude, yielding a renormalizable and asymptotically free theory in the UV-regime. It is unclear if scattering amplitudes obtained by crossing symmetry are UV-finite.

The last part of the thesis analyzes the hyperbolic tangent form factors introduced in [43, 44]. In chapter 6, we analyzed the properties of these form factors and came to the following conclusions.

- The function $\mathfrak{s}\tanh(\mathfrak{s})$ is a positive function, ensuring that the only pole of the propagator is situated at the origin. The ghost mode of Stelle gravity is avoided.
- The scattering amplitude of the $\mathfrak{s}$-channel diagram is finite and scale-free in the high-energy limit. In this regime the growth of the amplitude is cancelled by the tanh contribution. The $\mathfrak{t}$-channel amplitude related by crossing symmetry was not finite. This amplitude scales with $\mathfrak{s}^2$, which violates the causality bound. In this case, it is essential that the scalar self-interaction is included. With an appropriate choice, also the $\mathfrak{t}$-channel is finite.
- The mechanism that underlies the finiteness of the amplitude can be found in the pole structure of the form factors. The poles of the propagator are all situated on the imaginary axis and approach a Regge behaviour, where the poles become equally distanced. Truncating the form factor to a finite order returns massive (ghost) modes which signal the violation of unitarity, mimicking the spin-two ghost of Stelle gravity.
- The model introduced here is similar to Lee-Wick models [97, 98], due to the nature of the pole structure of the tanh-model. Lee-Wick models also have poles in the imaginary plane, and it is known that at time-scales set by the real part of these poles, causality is violated. The poles in the tanh-model are massless however. Following [102], this guarantees to ensure that microcausality is preserved.

- There are no degrees of freedom in the partial wave amplitudes for $j \geq 3$. This is in contrast to the Veneziano and Virasoro-Shapiro amplitudes, which provide a stringy UV-completion through an infinite tower of massive spin resonances.

A next step would be to calculate the form factors from first principles. In [40], a first step in this direction is made. It has been shown that $R + C^2$ gravity projected on the Wetterich equation gives a non-Gaussian fixed point in the UV, and it fixes the asymptotic behaviour of the form factor f_{CC}. An accurate approximation has then been shown to remove the spacetime singularity induced by black holes. Extending the discussion to the form factors of this thesis would then give the full momentum correction to the Newtonian potential.

Another interesting part would be to include other types of matter to the discussion. For example, one could adopt a similar procedure to derive scattering amplitudes for gravity-mediated photon interactions. Although the approach is straightforward conceptually, the explicit calculations become tedious. Scalar-photon scattering is interesting in this regard. It is a logical extension of our work in [43, 44] and requires the introduction of the photon to the action. Besides the typical $F_{\mu\nu}F^{\mu\nu}$ part, all non-equivalent RFF monomials contributing to the graviton-photon three-point vertex should be considered. This is still very much doable (it turns out that there are nine monomials in total), but the number is ever increasing with the introduction of extra tensor indices and it is not always easy to reduce the list of monomials to a minimal basis. Besides the number of monomials, also the number of amplitudes increases. External particles can be in different helicity states, and all amplitudes need to be considered. Nevertheless, programming packages such as *xAct* in *Mathematica* make this feasible. Having the full amplitude at hand, it is then interesting to see if the theory can be linked to experiment in an effective field theory setting. Typical examples are the Shapiro time-delay or superluminal propagation of gravitational waves [108–110]. In particular, it would be very interesting to calculate quantum corrections to the gravitational deflection of light. A massive object can be modelled as a massive scalar field without any quantum fluctuations. Performing a loop computation for a fluctuating photon and graviton field, generates the one-loop form factors. The total scattering amplitude provides a plug-and-play solution, where the form factors are to be substituted directly by the one-loop results. Hence, the form factor formalism provides an easy and methodical approach to study the $\phi\gamma \to \phi\gamma$ scattering amplitude and all its related features.

Appendices

APPENDIX A

Kinematics

In this appendix, the kinematical conventions of this thesis are defined. This will include the sign convention of the space-time metric, the definition of the incoming and outgoing particles in terms of centre-of-mass coordinates, and the relations of the Mandelstam variables to the scattering angle θ.

Most literature regarding general relativity uses the mostly-plus convention, while most literature on quantum field theory uses the mostly-minus convention. In this thesis, I choose to adopt the conventions of QFT,

$$\eta_{\mu\nu} = \text{diag}(1, -1, -1, -1). \tag{A.1}$$

The on-shell condition for a massive scalar field reads,

$$p^2 = \eta_{\mu\nu} p^\mu p^\nu = (p^0)^2 - \boldsymbol{p}^2 = m^2. \tag{A.2}$$

The bold symbol, $\boldsymbol{p}$, indicates the three-vector component of the tensor p^μ. This relation allows us to express p^0 in the mass and momentum of the scalar field. A convenient choice is to switch to the centre-of-mass frame, where the total three-momentum vanishes. This can be represented in the four-momentum of the incoming and outgoing fields

$$\begin{aligned} p_{1\mu} &= \left(\sqrt{\boldsymbol{p}^2 + m_\phi^2}, \boldsymbol{p}\right) & p_{2\mu} &= \left(\sqrt{\boldsymbol{p}^2 + m_\phi^2}, -\boldsymbol{p}\right) \\ p_{3\mu} &= \left(-\sqrt{\boldsymbol{q}^2 + m_\chi^2}, \boldsymbol{q}\right) & p_{4\mu} &= \left(-\sqrt{\boldsymbol{q}^2 + m_\chi^2}, -\boldsymbol{q}\right) \end{aligned} \tag{A.3}$$

Using this convention, all momenta in the Feynman diagrams are incoming. This is indicated by the arrows of the Feynman diagrams in figures 3.1, 4.1, 4.2 and 4.3. Next, we demand energy-momentum conservation of the incoming and outgoing particles,

$$\boldsymbol{p}^2 + m_\phi^2 = \boldsymbol{q}^2 + m_\chi^2. \tag{A.4}$$

In general, the length of the incoming and outgoing three-momenta, $\boldsymbol{p}$ and $\boldsymbol{q}$ respectively, are different. The exception is the case where the masses are equal. In this case, equation (A.4) implies that $|\boldsymbol{p}| = |\boldsymbol{q}|$. In both cases, the incoming and outgoing momenta define a scattering angle θ by

$$\boldsymbol{p} \cdot \boldsymbol{q} = \sqrt{\boldsymbol{p}^2 \cdot \boldsymbol{q}^2} \cos\theta \tag{A.5}$$

In the centre-of-mass frame, we can introduce the Mandelstam variables. They are combinations of the momenta, which often occur in scattering amplitudes,

$$\mathfrak{s} = \big(p_1 + p_2\big)^2 = 4\big(\boldsymbol{p}^2 + m_\phi^2\big) \tag{A.6}$$

$$\mathfrak{t} = \big(p_1 + p_3\big)^2 = -\boldsymbol{p}^2 - \boldsymbol{q}^2 - 2\sqrt{\boldsymbol{p}^2 \cdot \boldsymbol{q}^2}\cos\theta \tag{A.7}$$

$$\mathfrak{u} = \big(p_1 + p_4\big)^2 = -\boldsymbol{p}^2 - \boldsymbol{q}^2 + 2\sqrt{\boldsymbol{p}^2 \cdot \boldsymbol{q}^2}\cos\theta. \tag{A.8}$$

Here $\mathfrak{s}$[5] is the centre-of-mass energy; the total energy of the scattering process measured in the centre-of-mass frame. We can invert equation (A.6) to express $\boldsymbol{p}^2$ (and $\boldsymbol{q}^2$) in terms of $\mathfrak{s}$,

$$\boldsymbol{p}^2 = \frac{1}{4}\mathfrak{s} - m_\phi^2, \quad \boldsymbol{q}^2 = \frac{1}{4}\mathfrak{s} - m_\chi^2. \tag{A.9}$$

This allows us to write all Mandelstam variables in terms of two variables: $\mathfrak{s}$ and θ,

$$\mathfrak{t} = -\left(\frac{\mathfrak{s}}{2} - m_\phi^2 - m_\chi^2 + \frac{1}{2}\sqrt{\big(\mathfrak{s} - 4m_\phi^2\big)\big(\mathfrak{s} - 4m_\chi^2\big)}\cos\theta\right), \tag{A.10}$$

$$\mathfrak{u} = -\left(\frac{\mathfrak{s}}{2} - m_\phi^2 - m_\chi^2 - \frac{1}{2}\sqrt{\big(\mathfrak{s} - 4m_\phi^2\big)\big(\mathfrak{s} - 4m_\chi^2\big)}\cos\theta\right). \tag{A.11}$$

Finally, we can easily check the well-known identity

$$\mathfrak{s} + \mathfrak{t} + \mathfrak{u} = 2\big(m_\phi^2 + m_\chi^2\big), \tag{A.12}$$

showing us the linear dependence of the Mandelstam variables. In the case that the incoming and outgoing particles are the same, equations (A.10) and (A.11) simplify. This can be seen as taking $m_\chi^2 = m_\phi^2$.

$$\mathfrak{t} = -\frac{1}{2}\big(\mathfrak{s} - 4m_\phi^2\big)\big(1 - \cos\theta\big) \tag{A.13}$$

$$\mathfrak{u} = -\frac{1}{2}\big(\mathfrak{s} - 4m_\phi^2\big)\big(1 + \cos\theta\big) \tag{A.14}$$

[5] To remove any confusion about the use of the fraktur typesetting, these are the normal Mandelstam variables which one could encounter in an everyday QFT-textbook.

APPENDIX B

Properties of the curvature tensors

B.1 Symmetries in the curvature tensors

1. We will work with the Christoffel symbol, which is the unique metric compatible connection satisfying

$$\Gamma^{\lambda}_{\ \mu\nu} = \Gamma^{\lambda}_{\ \nu\mu}, \qquad D_\lambda g_{\mu\nu} = 0. \tag{B.1}$$

2. The Riemann tensor has the following set of internal symmetries:

$$\begin{aligned} R_{\mu\nu\rho\sigma} &= -R_{\nu\mu\rho\sigma} = -R_{\mu\nu\sigma\rho}, \\ R_{\mu\nu\rho\sigma} &= R_{\rho\sigma\mu\nu}. \end{aligned} \tag{B.2}$$

3. The Riemann tensor satisfies the two Bianchi indentities:

$$R_{\mu[\nu\rho\sigma]} = 0, \tag{B.3}$$

$$D_{[\alpha}R_{\mu\nu]\rho\sigma} = 0. \tag{B.4}$$

   In this notation, the square brackets denote the antisymmetrization of a tensor in the indicated indices. Similarly, the symmetrization of a tensor is denoted with parentheses. Formally, for an arbitrary tensor T of rank n,

$$T_{(\mu_1,\ldots,\mu_n)} = \frac{1}{n!}\sum_{\sigma\in\mathfrak{S}_n} T_{\sigma(\mu_1),\ldots,\sigma(\mu_n)}, \tag{B.5}$$

$$T_{[\mu_1,\ldots,\mu_n]} = \frac{1}{n!}\sum_{\sigma\in\mathfrak{S}_n} \mathrm{sgn}(\sigma) T_{\sigma(\mu_1),\ldots,\sigma(\mu_n)}. \tag{B.6}$$

   Here, $\mathfrak{S}_n$ is the symmetric group of order n.

4. The Ricci tensor and Ricci scalar are defined as

$$R_{\mu\nu} = g^{\mu\rho}R_{\mu\nu\rho\sigma}, \tag{B.7}$$

$$R = g^{\mu\nu}R_{\mu\nu}. \tag{B.8}$$

5. For the Ricci tensor and Ricci scalar, we have the relation.

$$D_\mu R^\mu_{\ \nu} = \frac{1}{2} D_\nu R. \tag{B.9}$$

It comes from contracting indices of the Riemann tensor in the second Bianchi identity, hence the name "contracted Bianchi identity".

B.2 Linearized Einstein field equations

The full metric is expanded around a flat Minkowskian background.

$$g_{\mu\nu} = \eta_{\mu\nu} + h_{\mu\nu}, \tag{B.10}$$

$$g^{\mu\nu} \simeq \eta^{\mu\nu} - h^{\mu\nu}, \tag{B.11}$$

$$\sqrt{-g} \simeq 1 + \frac{1}{2} h. \tag{B.12}$$

Here $\simeq$ symbol means that the expansion is truncated at first order in h. This gives the following expansion of the Christoffel symbol, the Riemann and Ricci curvature tensors, and the Ricci curvature scalar

$$\Gamma^\lambda_{\ \mu\nu} \simeq \frac{1}{2}\Big(\partial_\mu h^\lambda_{\ \nu} + \partial_\nu h^\lambda_{\ \mu} - \partial^\lambda h_{\mu\nu}\Big), \tag{B.13}$$

$$R_{\mu\nu\rho\sigma} \simeq \frac{1}{2}\Big(\partial_\mu\partial_\sigma h_{\nu\rho} + \partial_\nu\partial_\rho h_{\mu\sigma} - \partial_\mu\partial_\rho h_{\nu\sigma} - \partial_\nu\partial_\sigma h_{\mu\rho}\Big), \tag{B.14}$$

$$R_{\mu\nu} \simeq \frac{1}{2}\Big(\partial_\alpha\partial_\mu h_\nu^{\ \alpha} + \partial_\alpha\partial_\nu h_\mu^{\ \alpha} - \partial^2 h_{\mu\nu} - \partial_\mu\partial_\nu h\Big), \tag{B.15}$$

$$R \simeq \partial_\beta\partial_\alpha h^{\alpha\beta} - \partial^2 h. \tag{B.16}$$

We also remark that the Weyl tensor has the following decomposition in four dimensions

$$C_{\mu\nu\rho\sigma} = R_{\mu\nu\rho\sigma} + \frac{1}{2}\Big(g_{\rho\nu}R_{\mu\sigma} + g_{\sigma\mu}R_{\nu\rho} - g_{\sigma\nu}R_{\mu\rho} - g_{\rho\mu}R_{\nu\sigma}\Big) + \frac{1}{6}\Big(g_{\rho\mu}g_{\sigma\nu} - g_{\rho\nu}g_{\sigma\mu}\Big)R \tag{B.17}$$

such that at first order in h, we have

$$\begin{aligned}
C_{\mu\nu\rho\sigma} \simeq\ & \frac{1}{2}\Big(\partial_\mu\partial_\sigma h_{\nu\rho} + \partial_\nu\partial_\rho h_{\mu\sigma} - \partial_\nu\partial_\sigma h_{\mu\rho} - \partial_\mu\partial_\rho h_{\nu\sigma}\Big) \\
& + \frac{1}{4}\Big(\eta_{\nu\sigma}\partial^2 h_{\mu\rho} - \eta_{\nu\rho}\partial^2 h_{\mu\sigma} - \eta_{\mu\sigma}\partial^2 h_{\nu\rho} + \eta_{\mu\rho}\partial^2 h_{\nu\sigma} \\
& \quad - \eta_{\nu\sigma}\partial^\alpha\partial_\mu h_{\rho\alpha} + \eta_{\nu\rho}\partial^\alpha\partial_\mu h_{\sigma\alpha} + \eta_{\mu\sigma}\partial^\alpha\partial_\nu h_{\rho\alpha} - \eta_{\mu\rho}\partial^\alpha\partial_\nu h_{\sigma\alpha} \\
& \quad - \eta_{\nu\sigma}\partial^\alpha\partial_\rho h_{\mu\alpha} + \eta_{\mu\sigma}\partial^\alpha\partial_\rho h_{\nu\alpha} + \eta_{\nu\rho}\partial^\alpha\partial_\sigma h_{\mu\alpha} - \eta_{\mu\rho}\partial^\alpha\partial_\sigma h_{\nu\alpha} \\
& \quad + \eta_{\nu\sigma}\partial_\mu\partial_\rho h - \eta_{\nu\rho}\partial_\mu\partial_\sigma h - \eta_{\mu\sigma}\partial_\nu\partial_\rho h + \eta_{\mu\rho}\partial_\nu\partial_\sigma h\Big) \\
& + \frac{1}{6}\Big(\eta_{\mu\rho}\eta_{\nu\sigma}\partial^\alpha\partial^\beta h_{\alpha\beta} - \eta_{\mu\sigma}\eta_{\nu\rho}\partial^\alpha\partial^\beta h_{\alpha\beta} + \eta_{\mu\sigma}\eta_{\nu\rho}\partial^2 h - \eta_{\mu\rho}\eta_{\nu\sigma}\partial^2 h\Big).
\end{aligned} \tag{B.18}$$

The Einstein-Hilbert action gives the vacuum equations of motion. To include the matter part into the equations, a matter Langrangian, $\mathcal{L}_M$, is added to the action. The stress-energy tensor is then proportional to the matter terms appearing in the equations of motion

$$T_{\mu\nu} \equiv -\frac{2}{\sqrt{-g}} \frac{\delta\big(\sqrt{-g}\mathcal{L}_M\big)}{\delta g^{\mu\nu}}. \tag{B.19}$$

Expanding the equations of motion up to first order, we obtain the linearized Einstein field equations

$$\begin{aligned} R_{\mu\nu} - \frac{1}{2} g_{\mu\nu} R & \\ &\simeq -\frac{1}{2}\Big(\partial^2 h_{\mu\nu} - \partial_\alpha \partial_\mu h_\nu{}^\alpha - \partial_\alpha \partial_\nu h_\mu{}^\alpha + \eta_{\mu\nu}\partial_\beta \partial_\alpha h^{\alpha\beta} - \eta_{\mu\nu}\partial^2 h + \partial_\mu \partial_\nu h\Big) \\ &= 8\pi G_N T_{\mu\nu} \end{aligned} \tag{B.20}$$

Imposing the harmonic gauge condition on the metric perturbation simplifies the linearized equations to

$$\partial^2 h_{\mu\nu} - \frac{1}{2}\eta_{\mu\nu}\partial^2 h = -16\pi G_N T_{\mu\nu}. \tag{B.21}$$

Taking the trace on both sides gives

$$\partial^2 h = 16\pi G_N T. \tag{B.22}$$

Plugging this back in, we get the inhomogeneous wave equation for the metric perturbation, equation (3.6)

$$\partial^2 h_{\mu\nu} = -16\pi G_N \Big(T_{\mu\nu} - \frac{1}{2}\eta_{\mu\nu} T\Big). \tag{B.23}$$

APPENDIX C

Propagator and vertex calculations

The following calculations have been confirmed with the *xAct* package suite in Mathematica [64]. *xAct* is relatively new and provides a wide variety of field and tensor manipulations suited for research in high energy physics or classical field theory. For the research done in this thesis, we have made particular use of the tensor computer algebra package *xTras*, [70], which provides additional features to calculate the appropriate vertices of a classical field theory. We have made great use of the following build-in functions:

- *AllContractions:* To calculate the minimal basis of monomials in sections 3.2.1 and 3.2.3.
- *SolveConstants:* To project the graviton propagator and graviton-matter vertex onto the basis of spin projection operators (see appendix D).
- *VarD:* To calculate variational derivatives of the quantum effective action.

C.1 Propagator calculations

The relevant contributions to the graviton propagator come from the curvature and gauge fixing terms. These were encoded in equation (3.19)

$$\Gamma_{\text{grav}} + \Gamma_{\text{gf}} = \frac{1}{16\pi G_N}\Bigg[\int \mathrm{d}^4x\sqrt{-g}\Big(-R - \frac{1}{6}Rf_{\text{RR}}(\Delta)R + \frac{1}{2}C_{\mu\nu\rho\sigma}f_{\text{CC}}(\Delta)C^{\mu\nu\rho\sigma}\Big) + \frac{1}{2\alpha}\int \mathrm{d}^4x\,\mathcal{F}_\mu\mathcal{F}^\mu\Bigg]. \tag{C.1}$$

They are found by expanding the curvature tensors in h. Here we make use of (B.16) and (B.18) of appendix B. We notice that the flat Minkowski background reduces the subsequent result. The Ricci scalar and Weyl tensor vanishes in this case. This means that the factors of h have to come from the linear expansion of the Ricci scalar and Weyl tensor, and we do not need to expand the Laplacian Δ or the metric determinant beyond zeroth order. Following this procedure, we get

$$
\begin{aligned}
\Gamma_{\text{grav}}+\Gamma_{\text{gf}} \simeq \frac{1}{16\pi G_N}\int \mathrm{d}^4x\Big(& -2h^{\alpha\beta}\partial_\alpha\partial_\beta h+2h^{\alpha\beta}\partial_\beta\partial_\gamma h_\alpha{}^\gamma+\frac{1}{2}\partial_\beta h\partial^\beta h+2\partial_\alpha h^{\alpha\beta}\partial_\gamma h_\beta{}^\gamma \\
& -2\partial^\beta h\partial_\gamma h_\beta{}^\gamma+2h^{\alpha\beta}\partial_\gamma\partial_\beta h_\alpha{}^\gamma-h\partial_\gamma\partial_\beta h^{\beta\gamma}-2h^{\alpha\beta}\partial^2 h_{\alpha\beta}+h\partial^2 h+\partial_\beta h_{\alpha\gamma}\partial^\gamma h^{\alpha\beta} \\
& -\frac{3}{2}\partial_\gamma h_{\alpha\beta}\partial^\gamma h^{\alpha\beta} \\
& -\frac{1}{6}\Big[\partial_\alpha\partial_\beta h^{\alpha\beta}-\partial^2 h\Big]f_{\text{RR}}(-\partial^2)\Big[\partial_\alpha\partial_\beta h^{\alpha\beta}-\partial^2 h\Big] \\
& +\frac{1}{32}\Big[\eta_{\nu\sigma}\partial^2 h_{\mu\rho}-\eta_{\nu\rho}\partial^2 h_{\mu\sigma}-\eta_{\mu\sigma}\partial^2 h_{\nu\rho}+\eta_{\mu\rho}\partial^2 h_{\nu\sigma}-\eta_{\nu\sigma}\partial_\alpha\partial_\mu h_\rho{}^\alpha+\eta_{\nu\rho}\partial_\alpha\partial_\mu h_\sigma{}^\alpha \\
& \quad +\eta_{\mu\sigma}\partial_\alpha\partial_\nu h_\rho{}^\alpha-\eta_{\mu\rho}\partial_\alpha\partial_\nu h_\sigma{}^\alpha-\eta_{\nu\sigma}\partial_\alpha\partial_\rho h_\mu{}^\alpha+\eta_{\mu\sigma}\partial_\alpha\partial_\rho h_\nu{}^\alpha+\eta_{\nu\rho}\partial_\alpha\partial_\sigma h_\mu{}^\alpha \\
& \quad -\eta_{\mu\rho}\partial_\alpha\partial_\sigma h_\nu{}^\alpha+\eta_{\nu\sigma}\partial_\mu\partial_\rho h-\eta_{\nu\rho}\partial_\mu\partial_\sigma h-\eta_{\mu\sigma}\partial_\nu\partial_\rho h+\eta_{\mu\rho}\partial_\nu\partial_\sigma h \\
& \quad -\frac{2}{3}\eta_{\mu\sigma}\eta_{\nu\rho}\partial_\alpha\partial_\beta h^{\alpha\beta}+\frac{2}{3}\eta_{\mu\rho}\eta_{\nu\sigma}\partial_\alpha\partial_\beta h^{\alpha\beta}+\frac{2}{3}\eta_{\mu\sigma}\eta_{\nu\rho}\partial^2 h-\frac{2}{3}\eta_{\mu\rho}\eta_{\nu\sigma}\partial^2 h \\
& \quad -2\partial_\mu\partial_\nu h_{\rho\sigma}-2\partial_\mu\partial_\rho h_{\nu\sigma}+2\partial_\mu\partial_\sigma h_{\nu\rho}+2\partial_\mu\partial_\nu h_{\rho\sigma}+2\partial_\nu\partial_\rho h_{\mu\sigma}-2\partial_\nu\partial_\sigma h_{\mu\rho}\Big] \\
& \quad \times f_{\text{CC}}(-\partial^2)\times \\
& \quad \Big[\eta^{\nu\sigma}\partial^2 h^{\mu\rho}-\eta^{\nu\rho}\partial^2 h^{\mu\sigma}-\eta^{\mu\sigma}\partial^2 h^{\nu\rho}+\eta^{\mu\rho}\partial^2 h^{\nu\sigma}-\eta^{\nu\sigma}\partial_\alpha\partial^\mu h^{\rho\alpha}+\eta^{\nu\rho}\partial_\alpha\partial^\mu h^{\sigma\alpha} \\
& \quad +\eta^{\mu\sigma}\partial_\alpha\partial^\nu h^{\rho\alpha}-\eta^{\mu\rho}\partial_\alpha\partial^\nu h^{\sigma\alpha}-\eta^{\nu\sigma}\partial_\alpha\partial^\rho h^{\mu\alpha}+\eta^{\mu\sigma}\partial_\alpha\partial^\rho h^{\nu\alpha}+\eta^{\nu\rho}\partial_\alpha\partial^\sigma h^{\mu\alpha} \\
& \quad -\eta^{\mu\rho}\partial_\alpha\partial^\sigma h^{\nu\alpha}+\eta^{\nu\sigma}\partial^\mu\partial^\rho h-\eta^{\nu\rho}\partial^\mu\partial^\sigma h-\eta^{\mu\sigma}\partial^\nu\partial^\rho h+\eta^{\mu\rho}\partial^\nu\partial^\sigma h \\
& \quad -\frac{2}{3}\eta^{\mu\sigma}\eta^{\nu\rho}\partial_\alpha\partial_\beta h^{\alpha\beta}+\frac{2}{3}\eta^{\mu\rho}\eta^{\nu\sigma}\partial_\alpha\partial_\beta h^{\alpha\beta}+\frac{2}{3}\eta^{\mu\sigma}\eta^{\nu\rho}\partial^2 h-\frac{2}{3}\eta^{\mu\rho}\eta^{\nu\sigma}\partial^2 h \\
& \quad -2\partial^\mu\partial^\nu h^{\rho\sigma}-2\partial^\mu\partial^\rho h^{\nu\sigma}+2\partial^\mu\partial^\sigma h^{\nu\rho}+2\partial^\mu\partial^\nu h^{\rho\sigma}+2\partial^\nu\partial^\rho h^{\mu\sigma}-2\partial^\nu\partial^\sigma h^{\mu\rho}\Big] \\
& +\frac{(\beta+1)^2}{32\alpha}\partial_\beta h\partial^\beta h+\frac{1}{2\alpha}\partial_\alpha h^{\alpha\beta}\partial_\gamma h_\beta{}^\gamma-\frac{\beta+1}{4\alpha}\partial_\beta h\partial_\gamma h^{\beta\gamma}\Big)
\end{aligned}
\tag{C.2}
$$

This result is not very illuminating, but it can be simplified significantly.The partial derivatives can be removed by switching to momentum space by a Fourier transformation of the metric perturbation. This replaces all $\partial_\mu \to iq_\mu$, with q_μ being the graviton momentum. This way, the tensor contractions can be pulled through the form factors. The Fourier transform is denoted by the operator $\hat{\mathcal{F}}$, and applying this operation to (C.2) gives

$$
\begin{aligned}
\hat{\mathcal{F}}\big(\Gamma_{\text{grav}}+\Gamma_{\text{gf}}\big) = \frac{1}{64\pi G_N}\Big(& q^2\big(7+q^2 f_{\text{CC}}(q^2)\big)h_{\alpha\beta}h^{\alpha\beta} \\
& -\Big[2+\frac{3(\beta+1)^2}{8\alpha}+\frac{1+q^2 f_{\text{CC}}(q^2)}{3}+\frac{2\big(1+q^2 f_{\text{RR}}(q^2)\big)}{3}\Big]q^2h^2 \\
& -2\Big[\frac{1+6\alpha}{\alpha}+1+q^2 f_{\text{CC}}(q^2)\Big]q^\alpha q^\beta h_\alpha{}^\gamma h_{\beta\gamma} \\
& +\Big[8+\frac{\beta+1}{\alpha}+\frac{2}{3}\big(1+q^2 f_{\text{CC}}(q^2)\big)+\frac{4}{3}\big(1+q^2 f_{\text{RR}}(q^2)\big)\Big]q^\alpha q^\beta h_{\alpha\beta}h \\
& +\frac{2}{3}\Big[f_{\text{CC}}(q^2)-f_{\text{RR}}(q^2)\Big]q^\alpha q^\beta q^\gamma q^\delta h_{\alpha\beta}h_{\gamma\delta}\Big).
\end{aligned}
\tag{C.3}
$$

We now take two functional derivatives with respect to the metric perturbation.

$$\begin{aligned}\left(\frac{\delta^2\hat{\mathcal{F}}\left(\Gamma_{\text{grav}}+\Gamma_{\text{gf}}\right)}{\delta h_{\mu\nu}\delta h_{\rho\sigma}}\right) = \frac{1}{64\pi G_N}\Big(&q^2\left(1+q^2 f_{\text{CC}}(q^2)\right)\left(\eta^{\mu\sigma}\eta^{\nu\rho}+\eta^{\mu\rho}\eta^{\nu\sigma}\right)\\ &+\Big[\frac{(\beta+1)^2}{4\alpha}-\frac{2}{3}\left(1+q^2 f_{\text{CC}}(q^2)\right)-\frac{4}{3}\left(1+q^2 f_{\text{RR}}(q^2)\right)\Big]q^2\eta^{\mu\nu}\eta^{\rho\sigma}\\ &+\Big[-\frac{\beta+1}{\alpha}+\frac{2}{3}\left(1+q^2 f_{\text{CC}}(q^2)\right)+\frac{4}{3}\left(1+q^2 f_{\text{RR}}(q^2)\right)\Big]\left(\eta^{\mu\nu}q^\rho q^\sigma+\eta^{\rho\sigma}q^\mu q^\nu\right)\\ &+\Big[\frac{1}{\alpha}-\left(1+q^2 f_{\text{CC}}(q^2)\right)\Big]\left(\eta^{\nu\sigma}q^\mu q^\rho+\eta^{\mu\sigma}q^\nu q^\rho+\eta^{\nu\rho}q^\mu q^\sigma+\eta^{\mu\rho}q^\nu q^\sigma\right)\\ &+\frac{4}{3}\Big[f_{\text{CC}}(q^2)-f_{\text{RR}}(q^2)\Big]q^\mu q^\nu q^\rho q^\sigma\Big)\end{aligned} \tag{C.4}$$

The final step in this calculation is to invert this expression. Although this can in principle be done, it is worth the wait to introduce a convenient basis of operators. In appendix D, we introduce the spin projection operators, which allows us to distinguish between the different spin components of the graviton. Then, we decompose equation (C.4) into this basis. Also decomposing the graviton propagator in this basis, we see that the components are easily obtained.

C.2 Vertex calculations

Here, I will follow the notation of [66]. The part of the action that contributes to this vertex is equation (3.29)

$$\begin{aligned}\Gamma_{\text{matter}} = \int \mathrm{d}^4x\sqrt{-g}\Big(&\phi f_{\phi\phi}(\Delta)\phi\\ &+ f_{\text{R}\phi\phi}(\Delta_1,\Delta_2,\Delta_3)R\phi\phi + f_{\text{Ric}\phi\phi}(\Delta_1,\Delta_2,\Delta_3)R^{\mu\nu}D_\mu\phi D_\nu\phi\Big).\end{aligned} \tag{C.5}$$

First we focus on the kinetic part $\Gamma_{\phi\phi}$. Contributions to the $h\phi\phi$-vertex are generated by expanding Δ. To first order in h, we get

$$\begin{aligned}\Delta\phi &= -g^{\mu\nu}D_\mu D_\nu\phi\\ &\simeq -\left(\eta^{\mu\nu}-h^{\mu\nu}\right)D_\mu\partial_\nu\phi\\ &= -\left(\eta^{\mu\nu}-h^{\mu\nu}\right)\left(\partial_\mu\partial_\nu\phi-\Gamma^\lambda_{\mu\nu}\partial_\lambda\phi\right)\\ &= \Box\phi + h^{\mu\nu}\partial_\mu\partial_\nu\phi+\eta^{\mu\nu}\Gamma^\lambda_{\mu\nu}\partial_\lambda\phi.\end{aligned} \tag{C.6}$$

The flat Minkowski background metric has a vanishing Christoffel symbol. That means up to first order in h we have

$$\begin{aligned}\Delta\phi &\simeq \Box\phi + h^{\mu\nu}\partial_\mu\partial_\nu\phi+\frac{1}{2}\eta^{\mu\nu}\eta^{\lambda\sigma}\left(\partial_\mu h_{\nu\sigma}+\partial_\nu h_{\mu\sigma}-\partial_\sigma h_{\mu\nu}\right)\partial_\lambda\phi\\ &= \Box\phi + h^{\mu\nu}\partial_\mu\partial_\nu\phi+\left(\partial_\mu h^{\mu\lambda}-\frac{1}{2}\partial^\lambda h\right)\partial_\lambda\phi\\ &= \Box\phi + \left(h^{\mu\nu}\partial_\mu\partial_\nu+\partial_\mu h^{\mu\nu}\partial_\nu-\frac{1}{2}\partial^\mu h\partial_\mu\right)\phi\\ &= \Box\phi + \mathfrak{d}_1\phi\end{aligned} \tag{C.7}$$

where d_1 is the following differential operator, which is linear in $h_{\mu\nu}$

$$\mathrm{d}_1 = h^{\mu\nu}\partial_\mu\partial_\nu + \partial_\mu h^{\mu\nu}\partial_\nu - \frac{1}{2}\partial^\mu h \partial_\mu. \tag{C.8}$$

With the techniques of [66], we are now able to deduce the full graviton-matter vertex. With "full" I mean that all calculations can be done explicitly, without relying on a expansion method of some kind. The prerequisite is that the form factors have a well-defined Laplace transform. In that case, we have

$$\begin{aligned}\Gamma_{\phi\phi} &= \frac{1}{2}\int \mathrm{d}^4x\sqrt{-g}\phi f_{\phi\phi}(\Delta)\phi \\ &= \frac{1}{2}\int \mathrm{d}^4x\sqrt{-\eta}\left(1+\frac{1}{2}h\right)\phi\int_0^\infty \mathrm{d}s\tilde{f}(s)\big(1+V(0;-s\Box,-s\mathrm{d}_1)\big)e^{-s\Box}\phi \\ &= \frac{1}{2}\int \mathrm{d}^4x\left[\frac{1}{2}h\phi f_{\phi\phi}(\Box)\phi + \int_0^\infty \mathrm{d}s\tilde{f}(s)\phi V(0;-s\Box,-s\mathrm{d}_1)e^{-s\Box}\phi\right].\end{aligned} \tag{C.9}$$

where the operator V is defined as

$$V(\epsilon;X,Y) = \sum_{j=0}^\infty \frac{1}{(j+1)!}\big[X+\epsilon Y,Y\big]_j \tag{C.10}$$

and the multicommutator $\big[X,Y\big]_j$ is defined recursively as

$$\big[X,Y\big]_j \equiv \big[X,\big[X,Y\big]_{j-1}\big], \qquad \big[X,Y\big]_0 = Y, \quad \forall j\in\mathbb{N}_{\geqslant 0}. \tag{C.11}$$

Writing the (C.9) in terms of this multicommutator expansion, we obtain

$$\Gamma_{\phi\phi} = \frac{1}{2}\int \mathrm{d}^4x\left[\frac{1}{2}h\phi f_{\phi\phi}(\Box)\phi + \int_0^\infty \mathrm{d}s\tilde{f}(s)\phi\sum_{j=0}^\infty\frac{1}{(j+1)!}\left[-s\Box,-s\mathrm{d}_1\right]_j e^{-s\Box}\phi\right] \tag{C.12}$$

Now, we pull s out of the commutator, and we make use of the identity

$$\int \mathrm{d}^4x\sqrt{-g}Y\left[\Box,Z\right]_j X = \int \mathrm{d}^4x\sqrt{-g}\sum_{l=0}^j\binom{j}{l}(-1)^l(\Box^{j-l}Y)Z(\Box^l X) \tag{C.13}$$

where X,Y and Z are (differential) operators. Applying this to (C.12) gives

$$\begin{aligned}\Gamma_{\phi\phi} &= \frac{1}{2}\int \mathrm{d}^4x\left[\frac{1}{2}h\phi f_{\phi\phi}(\Box)\phi + \int_0^\infty \mathrm{d}s\tilde{f}(s)\sum_{j=0}^\infty\frac{(-s)^{j+1}}{(j+1)!}\sum_{l=0}^j\binom{j}{l}(-1)^l(\Box^{j-l}\phi)\mathrm{d}_1\Box^l e^{-s\Box}\phi\right] \\ &= \frac{1}{2}\int \mathrm{d}^4x\Bigg[\frac{1}{2}f_{\phi\phi}(\Box_3)h\phi\phi \\ &\qquad + \int_0^\infty \mathrm{d}s\tilde{f}(s)\sum_{j=0}^\infty\frac{(-s)^{j+1}}{(j+1)!}\sum_{l=0}^j\binom{j}{l}(-1)^l\Box_2^{j-l}\tilde{\mathrm{d}}^{\mu\nu}_{1,3}\Box_3^l e^{-s\Box_3}h_{\mu\nu}\phi\phi\Bigg]\end{aligned} \tag{C.14}$$

The indices of the box operators indicate on which object they act. This way, $\Box_1$ acts on h, $\Box_2$ on the first ϕ and $\Box_3$ and the second ϕ. From d_1, we get differential operators acting on h and the last

ϕ. This is captured in $\tilde{\mathrm{d}}_{1,3}$, which is derived from

$$\begin{aligned}\phi \mathrm{d}_1 \phi &= \phi \left(h^{\mu\nu}\partial_\mu\partial_\nu + \partial_\mu h^{\mu\nu}\partial_\nu - \frac{1}{2}\partial^\mu h \partial_\mu \right) \phi \\ &= \left(\partial_3^\mu \partial_3^\nu + \partial_1^\mu \partial_3^\nu - \frac{1}{2}\partial_1^\alpha \partial_{3\alpha}\eta^{\mu\nu} \right) h_{\mu\nu}\phi\phi \\ &= \tilde{\mathrm{d}}_{1,3}^{\mu\nu} h_{\mu\nu}\phi\phi \end{aligned} \tag{C.15}$$

such that

$$\tilde{\mathrm{d}}_{1,3}^{\mu\nu} = \partial_3^\mu \partial_3^\nu + \partial_1^\mu \partial_3^\nu - \frac{1}{2}\partial_1^\alpha \partial_{3\alpha}\eta^{\mu\nu}$$

As remarked by the authors of [66], both sums and the s-integral can be done explicitly. This leaves

$$\Gamma_{\phi\phi} = \frac{1}{2}\int \mathrm{d}^4x \left[\frac{1}{2} f_{\phi\phi}(\Box_3) h\phi\phi + \frac{f_{\phi\phi}(\Box_2) - f_{\phi\phi}(\Box_3)}{\Box_2 - \Box_3} \tilde{\mathrm{d}}_{1,3}^{\mu\nu} h_{\mu\nu}\phi\phi \right]. \tag{C.16}$$

This finalizes the result. The contribution of $\Gamma_{\phi\phi}$ to the graviton-matter vertex comes from

$$\Gamma_{\phi\phi} \simeq \frac{1}{2}\int \mathrm{d}^4x \left[\frac{1}{2} f_{\phi\phi}(\Box_3)\eta^{\mu\nu} + \frac{f_{\phi\phi}(\Box_2) - f_{\phi\phi}(\Box_3)}{\Box_2 - \Box_3} \left(\partial_3^\mu \partial_3^\nu + \partial_1^\mu \partial_3^\nu - \frac{1}{2}\partial_1^\alpha \partial_{3\alpha}\eta^{\mu\nu} \right) \right] h_{\mu\nu}\phi\phi. \tag{C.17}$$

A similar result can be obtained for the other monomials in equation (C.5). The calculation for this as a little less tedious. The h contribution has to come from the curvature tensor, because we have a flat Minkowski background. The metric and form factors do not need to be expanded for the $h\phi\phi$-contribution.

$$\begin{aligned}\int \mathrm{d}^4x\sqrt{-g} f_{\mathrm{R}\phi\phi}(\Delta_1,\Delta_2,\Delta_3) R\phi\phi &= \int \mathrm{d}^4x f_{\mathrm{R}\phi\phi}(\Box_1,\Box_2\Box_3) \left(\partial^\nu\partial^\mu h_{\mu\nu} - \partial^2 h \right)\phi\phi \\ &= \int \mathrm{d}^4x f_{\mathrm{R}\phi\phi}(\Box_1,\Box_2\Box_3) \left(\partial_1^\nu\partial_1^\mu - \eta^{\mu\nu}\partial^2 \right) h_{\mu\nu}\phi\phi, \end{aligned} \tag{C.18}$$

and

$$\begin{aligned}&\int \mathrm{d}^4x\sqrt{-g} f_{\mathrm{Ric}\phi\phi}(\Delta_1,\Delta_2,\Delta_3) R^{\mu\nu} D_\mu D_\nu \phi\phi \\ &= \int \mathrm{d}^4x f_{\mathrm{Ric}\phi\phi}(\Box_1,\Box_2,\Box_3) \left(\partial_\nu\partial_\alpha h_\beta^{\ \nu} - \frac{1}{2}\partial_\beta\partial_\alpha h - \frac{1}{2}\partial^2 h_{\alpha\beta} \right) \partial^\beta\partial^\alpha\phi\phi \\ &= \int \mathrm{d}^4x f_{\mathrm{Ric}\phi\phi}(\Box_1,\Box_2,\Box_3) \left(\partial_1^\nu\partial_{1\alpha}\partial_2^\mu\partial_2^\alpha - \frac{1}{2}\eta^{\mu\nu}\partial_{1\alpha}\partial_{1\beta}\partial_2^\alpha\partial_2^\beta - \frac{1}{2}\partial_1^2\partial_2^\mu\partial_2^\nu \right) h_{\mu\nu}\phi\phi. \end{aligned} \tag{C.19}$$

The remainder of the computation is straightforward. Collecting the terms from equations (C.17), (C.18) and (C.19) the next step is the Fourier transform of the fields h and ϕ to obtain the vertex in momentum space. Effectively, this means we set $\partial_1 \to iq$, $\partial_2 \to ip_{\phi_1}$ and $\partial_3 \to ip_{\phi_2}$. The result is

then read of from the remaining term in the brackets, giving (3.37)

$$\begin{aligned}\mathcal{V}^{\mu\nu}_{h\phi\phi}(q,p_{\phi_1},p_{\phi_2}) = &\frac{1}{4}\eta^{\mu\nu}f_{\phi\phi}(p^2_{\phi_1})\\ &-\frac{1}{2}\frac{f_{\phi\phi}(p^2_{\phi_1})-f_{\phi\phi}(p^2_{\phi_2})}{p^2_{\phi_1}-p^2_{\phi_2}}\left(p^\mu_{\phi_1}p^\nu_{\phi_1}-\frac{1}{2}\eta^{\mu\nu}q\cdot p_{\phi_1}+\frac{1}{2}\left(q^\mu p^\nu_{\phi_1}+q^\nu p^\mu_{\phi_1}\right)\right)\\ &+f_{\mathrm{R}\phi\phi}(q^2,p^2_{\phi_1},p^2_{\phi_2})\left(q^2\eta^{\mu\nu}-q^\mu q^\nu\right)\\ &-\frac{1}{2}f_{\mathrm{Ric}\phi\phi}(q^2,p^2_{\phi_1},p^2_{\phi_2})\left(\frac{1}{2}\left(q^2+p^2_{\phi_1}-p^2_{\phi_2}\right)\left(q^\mu p^\nu_{\phi_1}+q^\nu p^\mu_{\phi_1}\right)+\right.\\ &\qquad\left.\frac{1}{4}\left(q^2+p^2_{\phi_1}-p^2_{\phi_2}\right)\eta^{\mu\nu}+q^2p^\mu_{\phi_1}p^\nu_{\phi_1}\right)\\ &+(p_{\phi_1}\leftrightarrow p_{\phi_2}).\end{aligned} \tag{C.20}$$

APPENDIX D

Spin projection operators

In this appendix, we introduce a set of operators which allows us to distinguish the different spin components of the graviton. A conventional choice are the Barnes-Rivers operators [111], which have been used with great success in four-dimensional quantum gravity [112], where they are dubbed spin-projectors. The name already reveal what these operators do. They decompose the graviton in various spin states. Any symmetric rank-two tensor such as the graviton can be decomposed into irreducible representations of $SO(3)$, labelled by a bold integer $\boldsymbol{j}$ and have dimension $2j+1$. An extensive discussion is given in [69], which shows that the graviton can be decomposed into two spin-zero multiplets, a spin-one singlet and a spin-two singlet. Schematically, $h_{\mu\nu} \in \mathbf{0} \oplus \mathbf{0} \oplus \mathbf{1} \oplus \mathbf{2}$.

The way to do this is to project the tensor along its transverse and longitudinal parts by introducing the operators

$$\theta_{\mu\nu} = \eta_{\mu\nu} - \omega_{\mu\nu}, \quad \omega_{\mu\nu} \equiv \frac{q^\mu q^\nu}{q^2}. \tag{D.1}$$

These satisfy

$$q^\mu \theta_{\mu\nu} = 0, \qquad q^\mu \omega_{\mu\nu} = q_\nu. \tag{D.2}$$

In four-dimensional theories, the four operators that project any symmetric rank-two tensor onto the irreducible representations of $SO(3)$ are represented as combinations of $\theta_{\mu\nu}$ and $\omega_{\mu\nu}$

$$\begin{aligned}
\mathcal{P}_2^{\mu\nu\rho\sigma} &= \frac{1}{2}\Big(\theta^{\mu\rho}\theta^{\nu\sigma} + \theta^{\mu\sigma}\theta^{\nu\rho}\Big) - \frac{1}{3}\theta^{\mu\nu}\theta^{\rho\sigma}, \\
\mathcal{P}_1^{\mu\nu\rho\sigma} &= \frac{1}{2}\Big(\theta^{\mu\rho}\omega^{\nu\sigma} + \theta^{\mu\sigma}\omega^{\nu\rho} + \theta^{\nu\rho}\omega^{\mu\sigma} + \theta^{\nu\sigma}\omega^{\mu\rho}\Big), \\
\mathcal{P}_{0,\mathrm{s}}^{\mu\nu\rho\sigma} &= \frac{1}{3}\theta^{\mu\nu}\theta^{\rho\sigma}, \\
\mathcal{P}_{0,\mathrm{w}}^{\mu\nu\rho\sigma} &= \omega^{\mu\nu}\omega^{\rho\sigma}.
\end{aligned} \tag{D.3}$$

In order to close the algebra, we need to introduce two additional projection operators, which symbolize that the two spin-zero multiplets can mix,

$$\begin{aligned}
\mathcal{P}_{0,\mathrm{sw}}^{\mu\nu\rho\sigma} &= \frac{1}{\sqrt{3}}\theta^{\mu\nu}\omega^{\rho\sigma}, \\
\mathcal{P}_{0,\mathrm{ws}}^{\mu\nu\rho\sigma} &= \frac{1}{\sqrt{3}}\omega^{\mu\nu}\theta^{\rho\sigma}.
\end{aligned} \tag{D.4}$$

The operators are defined such that $\mathcal{P}^2 = \mathcal{P}$. Together, these six projections operators satisfy the following algebraic relations and completeness relation[6]. Removing the tensor indices for clarity, they are

$$\begin{aligned} \mathcal{P}_{0,ab}\mathcal{P}_{0,cd} &= \delta_{ad}\delta_{bc}\mathcal{P}_{0,a}, & \mathcal{P}_{i,c}\mathcal{P}_{0,ab} &= \delta_{i0}\delta_{ac}\mathcal{P}_{0,ab}, \\ \mathcal{P}_{0,ab}\mathcal{P}_{i,c} &= \delta_{i0}\delta_{bc}\mathcal{P}_{i,ab}, & \mathcal{P}_{i,a}\mathcal{P}_{j,b} &= \delta_{ij}\delta_{ab}\mathcal{P}_{j,a}, \end{aligned} \qquad \mathcal{P}_2 + \mathcal{P}_1 + \mathcal{P}_{0,\mathrm{s}} + \mathcal{P}_{0,\mathrm{w}} = \mathbb{1} \tag{D.5}$$

In this notation, $i, j = 0, 1, 2$ and $a, b, c, d = \mathrm{s}, \mathrm{w}$. Also, $a \neq b$ and $c \neq d$. Finally, we can see the important properties of the operators. First, the transverse and traceless conditions met by $\mathcal{P}_2$ and $\mathcal{P}_1$ are given

$$\eta_{\mu\nu}\mathcal{P}_2^{\mu\nu\rho\sigma} = \eta_{\rho\sigma}\mathcal{P}_2^{\mu\nu\rho\sigma} = 0 \quad \text{(traceless)} \tag{D.6}$$

$$q_\mu\mathcal{P}_2^{\mu\nu\rho\sigma} = q_\mu\mathcal{P}_1^{\mu\nu\rho\sigma} = 0 \quad \text{(transverse)}. \tag{D.7}$$

Secondly, contracting the background metric with the projection operators gives us the correct dimension of the irreducible representations the operators project on. This was already hinted by their lower index,

$$\eta_{\mu\rho}\eta_{\nu\sigma}\mathcal{P}_j^{\mu\nu\rho\sigma} = 2j + 1. \tag{D.8}$$

Using this basis of operators, we are now in the position to calculate the expansion coefficients of the graviton propagator, calculated from (3.19), following the prescription of section 3.3. The coefficients coincide with the ones calculated in [43], where we used a different basis. The basis there consists of five independent tensor structures which satisfy the symmetry conditions and can be constructed from the background metric and the graviton four-momentum. They are

$$\begin{aligned} \mathcal{P}_{\mathrm{Tr}}^{\mu\nu\rho\sigma} &= \eta^{\mu\nu}\eta^{\rho\sigma}, & \mathcal{P}_{\mathrm{Id}}^{\mu\nu\rho\sigma} &= \eta^{\mu(\rho}\eta^{\sigma)\nu}, \\ \mathcal{P}_{\eta qq}^{\mu\nu\rho\sigma} &= \frac{\eta^{\mu\nu}q^\rho q^\sigma + \eta^{\rho\sigma}q^\mu q^\nu}{q^2}, & \mathcal{P}_{q\eta q}^{\mu\nu\rho\sigma} &= \frac{q^{(\mu}\eta^{\nu)(\rho}q^{\sigma)}}{q^2}, \\ \mathcal{P}_{q^4}^{\mu\nu\rho\sigma} &= \frac{q^\mu q^\nu q^\rho q^\sigma}{q^4}. \end{aligned} \tag{D.9}$$

We remark that the parentheses around the indices again indicate symmetrization conform (B.5). The transformation rules between the two are given below.

$$\begin{aligned} \mathcal{P}_2^{\mu\nu\rho\sigma} &= \frac{1}{2}\mathcal{P}_{\mathrm{Id}}^{\mu\nu\rho\sigma} - \frac{1}{3}\mathcal{P}_{\mathrm{Tr}}^{\mu\nu\rho\sigma} - \frac{1}{2}\mathcal{P}_{q\eta q}^{\mu\nu\rho\sigma} - \frac{1}{3}\mathcal{P}_{\eta qq}^{\mu\nu\rho\sigma} + \frac{2}{3}\mathcal{P}_{q^4}^{\mu\nu\rho\sigma} \\ \mathcal{P}_1^{\mu\nu\rho\sigma} &= \frac{1}{2}\mathcal{P}_{q\eta q}^{\mu\nu\rho\sigma} - 2\mathcal{P}_{q^4}^{\mu\nu\rho\sigma} \\ \mathcal{P}_{0,\mathrm{s}}^{\mu\nu\rho\sigma} &= \frac{1}{3}\left(\mathcal{P}_{\mathrm{Tr}}^{\mu\nu\rho\sigma} - \mathcal{P}_{\eta qq}^{\mu\nu\rho\sigma} + \mathcal{P}_{q^4}^{\mu\nu\rho\sigma}\right) \\ \mathcal{P}_{0,\mathrm{w}}^{\mu\nu\rho\sigma} &= \mathcal{P}_{q^4}^{\mu\nu\rho\sigma} \\ \mathcal{P}_{0,\mathrm{ws}}^{\mu\nu\rho\sigma} + \mathcal{P}_{0,\mathrm{sw}}^{\mu\nu\rho\sigma} &= \frac{1}{\sqrt{3}}\mathcal{P}_{\eta qq}^{\mu\nu\rho\sigma} - \frac{2}{\sqrt{3}}\mathcal{P}_{q^4}^{\mu\nu\rho\sigma} \end{aligned} \tag{D.10}$$

[6] In unit tensor with four indices is defined as $\mathbb{1}^{\mu\nu}{}_{\rho\sigma} = \frac{1}{2}\left(\delta^\mu{}_\rho\delta^\nu{}_\sigma + \delta^\mu{}_\sigma\delta^\nu{}_\rho\right)$. The absence of $\mathcal{P}_{0,\mathrm{sw}}$ and $\mathcal{P}_{0,\mathrm{ws}}$ signifies that they really or not projection operators.

D.1 Propagator decomposition

We now use the power of the spin projectors to decompose (C.4). We define the decomposition in the following way

$$\left(\frac{\delta^2\hat{\mathcal{F}}\big(\Gamma_{\text{grav}}+\Gamma_{\text{gf}}\big)}{\delta h_{\mu\nu}\delta h_{\rho\sigma}}\right) = a_2(q^2)\mathcal{P}_2^{\mu\nu\rho\sigma} + a_1(q^2)\mathcal{P}_1^{\mu\nu\rho\sigma} + a_{0,\text{s}}(q^2)\mathcal{P}_{0,\text{s}}^{\mu\nu\rho\sigma} + a_{0,\text{w}}(q^2)\mathcal{P}_{0,\text{w}}^{\mu\nu\rho\sigma} + a_{0,\text{sw}}(q^2)\mathcal{P}_{0,\text{sw}}^{\mu\nu\rho\sigma} + a_{0,\text{ws}}(q^2)\mathcal{P}_{0,\text{ws}}^{\mu\nu\rho\sigma} \tag{D.11}$$

We then used Mathematica, to find the momentum-dependent coefficients.

$$\begin{aligned}
a_2(q^2) &= \frac{1}{32\pi G_N}q^2\big(1+q^2 f_{\text{CC}}(q^2)\big)\\
a_1(q^2) &= \frac{1}{32\pi G_N\alpha}q^2\\
a_{0,\text{s}}(q^2) &= \frac{1}{32\pi G_N}\left[\frac{3(\beta+1)^2}{8\alpha}q^2 - 2q^2\big(1+q^2 f_{\text{RR}}(q^2)\big)\right]\\
a_{0,\text{w}}(q^2) &= \frac{1}{32\pi G_N}\frac{(\beta-3)^2}{8\alpha}q^2\\
a_{0,\text{sw}}(q^2) = a_{0,\text{ws}}(q^2) &= \frac{1}{32\pi G_N}\sqrt{3}\frac{(\beta-3)(\beta+1)}{8\alpha}q^2
\end{aligned}$$

Following section 2.2 we have seen that all that is left to do is inverting the expression. Concretely, we want to find a tensor $D^{\mu\nu\rho\sigma}$, the graviton propagator, which satisfies

$$\left(\frac{\delta^2\hat{\mathcal{F}}\big(\Gamma_{\text{grav}}+\Gamma_{\text{gf}}\big)}{\delta h_{\mu\nu}h_{\rho\sigma}}\right)D_{\rho\sigma}{}^{\alpha\beta} = \mathbb{1}^{\mu\nu\alpha\beta}. \tag{D.12}$$

Decomposing the propagator into the basis of spin projectors, we wish to solve this equation for the coefficients $b(q^2)$, which are defined as

$$D^{\mu\nu\rho\sigma}(q^2) = b_2(q^2)\mathcal{P}_2^{\mu\nu\rho\sigma} + b_1(q^2)\mathcal{P}_1^{\mu\nu\rho\sigma} + b_{0,\text{s}}(q^2)\mathcal{P}_{0,\text{s}}^{\mu\nu\rho\sigma} + b_{0,\text{w}}(q^2)\mathcal{P}_{0,\text{w}}^{\mu\nu\rho\sigma} + b_{0,\text{sw}}(q^2)\mathcal{P}_{0,\text{sw}}^{\mu\nu\rho\sigma} + b_{0,\text{ws}}(q^2)\mathcal{P}_{0,\text{ws}}^{\mu\nu\rho\sigma} \tag{D.13}$$

This is easier than it seems. The tensor, vector and scalar sectors do not mix, which means we are basically inverting a block diagonal matrix and that $b_2(q^2)$ and $b_1(q^2)$ are given by the inverse of $a_2(q^2)$ and $a_1(q^2)$ respectively. To obtain the scalar modes boils down to inverting a 2×2-matrix. Carefully accounting for factors of i, we obtain the components of the graviton propagator.

$$\begin{aligned}
b_2(q^2) &= 32\pi G_N G_{\text{CC}}(q^2)\\
b_1(q^2) &= \frac{32\pi G_N\alpha}{q^2}\\
b_{0,\text{s}}(q^2) &= -16\pi G_N G_{\text{RR}}(q^2)\\
b_{0,\text{w}}(q^2) &= 16\pi G_N\left(\frac{16\alpha}{(\beta-3)^2}\frac{1}{q^2} - 3\Big(\frac{\beta+1}{\beta-3}\Big)^2 G_{\text{RR}}(q^2)\right)\\
b_{0,\text{sw}}(q^2) = b_{0,\text{ws}}(q^2) &= 16\sqrt{3}\pi G_N\frac{\beta+1}{\beta-3}G_{\text{RR}}(q^2)
\end{aligned} \tag{D.14}$$

where

$$G_{\mathrm{XX}}(q^2) = \frac{1}{q^2\big(1 + q^2 f_{\mathrm{XX}}(q^2)\big)}. \tag{D.15}$$

In total, the graviton propagator is given by

$$\begin{aligned} D^{\mu\nu\rho\sigma}(q^2) = 16\pi G_N \Bigg(& 2G_{\mathrm{CC}}(q^2)\mathcal{P}_2^{\mu\nu\rho\sigma} + \frac{2\alpha}{q^2}\mathcal{P}_1^{\mu\nu\rho\sigma} - G_{\mathrm{RR}}(q^2)\mathcal{P}_{0,\mathrm{s}}^{\mu\nu\rho\sigma} \\ & + \left[\frac{16\alpha}{(\beta-3)^2}\frac{1}{q^2} - 3\Big(\frac{\beta+1}{\beta-3}\Big)^2 G_{\mathrm{RR}}(q^2)\right]\mathcal{P}_{0,\mathrm{w}}^{\mu\nu\rho\sigma} \\ & + \sqrt{3}\frac{\beta+1}{\beta-3}G_{\mathrm{RR}}(q^2)\big(\mathcal{P}_{0,\mathrm{sw}}^{\mu\nu\rho\sigma} + \mathcal{P}_{0,\mathrm{ws}}^{\mu\nu\rho\sigma}\big)\Bigg). \end{aligned} \tag{D.16}$$

Bibliography

[1] B. Abbott *et al.*, "Observation of Gravitational Waves from a Binary Black Hole Merger," *Phys. Rev. Lett.*, vol. 116, no. 6, p. 061102, 2016.

[2] K. Akiyama *et al.*, "First M87 Event Horizon Telescope Results. I. The Shadow of the Supermassive Black Hole," *Astrophys. J.*, vol. 875, no. 1, p. L1, 2019.

[3] G. Aad *et al.*, "Observation of a new particle in the search for the Standard Model Higgs boson with the ATLAS detector at the LHC," *Phys. Lett. B*, vol. 716, pp. 1–29, 2012.

[4] S. Chatrchyan *et al.*, "Observation of a New Boson at a Mass of 125 GeV with the CMS Experiment at the LHC," *Phys. Lett. B*, vol. 716, pp. 30–61, 2012.

[5] B. Odom, D. Hanneke, B. D'Urso, and G. Gabrielse, "New Measurement of the Electron Magnetic Moment Using a One-Electron Quantum Cyclotron," *Phys. Rev. Lett.*, vol. 97, p. 030801, Jul 2006.

[6] G. 't Hooft and M. Veltman, "One-loop divergencies in the theory of gravitation," *Annales de l'I.H.P. Physique théorique*, vol. 20, no. 1, pp. 69–94, 1974.

[7] S. Christensen and M. Duff, "Quantizing gravity with a cosmological constant," *Nuclear Physics B*, vol. 170, no. 3, pp. 480 – 506, 1980.

[8] M. H. Goroff and A. Sagnotti, "Quantum gravity at two loops," *Phys. Lett. B*, vol. 160, pp. 81–86, 1985.

[9] G. Amelino-Camelia, "Quantum-Spacetime Phenomenology," *Living Rev. Rel.*, vol. 16, p. 5, 2013.

[10] S. Hossenfelder and L. Smolin, "Phenomenological Quantum Gravity," *Phys. Canada*, vol. 66, pp. 99–102, 2010.

[11] S. Hossenfelder, "Experimental Search for Quantum Gravity," *Classical and Quantum Gravity: Theory, Analysis and Applications*, pp. 6–9, 10 2010.

[12] J. F. Donoghue and B. R. Holstein, "Low Energy Theorems of Quantum Gravity from Effective Field Theory," *J. Phys. G*, vol. 42, no. 10, p. 103102, 2015.

[13] C. P. Burgess, "Quantum Gravity in Everyday Life: General Relativity as an Effective Field Theory," *Living Rev. Rel.*, vol. 7, pp. 5–56, 2004.

[14] J. F. Donoghue, "General relativity as an effective field theory: The leading quantum corrections," *Phys. Rev. D*, vol. 50, pp. 3874–3888, 1994.

[15] L. Smolin, "The Classical limit and the form of the Hamiltonian constraint in nonperturbative quantum general relativity," *arXiv preprint gr-qc/9609034*, 9 1996.

[16] J. Lewandowski and D. Marolf, "Loop constraints: A Habitat and their algebra," *Int. J. Mod. Phys. D*, vol. 7, pp. 299–330, 1998.

[17] R. Gambini, J. Lewandowski, D. Marolf, and J. Pullin, "On the consistency of the constraint algebra in spin network quantum gravity," *Int. J. Mod. Phys. D*, vol. 7, pp. 97–109, 1998.

[18] K. Stelle, "Renormalization of Higher Derivative Quantum Gravity," *Phys. Rev. D*, vol. 16, 08 1977.

[19] K. S. Stelle, "Classical Gravity with Higher Derivatives," *Gen. Rel. Grav.*, vol. 9, pp. 353–371, 1978.

[20] I. Kuntz, "Exorcising ghosts in quantum gravity," *The European Physical Journal Plus*, vol. 135, p. 859, Oct 2020.

[21] M. Raidal and H. Veermäe, "On the quantisation of complex higher derivative theories and avoiding the Ostrogradsky ghost," *Nuclear Physics B*, vol. 916, pp. 607 – 626, 2017.

[22] A. Bonanno, A. Eichhorn, H. Gies, J. M. Pawlowski, R. Percacci, M. Reuter, F. Saueressig, and G. P. Vacca, "Critical Reflections on Asymptotically Safe Gravity," *Frontiers in Physics*, vol. 8, p. 269, 2020.

[23] D. Becker, C. Ripken, and F. Saueressig, "On avoiding Ostrogradski instabilities within Asymptotic Safety," *JHEP*, vol. 12, p. 121, 2017.

[24] N. Christiansen, D. F. Litim, J. M. Pawlowski, and M. Reichert, "Asymptotic safety of gravity with matter," *Phys. Rev. D*, vol. 97, no. 10, p. 106012, 2018.

[25] A. Codello, R. Percacci, and C. Rahmede, "Ultraviolet properties of f(R)-gravity," *Int. J. Mod. Phys. A*, vol. 23, pp. 143–150, 2008.

[26] T. Denz, J. M. Pawlowski, and M. Reichert, "Towards apparent convergence in asymptotically safe quantum gravity," *Eur. Phys. J. C*, vol. 78, no. 4, p. 336, 2018.

[27] J. A. Dietz and T. R. Morris, "Asymptotic safety in the f(R) approximation," *JHEP*, vol. 01, p. 108, 2013.

[28] A. Eichhorn and M. Schiffer, "$d = 4$ as the critical dimensionality of asymptotically safe interactions," *Phys. Lett. B*, vol. 793, pp. 383–389, 2019.

[29] K. Falls, D. F. Litim, K. Nikolakopoulos, and C. Rahmede, "Further evidence for asymptotic safety of quantum gravity," *Phys. Rev. D*, vol. 93, no. 10, p. 104022, 2016.

[30] D. Benedetti, P. F. Machado, and F. Saueressig, "Asymptotic Safety in Higher-Derivative Gravity," *Mod. Phys. Lett. A*, vol. 24, pp. 2233–2241, 2009.

[31] J. Biemans, A. Platania, and F. Saueressig, "Quantum gravity on foliated spacetimes: Asymptotically safe and sound," *Phys. Rev. D*, vol. 95, no. 8, p. 086013, 2017.

[32] H. Gies, B. Knorr, S. Lippoldt, and F. Saueressig, "Gravitational Two-Loop Counterterm is Asymptotically Safe," *Phys. Rev. Lett.*, vol. 116, p. 211302, May 2016.

[33] A. Codello, R. Percacci, and C. Rahmede, "Investigating the Ultraviolet Properties of Gravity with a Wilsonian Renormalization Group Equation," *Annals Phys.*, vol. 324, pp. 414–469, 2009.

[34] Y. Kluth and D. Litim, "Fixed Points of Quantum Gravity and the Dimensionality of the UV Critical Surface," *arXiv e-prints*, p. arXiv:2008.09181, Aug. 2020.

[35] R. Percacci, *An Introduction to Covariant Quantum Gravity and Asymptotic Safety*, vol. 3 of *100 Years of General Relativity*. World Scientific, 2017.

[36] M. Reuter and F. Saueressig, *Quantum Gravity and the Functional Renormalization Group: The Road towards Asymptotic Safety*. Cambridge Monographs on Mathematical Physics, Cambridge University Press, 2019.

[37] C. Ripken, *Structural and observational aspects of asymptotically safe Quantum Gravity*. PhD thesis, Radboud University, 9 2020.

[38] J. F. Donoghue, "A Critique of the Asymptotic Safety Program," *Front. in Phys.*, vol. 8, p. 56, 2020.

[39] A. Barvinsky and G. Vilkovisky, "Covariant perturbation theory (II). second order in the curvature. general algorithms," *Nuclear Physics B*, vol. 333, no. 2, pp. 471 – 511, 1990.

[40] L. Bosma, B. Knorr, and F. Saueressig, "Resolving Spacetime Singularities within Asymptotic Safety," *Phys. Rev. Lett.*, vol. 123, no. 10, p. 101301, 2019.

[41] E. Belgacem, Y. Dirian, S. Foffa, and M. Maggiore, "Nonlocal gravity. Conceptual aspects and cosmological predictions," *JCAP*, vol. 03, p. 002, 2018.

[42] E. Belgacem, Y. Dirian, A. Finke, S. Foffa, and M. Maggiore, "Gravity in the infrared and effective nonlocal models," *JCAP*, vol. 04, p. 010, 2020.

[43] T. Draper, B. Knorr, C. Ripken, and F. Saueressig, "Graviton-Mediated Scattering Amplitudes from the Quantum Effective Action," *JHEP*, vol. 11, p. 136, 2020.

[44] T. Draper, B. Knorr, C. Ripken, and F. Saueressig, "Finite Quantum Gravity Amplitudes: No Strings Attached," *Phys. Rev. Lett.*, vol. 125, no. 18, p. 181301, 2020.

[45] A. Zee, *Quantum Field Theory in a Nutshell*. Princeton University Press, 11 2003.

[46] M. Srednicki, *Quantum Field Theory*. Cambridge University Press, 1 2007.

[47] M. E. Peskin and D. V. Schroeder, *An Introduction to Quantum Field Theory*. Reading, USA: Addison-Wesley, 1995.

[48] M. Maggiore, "Phantom dark energy from nonlocal infrared modifications of General Relativity," *Phys. Rev. D*, vol. 89, no. 4, p. 043008, 2014.

[49] M. Maggiore and M. Mancarella, "Non-local gravity and dark energy," *Phys. Rev. D*, vol. 90, no. 2, p. 023005, 2014.

[50] L. D. Faddeev, "The Feynman integral for singular Lagrangians," *Theoretical and Mathematical Physics*, vol. 1, pp. 1–13, Oct 1969.

[51] L. D. Faddeev and V. N. Popov, "Feynman diagrams for the yang-mills field," *Physics Letters B*, vol. 25, no. 1, pp. 29–30, 1967.

[52] V. Popov and L. Faddeev, "Kiev report itp 67-36. 1967, unpublished," *Trans. NAL Report THY-57 (D. Gordon and BW Lee, Eds.)*, 1972.

[53] M. Froissart, "Asymptotic Behavior and Subtractions in the Mandelstam Representation," *Phys. Rev.*, vol. 123, pp. 1053–1057, Aug 1961.

[54] M. Froissart, "Froissart bound," *Scholarpedia*, vol. 5, no. 5, p. 10353, 2010. revision #91280.

[55] F. Cerulus and A. Martin, "A lower bound for large angle elastic scattering at high energies," *Physics Letters*, vol. 8, no. 1, pp. 80 – 82, 1964.

[56] H. Epstein and A. Martin, "Rigorous lower bound on the scattering amplitude at large angles," *Phys. Rev. D*, vol. 99, no. 11, p. 114025, 2019.

[57] X. O. Camanho, J. D. Edelstein, J. Maldacena, and A. Zhiboedov, "Causality Constraints on Corrections to the Graviton Three-Point Coupling," *JHEP*, vol. 02, p. 020, 2016.

[58] A. Adams, N. Arkani-Hamed, S. Dubovsky, A. Nicolis, and R. Rattazzi, "Causality, Analyticity and an IR Obstruction to UV Completion," *JHEP*, vol. 10, p. 014, 2006.

[59] S. Weinberg, "Ultraviolet divergences in quantum theories of gravitation.," in *General Relativity: An Einstein centenary survey* (S. W. Hawking and W. Israel, eds.), pp. 790–831, Jan. 1979.

[60] M. A. Virasoro, "Alternative Constructions of Crossing-Symmetric Amplitudes with Regge Behavior," *Phys. Rev.*, vol. 177, pp. 2309–2311, Jan 1969.

[61] J. Shapiro, "Electrostatic analogue for the Virasoro model," *Physics Letters B*, vol. 33, no. 5, pp. 361 – 362, 1970.

[62] G. Veneziano, "Construction of a crossing-symmetric, Regge-behaved amplitude for linearly rising trajectories," *Il Nuovo Cimento A (1965-1970)*, vol. 57, pp. 190–197, Sep 1968.

[63] A. Eichhorn, "Status of the asymptotic safety paradigm for quantum gravity and matter," *Found. Phys.*, vol. 48, no. 10, pp. 1407–1429, 2018.

[64] J. Martín-García, "xAct: Efficient Tensor Computer Algebra for Mathematica," 2004.

[65] C. de Rham, "Massive Gravity," *Living Rev. Rel.*, vol. 17, p. 7, 2014.

[66] B. Knorr, C. Ripken, and F. Saueressig, "Form Factors in Asymptotic Safety: conceptual ideas and computational toolbox," *Classical and Quantum Gravity*, vol. 36, p. 234001, Nov 2019.

[67] S. A. Fulling, R. C. King, B. G. Wybourne, and C. J. Cummins, "Normal forms for tensor polynomials. I. the Riemann tensor," *Classical and Quantum Gravity*, vol. 9, pp. 1151–1198, may 1992.

[68] R. J. Riegert, "The particle content of linearized conformal gravity," *Physics Letters A*, vol. 105, no. 3, pp. 110 – 112, 1984.

[69] L. Buoninfante, *Ghost and singularity free theories of gravity.* PhD thesis, Università degli Studi di Salerno.

[70] T. Nutma, "xTras : A field-theory inspired xAct package for Mathematica," *Comput. Phys. Commun.*, vol. 185, pp. 1719–1738, 2014.

[71] H. Gies, B. Knorr, and S. Lippoldt, "Generalized Parametrization Dependence in Quantum Gravity," *Physical Review D*, vol. 92, Oct 2015.

[72] D. C. Dunbar and P. S. Norridge, "Infinities within Graviton Scattering Amplitudes," *Class. Quant. Grav.*, vol. 14, pp. 351–365, 1997.

[73] V. Zakharov, "Spin of virtual gravitons," *J. Exptl. Theoret. Phys.*, vol. 21, pp. 199 – 203, 7 1965.

[74] R. Alonso and A. Urbano, "Amplitudes, resonances, and the ultraviolet completion of gravity," *Phys. Rev. D*, vol. 100, no. 9, p. 095013, 2019.

[75] A. Datta, E. Gabrielli, and B. Mele, "Violation of angular momentum selection rules in quantum gravity," *Physics Letters B*, vol. 579, p. 189–199, Jan 2004.

[76] S. Weinberg, "Infrared Photons and Gravitons," *Phys. Rev.*, vol. 140, pp. B516–B524, Oct 1965.

[77] R. P. Feynman, "Quantum theory of gravitation," *Acta Phys. Polon.*, vol. 24, pp. 697–722, 1963.

[78] N. E. J. Bjerrum-Bohr, J. F. Donoghue, and B. R. Holstein, "Quantum Gravitational Corrections to the Nonrelativistic Scattering Potential of Two Masses," 2002.

[79] A. Akhundov, S. Bellucci, and A. Shiekh, "Gravitational interaction to one loop in effective quantum gravity," *Phys. Lett. B*, vol. 395, pp. 16–23, 1997.

[80] S. Talaganis, T. Biswas, and A. Mazumdar, "Towards understanding the ultraviolet behavior of quantum loops in infinite-derivative theories of gravity," *Classical and Quantum Gravity*, vol. 32, p. 215017, Oct 2015.

[81] J. F. Donoghue, "Leading Quantum Correction to the Newtonian Potential," *Physical Review Letters*, vol. 72, p. 2996–2999, May 1994.

[82] N. Ohta and L. Rachwal, "Effective Action from the Functional Renormalization Group," *Eur. Phys. J. C*, vol. 80, no. 9, p. 877, 2020.

[83] A. Codello, R. Percacci, L. Rachwał, and A. Tonero, "Computing the Effective Action with the Functional Renormalization Group," *Eur. Phys. J. C*, vol. 76, no. 4, p. 226, 2016.

[84] A. Codello and R. K. Jain, "On the covariant formalism of the effective field theory of gravity and leading order corrections," *Class. Quant. Grav.*, vol. 33, no. 22, p. 225006, 2016.

[85] A. Codello and R. K. Jain, "On the covariant formalism of the effective field theory of gravity and its cosmological implications," *Class. Quant. Grav.*, vol. 34, no. 3, p. 035015, 2017.

[86] C. Wetterich, "Effective Nonlocal Euclidean Gravity," *Gen. Rel. Grav.*, vol. 30, pp. 159–172, 1998.

[87] A. Pais and G. E. Uhlenbeck, "On Field Theories with Non-Localized Action," *Phys. Rev.*, vol. 79, pp. 145–165, Jul 1950.

[88] T. Biswas, E. Gerwick, T. Koivisto, and A. Mazumdar, "Towards singularity and ghost free theories of gravity," *Phys. Rev. Lett.*, vol. 108, p. 031101, 2012.

[89] S. Talaganis and A. Mazumdar, "High-energy scatterings in infinite-derivative field theory and ghost-free gravity," *Classical and Quantum Gravity*, vol. 33, p. 145005, Jun 2016.

[90] T. Biswas and S. Talaganis, "String-inspired infinite-derivative theories of gravity: A brief overview," *Modern Physics Letters A*, vol. 30, p. 1540009, Jan 2015.

[91] A. Ghoshal, A. Mazumdar, N. Okada, and D. Villalba, "Stability of infinite derivative Abelian Higgs models," *Phys. Rev. D*, vol. 97, no. 7, p. 076011, 2018.

[92] M. Reuter, "Nonperturbative evolution equation for quantum gravity," *Phys. Rev. D*, vol. 57, pp. 971–985, 1998.

[93] U. Ellwanger, "Flow equations for N point functions and bound states," pp. 206–211, 9 1993.

[94] T. R. Morris, "The exact renormalization group and approximate solutions," *Int. J. Mod. Phys. A*, vol. 9, pp. 2411–2450, 1994.

[95] J. Daas, "Fermions in the Asymptotic Safety Program," Master's thesis, Radboud University, 7 2020.

[96] A. Bonanno and M. Reuter, "Renormalization group improved black hole spacetimes," *Physical Review D*, vol. 62, Jul 2000.

[97] T. Lee and G. Wick, "Negative metric and the unitarity of the S-matrix," *Nucl. Phys. B*, vol. 9, pp. 209–243, 1969.

[98] T. D. Lee and G. C. Wick, "Finite Theory of Quantum Electrodynamics," *Phys. Rev. D*, vol. 2, pp. 1033–1048, Sep 1970.

[99] D. G. Boulware and D. J. Gross, "Lee-Wick indefinite metric quantization: A functional integral approach," *Nuclear Physics B*, vol. 233, no. 1, pp. 1–23, 1984.

[100] J. F. Donoghue and G. Menezes, "Unitarity, stability and loops of unstable ghosts," *Phys. Rev. D*, vol. 100, no. 10, p. 105006, 2019.

[101] S. Coleman, "Acausality," in *7th International School of Subnuclear Physics (Ettore Majorana): Subnuclear Phenomena*, pp. 282–327, 1969.

[102] B. Grinstein, D. O'Connell, and M. B. Wise, "Causality as an emergent macroscopic phenomenon: The Lee-Wick O(N) model," *Phys. Rev. D*, vol. 79, p. 105019, May 2009.

[103] N. Nakanishi, "Lorentz Noninvariance of the Complex-Ghost Relativistic Field Theory," *Phys. Rev. D*, vol. 3, pp. 811–814, Feb 1971.

[104] N. Nakanishi, "Remarks on the Complex-Ghost Relativistic Field Theory," *Phys. Rev. D*, vol. 3, pp. 3235–3237, Jun 1971.

[105] T. D. Lee and G. C. Wick, "Questions of Lorentz Invariance in Field Theories with Indefinite Metric," *Phys. Rev. D*, vol. 3, pp. 1046–1047, Feb 1971.

[106] R. Cutkosky, P. Landshoff, D. Olive, and J. Polkinghorne, "A non-analytic S-matrix," *Nuclear Physics B*, vol. 12, no. 2, pp. 281–300, 1969.

[107] A. Platania and C. Wetterich, "Non-perturbative unitarity and fictitious ghosts in quantum gravity," *Physics Letters B*, vol. 811, p. 135911, 2020.

[108] L. Alberte, C. de Rham, S. Jaitly, and A. J. Tolley, "Positivity bounds and the massless spin-2 pole," *Phys. Rev. D*, vol. 102, p. 125023, 2020.

[109] C. de Rham and A. J. Tolley, "Speed of gravity," *Phys. Rev. D*, vol. 101, no. 6, p. 063518, 2020.

[110] C. de Rham and A. J. Tolley, "Causality in curved spacetimes: The speed of light and gravity," *Phys. Rev. D*, vol. 102, no. 8, p. 084048, 2020.

[111] R. J. Rivers, "Lagrangian theory for neutral massive spin-2 fields," *Il Nuovo Cimento (1955-1965)*, vol. 34, pp. 386–403, Oct 1964.

[112] P. Van Nieuwenhuizen, "On ghost-free tensor Lagrangians and linearized gravitation," *Nucl. Phys. B*, vol. 60, pp. 478–492, 1973.